AF TECHNICAL REPORT No. 6334 DECEMBER 1950

DIFFUSER EFFICIENCY AND FLOW PROCESS OF SUPERSONIC WIND TUNNELS WITH FREE JET TEST SECTION

RUDOLF HERMANN, Ph.D.

AIR ENGINEERING DEVELOPMENT DIVISION

United States Air Force
Air Materiel Command
Wright-Patterson Air Force Base, Dayton, Ohio

AF TECHNICAL REPORT NO. 6334 December 1950

DIFFUSER EFFICIENCY AND FLOW PROCESS OF SUPERSONIC WIND TUNNELS WITH FREE JET TEST SECTION

Rudolf Hermann, Ph.D.

Air Engineering Development Division

United States Air Force
Air Materiel Command
Wright-Patterson Air Force Base, Dayton, Ohio

Air Force-WPAFB-(A)-O-19 FEB 51 250

FOREWORD

Some results of this report have been briefly presented before as a lecture, entitled, "Theoretical Calculation of the Diffuser Efficiency of Supersonic Wind Tunnels with Free Jet Test Section", at the Heat Transfer and Fluid Mechanics Institute, Berkeley, California, in June 1949 by the author, Dr. Rudolf Hermann. (See Reference 25)

This report represents a much more detailed analytical study and a comprehensive comparison with available experiments. Both the above mentioned lecture and the present report deal with the special case of pressure equilibrium, when the pressure surrounding the free jet is equal to the pressure in the Laval nozzle exit cross-section.

Another report by the same author, not yet published, deals with the general case of pressure non-equilibrium and is entitled, "Diffuser Efficiency of Free Jet Supersonic Wind Tunnels at Variable Test Chamber Pressure." (See Reference 26)

The author wishes to express his thanks to Dr. R. H. Mills for his steady interest in these problems and his stimulating discussions; to Mr. E. Walk, long-time associate, for his careful and extensive numerical evaluation of the equations and laborious preparation of the graphs; to Mr. H. U. Eckert for critical study of the draft and his valuable comments; to Messrs. J. A. Spanogle and M. O. Lawson for their help in editing the English text; to Miss M. Le Comte and Miss V. Bowman for preparing the typewritten drafts and final copy.

ABSTRACT

In the wind tunnel arrangement under consideration, the air leaves the Laval nozzle as a free jet and is recaptured by the diffuser, which is of the convergent-divergent design. A theoretical analysis of the flow process through this type of supersonic wind tunnel is presented and the diffuser efficiency is calculated for the case of equilibrium between test chamber pressure and pressure in the nozzle exit, assuming one-dimensional, inviscous, steady flow.

Using the basic equations of continuity, energy and momentum flux through a bounding surface, an exact solution of the problem is obtained, which is applicable up to Mach number infinite.

One of the basic results is, that in the recapturing zone of the diffuser a transition occurs from supersonic to subsonic flow, which is followed by an acceleration in the convergent portion up to sonic velocity at the second throat. The transition is not a normal shock and involves a total pressure loss greater than that of a normal shock at the test section Mach number. A mathematical solution with supersonic velocity after the transition process has no physical existence.

A comprehensive comparison of the analytical results with available experiments in supersonic wind tunnels up to Mach numbe 4.4 regarding diffuser efficiency and second throat area shows good agreemert.

PUBLICATION REVIEW

The publication of this report does not constitute approva by the Air Force of the findings or the conclusions contained therein. It is published only for the exchange and stimulation of ideas.

FOR THE COMMANDING GENERAL:

George E. Schaetzel

GEORGE E. SCHAETZEL
Colonel, USAF
Deputy for Operations
Air Engineering Development Division

CONTENTS

CONTENTS (contd)

ILLUSTRATIONS

DIFFUSER EFFICIENCY AND FLOW PROCESS OF SUPERSONIC WIND TUNNELS WITH FREE JET TEST SECTION

Section 1 - Introduction - Diffusers, Flow Process and Efficiency Definitions.

A. Diffusers in Wind Tunnels with Free Jet and Closed Test Section

Supersonic wind tunnels, like subsonic wind tunnels, may be placed in one of two categories according to the bounding surface of the air stream in the test section, i.e., those with open or free jet test section and those with closed or rigid wall test section. The characteristic of the first type is the constant pressure around and along the surface of the free jet, while the direction of the streamlines at the surface is not determined. The characteristic of the second type is the fixed direction of the velocity along the rigid walls of the test section, while the pressure inside the flow or along the walls of the test section are dependent variables. It is well known for the subsonic incompressible and compressible velocity range, that the influence of the limited size of a wind tunnel stream on the aerodynamic test data (drag, lift) depends on the boundary conditions and the so-called wind tunnel corrections are quite different for the two types.

A similar behavior exists with regard to the diffuser efficiency of a supersonic wind tunnel. The following analysis, assuming one dimensional flow, will show that the flow process in a diffuser of a supersonic wind tunnel with free jet test section is completely determined by the preceding free jet and its spreading due to the turbulent mixing zones at its surface. Thus the area F_2 at the entrance of the supersonic diffuser must be larger than the cross section area F_1 of the stream leaving the nozzle ($F_2 > F_1$). The cross section ratio $f = F_1/F_2$ enters the fundamental equations (Section 2), and determines its solution (Section 3). It is therefore an important parameter of the diffuser efficiency (Section 4) and other related wind tunnel characteristics, for instance, the second throat area (Section 5). In case of a supersonic wind tunnel with closed test section this parameter does not, of course, appear, and the flow process in the diffuser will be quite different. Therefore, it is necessary to differentiate clearly between the diffuser efficiency of the supersonic wind tunnel with free jet test section and that for the closed test section.

A third type of wind tunnel test section is sometimes used or proposed, the so-called "half-open, half-closed" wind tunnel, which offers advantages in minimizing the wind tunnel corrections in the incompressible and in the compressible subsonic region. Assuming a rectangular shaped cross section, two of the air stream surfaces are bounded by still air as in the free jet type, while the other two are bounded by rigid walls as in the closed type. Analytical explanation of the flow process in the diffuser downstream of such a test section

seems to be more difficult than in the case of the two other types.

It might be briefly mentioned that the results obtained for the diffuser of a free jet supersonic wind tunnel are not applicable to diffusers in supersonic ram jets, or vice versa. The basic differences in these cases are as follows:

1. Fixed mass flow, given through the preceding Laval nozzle, in the wind tunnel and variable mass flow with traveling shock ("spilling") in case of ram jet.

2. Finite size of the jet with a spreading turbulent mixing zone collected by the wind tunnel diffuser and infinite uniform medium without any friction layer approaching the intake of the ram jet diffuser.

B. Flow Process and Tasks of the Diffuser

The following analysis will consider a conventional type of a supersonic wind tunnel with a free jet test section (See Fig. 1) - to the author's knowledge first established in Goettingen by L. Prandtl and A. Busemann in 1928 (Ref. 1). The air flows from the open atmosphere or from a settling chamber through a straightener and entrance cone into the Laval nozzle and attains sonic velocity in the minimum section called the first throat. The stream leaves the exit cross section of the Laval nozzle with supersonic velocity as a free jet bounded by air. In most of the supersonic tunnels an air tight test chamber surrounds the free jet, whose pressure then is independent of the atmosphere. The free jet is collected by the diffuser. In contrast to subsonic wind tunnels, the supersonic wind tunnel diffuser consists of two parts; the first is a converging diffuser portion which ends up in a minimum section called the second throat, and the second a diverging diffuser portion, which finally leads to the blowers.

The main taks of the diffuser is the transfer of the large kinetic energy at low pressure of the test section stream into high pressure at nearly vanishing kinetic energy at the end of the diffuser. This purpose is the same in all subsonic and supersonic wind tunnels with either free jet or closed test section. Due to the increasing kinetic energy in supersonic tunnels and the large driving power needed for operation, the efficiency of the pressure recovery is becoming more and more important. The second task of the diffuser, which is confined only to supersonic wind tunnels with free jet test section, is the control of the air pressure p_c in the test chamber, which, at supersonic velocity of the jet, is not necessarily equal to the pressure p_1 of the air stream in the exit cross section of the Laval nozzle. To fulfill these two requirements, the diffuser is usually designed with adjustable throat cross section and adjustable walls, upstream and downstream from the throat, forming a reasonable aerodynamic shape.

The reason for building the first part of the diffuser convergent is the assumption more or less generally made up to the present time that the incoming supersonic velocity should be continuously decelerated which results in increasing pressure. The optimum recovery would be reached, if the sonic velocity is attained in the second throat, so that subsonic velocities only, without further shocks, occur in the divergent part of the diffuser. Actually, this ideal case is only approached as the velocity in the throat is still slightly supersonic and is followed by a normal shock close downstream, which leads to subsonic velocity. In any case, the convergent part of the diffuser should act as a "converted" Laval nozzle declerating the supersonic flow of the diffuser entrance to approximately sonic velocity in the throat and to subsonic in the diverging part. It follows from the theoretical one-dimensional calculations below that this concept is wrong for the open jet tunnel. When the jet is recaptured a sudden transition from the supersonic to subsonic flow occurs close to the entrance section of the diffuser (See Sec. 4C, 2 and 3), which is followed by a new acceleration in the converging part of the diffuser to exact sonic speed in the second throat. The so-called supersonic diffuser acts as a "conventional" accelerating Laval nozzle, not as a decelerating "converted" Laval nozzle. (See Sec. 5A).

The mechanism of controlling the test chamber pressure by the adjustable diffuser throat has never been exactly understood. Actually it works satisfactorily in many but not in all cases. Because this pressure control is an "upstream action" in supersonic flow, sometimes the thick boundary layers inside the diffuser were assumed to transmit the pressure upstream. This concept is incorrect and has to be revised. Pressure control, so important for actual model testing in the tunnel, can be explained by one-dimensional calculation without consideration of any boundary layer (see Sec. 5A).

The subsequent calculations were instigated by some results of measurements carried out in the Peenemuende supersonic free jet wind tunnel by my former associate, H. Ramm (Ref. 2) in 1943, reported 1945. Pressure distribution measurements along the entire wind tunnel and especially those in the diffuser proved that most of the losses occur in the first part of the diffuser and are not distributed over the whole diffuser and tunnel. Therefore, it seemed logical that a theoretical analysis of the flow process between nozzle exit and diffuser throat would produce significant results. Having obtained the main theoretical results in 1946 some of the previous tests results acquired greater significance. Afterwards (in 1947), a new detailed discussion of his measurements was given by H. Ramm (Ref. 3).

Nevertheless, the following analysis of the diffuser efficiency is purely theoretical and does not use any empirical values. A comparison of the results with all experimental data available to the author is given in Section 6.

C. Various Definitions of Diffuser Efficiency and Energy Ratio

To obtain a convenient measure for the pressure recovery of the diffuser various definitions of different kinds of efficiency have been introduced. If they are defined correctly, that means utilizing thermodynamic states, they can be transformed one into another as a function

of Mach No. and it is a matter of convenience which one to use. Some of those definitions which fulfill the mentioned requirement are discussed in the following.

1. Pressure Efficiency and Energy Efficiency

J. Ackeret (Ref. 4) gives two possible definitions to use for evaluation of experimental data in the compressible subsonic region. However, he does not give theoretical calculations of any diffuser flow process or efficiency. One of these definitions is the "pressure efficiency" given by

$$\eta_P = \frac{p_e - p_i}{p_o - p_i}$$

where p_o = total pressure before the diffuser, p_i = static pressure in the inlet cross section of the diffuser; p_e = static or total pressure in the exit cross section of the diffuser where the velocity head can be neglected. (For evaluation purposes the total pressure is taken). It compares the actual pressure increase in the diffuser with the maximum possible increase at isentropic flow. Obviously this definition originated in the theory of incompressible flow, where the denominator represents the kinetic energy in the smallest section of a venturi meter. The pressure efficiency for reasonable diffusers in the incompressible or subsonic compressible range is of the order of 0.8. At high supersonic Mach Nos. it decreases rapidly and drops down to inconveniently small values; for instance, $\eta_P = 0.05$ at Mach No. 5 and $\eta_P = 0.002$ at Mach No. 10.

The other definition is the "energy efficiency" given by

$$\eta_E = 1 - \frac{T_B - T_o}{T_o - T_i}$$

where T_o = stagnation temperature; T_i = temperature in the inlet cross section of the diffuser; T_B = blower outlet temperature after adiabatic compression of the air leaving the diffuser up to the original total pressure p_o. It compares the difference of the kinetic energy in the test section and the blower energy with the kinetic energy in the test section. Obviously this definition is desired for wind tunnel purposes, where a complete cycle is required and the blower energy necessary to maintain this cycle is of primary interest. The "energy efficiency" in the subsonic range for reasonable diffusers has similar values (about 0.8) as the "pressure efficiency." Its major disadvantage, however, is that its value decreases rapidly with Mach No., passes zero and becomes negative at higher Mach Nos., even at diffusers with reasonable pressure recovery. (For instance, at Ma = 4: $\eta_E = -0.25$; at Ma = 10: $\eta_E = -4.0$). For a bad diffuser with no pressure recovery at all, the energy efficiency becomes zero for incompressible flow only, but negative even at subsonic compressible Mach Nos. (See Sec. 5, D).

2. Diffuser Efficiency (by Crocco) differentially defined.

L. Crocco (Ref. 5) has introduced another definition of the diffuser efficiency, assuming a step by step compression along the diffuser. He defines differentially an efficiency η_{Cr} at the ratio between actual and isentropic relative increase of static pressure with correspondingly equal

decrease of kinetic energy. η_{cr} is unknown but is assumed constant over the whole compression. This way he obtains a formula, which in the notations used above, can be transformed into

$$\eta_{cr} = \frac{\ln \frac{p_e}{p_i}}{\ln \frac{p_o}{p_i}}$$

Crocco gives no theoretical calculation of the diffuser process or the efficiency itself. He calculates η_{cr} with the aid of this formula by evaluation of total pressure measurements p_e of specific wind tunnel tests. These efficiency values converted into the η definition used in this paper are discussed later (see Sec. 6, E and Fig. 20. Curve 8).

Efficiency values η_{cr} of reasonable diffusers avoid the above mentioned inconveniences involved in Ackeret's η_P or η_E values at high Mach Nos. and stay in a convenient order of magnitude (for instance, 0.4 at Mach No. 10). At pressure ratios near unity the formula for η_{cr} approaches asymptotically the formula for η_P, thus furnishing conventional values of the order of 0.8 in the subsonic range. However, Crocco seems not to differentiate between diffusers behind closed or free jet test section. In case of a free jet tunnel, his concept of a step by step compression along the diffuser is incorrect according to the results of the following analysis. Hence the values of efficiency η_{cr} obtained thereby are fictitious. In spite of their convenient order of magnitude, they have no physical meaning.

3. The Energy Ratio

In order to describe the performance of wind tunnels the so-called energy ratio is also often used. Hereby the kinetic energy inside the test section L_{Kin} is considered as desired energy and compared with the energy consumption of the blowers L_B

$$\zeta = \frac{L_{Kin}}{L_B}$$

L_B is generally defined as the work per unit time either at isothermic or at adiabatic compression, and ζ is called the isothermic or adiabatic energy ratio respectively. Sometimes the energy output of the driving motor of the blower is considered as L_B. A detailed discussion of the values of the energy ratio calculated with the diffuser efficiency obtained by this analysis is given later (See Sec. 5, D, and Fig. 16, 17). It might be mentioned that the fraction in the definition of the energy efficiency η_E is the reciprocal value of the adiabatic energy ratio.

In discussing the definition of energy ratio we have to consider that the kinetic energy in the test section L_{Kin} is desired and needed to fulfill the task of the tunnel. But a wind tunnel is not an engine which takes power L_B from outside and delivers L_{Kin} as external useful work. The steady flow of air in a wind tunnel from the stagnation chamber to the section upstream of the blower has, even with losses in the diffuser or elsewhere, constant energy, if all kinds of energy are considered and non-conduting tunnel walls are assumed. In case of wind tunnels with a closed circuit the air circulates in a complete thermodynamic cycle. The energy L_B put into the air flow by

the motor of the blower has to be removed entirely as heat by the cooling system. If the compressor power is used in defining energy ratio or efficiency of the diffuser or of the whole tunnel, it is necessary to prescribe a specific compression and cooling process. This might be an adiabatic or isothermic or any other kind of polytropic compression and a cooling process between arbitrarily defined values of pressures and temperatures. Cooling can take place before, in between, or behind the compression. Therefore, the definition of the energy ratio ζ or the energy efficiency η_E of the diffuser depends on a specific but arbitrarily chosen cycle.

4. Efficiency Definition Used in this Paper

The definition for efficiency used in this paper is different from those mentioned above. All so-called losses, which occur by friction along the tunnel walls, by the model drag, by compression shocks, in the diffuser or elsewhere actually mean no loss but a devaluation of total energy, which is equivalent to an increase of entropy. From this point of view, the air flow in a wind tunnel can be considered in the same manner as any compressible flow at constant energy but with entropy increase. In order to characterize such an entropy increase for aerodynamic purposes it is convenient to use the ratio of the total pressures p_o' / p_o after and before the losses occur, as done in case of compression shocks by A. Busemann (Ref. 6, Par. 27, page 437). The total pressure ratio was widely used also by W. Tollmien (Ref. 7) and called "Drosselfaktor" K (throttling factor). It is connected with the entropy increase from s_o to s_o' by the equation

$$K = \frac{p_o'}{p_o} = e^{-\frac{s_o' - s_o}{R}}$$

The use of total pressure ratio is therefore equivalent to the determination of the entropy increase; however, no energy consideration is involved.

Defining the diffuser efficiency η_D we compare the total pressure ratio of the diffuser K_D with the total pressure ratio of a normal shock K_{NS} at the test section Mach Number

$$\eta_D = \frac{K_D}{K_{NS}} = \left(\frac{p_o'}{p_o}\right)_{DIFFUSER} : \left(\frac{p_o'}{p_o}\right)_{NORMAL\ SHOCK}$$

We call this coefficient of total pressure ratios for the purpose of briefness "diffuser efficiency", even though it is not a ratio of energies and its value can be smaller or larger than one. (For subsonic test section velocities the denominator is taken as unity).

The order of magnitude of the η_D values actually obtained will show the convenience of this definition, especially in the range of high Mach Numbers. This is valid for wind tunnel diffusers after free jet or closed test section as well as for ramjet diffusers. Moreover, this efficiency definition is suggested in the case of the free jet wind tunnel diffuser by the results of the following analysis. They show that the flow process in the diffuser, while not that of a normal shock does have some similarity to a normal shock. Besides, there exists a finite non-vanishing limiting value of η_D for Mach No. infinity, which is approached very well already from Mach Nos. 3 or 5 upwards. None of the other definitions mentioned above offer the same advantage. This definition has been used before by

the author and his associates at Peenemuende and Kochel, Germany, since 1942 for wind tunnel design purpose without knowledge of the subsequent calculations.

Section 2 - Establishing the Fundamental Equations

A. The Spreading of the Jet and the Transformation Zone in the Diffuser

The airstream emerges from the exit cross section F_1 of the Laval nozzle (See Fig. 1) with supersonic velocity w_1 as a free jet surrounded by the air in the test chamber which is supposed to be at rest in a greater distance from the jet. The length l of the free jet depends upon various test requirements and is conventionally between approximately one and two times the height H of the Laval nozzle exit. The free jet spreads out, increasing its area, due to a turbulent mixing process at its surface, resulting in wedge shaped turbulent mixing zones. This process has been analyzed for incompressible flow by W. Tollmien (Ref. 8) and A. Kuethe (Ref. 9) using the concept of the turbulent mixing length of L. Prandtl and recently by H. W. Liepmann and J. Laufer (Ref. 10) with detailed results on the turbulent structure in accordance with von Karman's (Ref. 11) concept. To obtain any pressure recovery the free jet has to be brought into the diffuser. This requires a "recapture" of the free jet in the intake F_2 of the diffuser. Here the free jet, with a given pressure as the boundary condition, is transformed into a flow between rigid walls with a given direction of velocity as determined by the walls. We assume that in this region a complete transfer of all values of state occurs which results in constant velocity, pressure and density all over the cross section. Furthermore, we assume that this transformation takes place in the intake portion of the diffuser with constant or nearly constant cross sectional area, corresponding to a slender diffuser design as used in many free jet supersonic tunnels, i.e., in Goettingen, Aachen, Peenemuende, and Kochel (See Sec. 6, D).

The spreading of the free jet requires that the intake cross section of the diffuser F_2 should be larger than the Laval nozzle exit cross section F_1. This is a conventional arrangement in all free jet wind tunnel designs. (See Fig. 18 and Sec. 6, A). Often, the entrance cross section of the diffuser is equipped with a bell-mouth, a knife edge, or another differently shaped pick-up. Such a device is, of course, important to the separation of the induced air from the nozzle air. Its interaction with the mixing zone and the determination of the minimum area F_2, which is required for a smooth recapturing process can be analyzed but need not be discussed in the present report. Here F_2 is one of the given boundaries.

B. Test Chamber Pressure

In case of a jet with supersonic velocity, the test chamber pressure p_c is in general not equal to the pressure p_1 in the nozzle exit, $p_c \neq p_1$. Only a specific opening of the second throat will produce pressure equilibrium $p_c = p_1$,

corresponding to a parallel jet in the core inside of the turbulent mixing zones. Larger second throat areas result in $p_c < p_1$, smaller ones in $p_c > p_1$. Test chamber pressure $p_c > p_1$ can be operated but, limited by the requirement that only oblique shocks occur at the nozzle exit, results in a reduced size of test rhombus with parallel flow. If p_c is so large that a normal shock occurs, no supersonic jet can be maintained. In case of a subsonic jet pressure equilibrium $p_c = p_1$ is established automatically, and the second throat area determines the velocity in the test section.

The present analysis is made for the special case of pressure equilibrium. A solution for the case of pressure non-equilibrium is given in another report (Ref. 26). It clarifies the exact mechanism of test chamber pressure control by means of an adjustable diffuser throat and gives a quantitative explanation of a slow starting process of the tunnel.

C. Assumptions and Fundamental Equations

We consider the flow as one-dimensional and steady and use the theorem of momentum for the axial momentum flux over a rectangular shaped bounding surface which extends from the nozzle exit to the end of the transformation zone and has a constant cross section F_2. The great advantage of such application of the momentum theorem is that the internal processes, such as mixing at the jet surface, recapturing and transformation in the diffuser intake section, need not be known in detail. The final state w_2, p_2, ϱ_2 in F_2 after completion of the transformation can be calculated by the initial state

w_1 ; p_1 ; ϱ_1 in F_1 and the amount of the boundaries F_1 and F_2. Evidently the whole transformation process is irreversible and is connected with an entropy increase which will eventually be determined by the calculation.

The following detailed assumptions and simplifications are made:

1. Steady one-dimensional flow parallel to the axis is assumed. This simplification is more valid when slender diffusers without sudden variation in cross section are considered. Especially the intake portion of the diffuser must be long enough to guarantee a complete transformation process (Sec. 2, A).

2. Air tight test chamber and chamber pressure constant with time are assumed. The air induced by the jet out of the test chamber must be separated and returned to the test chamber, before the transformation process is completed. This results in equality of mass entering and leaving the bounded volume and thus, the continuity equation becomes

$$F_1 \varrho_1 w_1 = F_2 \varrho_2 w_2 \qquad (1a)$$

The assumption of an air tight test chamber is of greater importance than might be realized. Calculations show that relatively small inleakage of air into the test section can produce quite a different flow process.

3. The flux of axial momentum through the bounding surfaces parallel to the axis and through the surface normal to the axis in the upstream section outside F_1 is neglected, because the components of the induced velocities are small compared with w_1. Thus, $F_1 \rho_1 w_1^2$ is the momentum entering and $F_2 \rho_2 w_2^2$ the momentum leaving the volume within the bounding surface. This is valid for a test chamber of reasonable size which allows the turbulent mixing zones to develop in a similar manner as it is known for jets in indefinite medium. Very small size of the test chamber might produce additional induced velocities.

4. The static pressure in the test chamber p_c is assumed to be constant along the bounding surface normal to the axis in the upstream cross section outside F_1, which is identical with neglecting the dynamic pressure of the induced velocities. (See Par. 3). Hence, the forces acting at the upstream cross section are $F_1 p_1 + (F_2 - F_1) p_c$ while the forces acting at the downstream cross section are $F_2 p_2$

5. The friction along the rigid walls inside the diffuser and the turbulent shearing stresses along the bounding surface outside the diffuser are neglected. Therefore, no other forces than pressure forces according to paragraph 4 enter the momentum equation. This equation states that the increase in momentum of the gas per unit time equals the net force acting on the gas in the same direction, and therefore becomes:

$$F_2 \rho_2 w_2^2 - F_1 \rho_1 w_1^2 = F_1 p_1 + (F_2 - F_1) p_c - F_2 p_2 \qquad (1b)$$

It is valid for the general case of pressure non-equilibrium. A more detailed investigation concerning the effect of the turbulent shearing stresses along the jet surface on the momentum equation (1b) and the energy equation (1c) shows that the assumptions made in Par. 5 and 6 hold much better than might be anticipated.

6. The wind tunnel walls are assumed to be insulated, so that no heat is transmitted out of the interior. No exterior work is performed by the gas even if the work of the turbulent shearing stresses along the jet surface on the chamber air is taken into account. In case of an airtight test chamber the air within belongs to the system because it is in permanent energy exchange with the stream emerging from the nozzle. Hence the total energy (kinetic energy plus enthalpy) entering the bounded volume must equal the outgoing total energy, even though dissipation is present. Thus, the energy equation gives

$$\frac{w_1^2}{2} + c_p T_1 = \frac{w_2^2}{2} + c_p T_2 = c_p T_o$$

where $c_p T_o$ is the enthalpy of the air at rest before entering the tunnel.

Using the equation of state: $\frac{p}{\varrho} = RT$

this is transformed into

$$\frac{w_1^2}{2} + \frac{\gamma}{\gamma-1}\frac{p_1}{\varrho_1} = \frac{w_2^2}{2} + \frac{\gamma}{\gamma-1}\frac{p_2}{\varrho_2} \qquad (1c)$$

Thus, we have a set of 3 independent equations (1a, 1b, 1c) for the solution of the three unknown variables w_2 p_2 ϱ_2 ; if the variables w_1 p_1 ϱ_1 ; the test chamber pressure p_c and the boundary areas F_1 and F_2 are given. The system of equations (1a, 1b, 1c) obtained under the given assumptions for the free jet diffuser process is obviously identical with that of a compressible pipe flow with sudden increase in cross section (See for instance - A. Busemann, Ref. 6, page 403). However, no detailed solution and discussion in relation to the free jet wind tunnel diffuser problem as analyzed here is--to the author's knowledge--given elsewhere. The losses connected with the pipe flow are sometimes called "Carnot impact or shock loss", although "impact" does not enter into this problem and the term "shock" has no relation to the compression shock waves at supersonic flow.

Section 3 - Solution of the System of Equations

In case of pressure equilibrium in the test chamber $p_c = p_1$, the system of the continuity equation (1a) and momentum equation (1b) becomes:

$$\left.\begin{aligned} F_1 \cdot w_1 \cdot \varrho_1 &= F_2 \cdot w_2 \cdot \varrho_2 \\ F_2 \varrho_2 w_2^2 - F_1 \varrho_1 w_1^2 &= F_2 (p_1 - p_2) \end{aligned}\right\} \qquad (2)$$

Combining both equations gives

$$F_1 w_1 \varrho_1 (w_2 - w_1) = F_2 (p_1 - p_2)$$

Using the abbreviation $\frac{F_1}{F_2} = f < 1$ one obtains

$$\left.\begin{aligned} \frac{p_1 - p_2}{w_2 - w_1} &= f \cdot w_1 \cdot \varrho_1 \\ \frac{w_2 \varrho_2}{w_1 \varrho_1} &= f \end{aligned}\right\} \qquad (2a)$$

We introduce the following dimensionless values for velocity, pressure, and mass flow:*

$$\frac{w}{a^*} = M \; ; \quad \frac{p}{p_0} = P \; ; \quad \frac{w\varrho}{a^* \varrho^*} = \Theta \qquad (2b)$$

and using

$$\frac{a^{*2}\varrho^*}{p_0} = \gamma \left(\frac{2}{\gamma+1}\right)^{\frac{\gamma}{\gamma-1}}$$

*Footnote: Distinguish $M = \frac{w}{a^*}$ and $Ma = \frac{w}{a}$ Mach No.; sometimes M is used to denote Mach No.

we obtain the relations

$$\left.\begin{aligned} \frac{P_2 - P_1}{M_1 - M_2} &= \gamma \left(\frac{2}{\gamma+1}\right)^{\frac{\gamma}{\gamma-1}} \cdot f \cdot \Theta_1 \\ \Theta_2 &= f \cdot \Theta_1 \end{aligned}\right\} \qquad (3)$$

System (3) plus the energy theorem (1c) converted into the same dimensionless values determines the three unknown variables M_2; P_2; Θ_2 if f and M_1; P_1; Θ_1 are given.

The initial state M_1 P_1 Θ_1 has the stagnation pressure p_0 and the initial entropy s_1. The final state M_2 P_2 Θ_2 has the stagnation pressure p_0' and the final entropy s_2. We introduce the ratio K of the total pressures before and after the losses occur

$$K = \frac{p_0'}{p_0} \qquad (4a)$$

which is connected with the entropy increase by the equation

$$\frac{s_2 - s_1}{R} = -\ln K \qquad (4b)$$

Then we express P and Θ as functions of M at constant entropy s_1 by application of the energy equation (1c) for isentropic processes:

$$\left.\begin{aligned} P(M; s_1) &= \left[1 - \frac{\gamma-1}{\gamma+1} M^2\right]^{\frac{\gamma}{\gamma-1}} \\ \Theta(M; s_1) &= \left[\frac{\gamma+1}{2}\right]^{\frac{1}{\gamma-1}} \cdot M \left[1 - \frac{\gamma-1}{\gamma+1} M^2\right]^{\frac{1}{\gamma-1}} \end{aligned}\right\} \qquad (5)$$

To obtain P and Θ as functions of M for another constant entropy s_2, the right hand side of the equations (5) have to be multiplied by the total pressure ratio K. Or in other words: Pressure and mass flow for different entropy are, at any velocity, proportional to the respective stagnation pressures. For this reason and with the use of P and Θ as function symbols, the values in equation (3) may be written

$$\left.\begin{aligned} P_1 &= P(M_1; s_1) \quad \left\{ \begin{aligned} P_2 &= P(M_2; s_2) = K \cdot P(M_2; s_1) \\ \Theta_2 &= \Theta(M_2; s_2) = K \cdot \Theta(M_2; s_1) \end{aligned}\right. \\ \Theta_1 &= \Theta(M_1; s_1) \end{aligned}\right\} \qquad (5a)$$

Equation (3) with (5a) becomes

$$\left.\begin{aligned} \frac{K \cdot P(M_2; s_1) - P(M_1; s_1)}{M_1 - M_2} &= \gamma \left(\frac{2}{\gamma+1}\right)^{\frac{\gamma}{\gamma-1}} \cdot f \cdot \Theta(M_1; s_1) \\ K \cdot \Theta(M_2; s_1) &= f \cdot \Theta(M_1; s_1) \end{aligned}\right\} \qquad (6)$$

This system (6) of two equations determines the two unknown variables M_2 and K, if M_1 and f are given.

Elimination of K and ommission of the parameter s_1 finally results in one equation for the one unknown M_2:

$$f\cdot\frac{P(M_2)}{\Theta(M_2)} - \frac{P(M_1)}{\Theta(M_1)} = \gamma\left(\frac{2}{\gamma+1}\right)^{\frac{\gamma}{\gamma-1}}\cdot f\cdot(M_1-M_2) \qquad (7)$$

Equations (5) give by dividing each other

$$\frac{P}{\Theta}(M) = \left(\frac{2}{\gamma+1}\right)^{\frac{1}{\gamma-1}}\cdot M^{-1}\left[1-\frac{\gamma-1}{\gamma+1}M^2\right] \qquad (8)$$

This ratio of dimensionless pressure and mass flow is independent of any special entropy value. The transcendental equation (7) is reduced by means of (8) to a quadratic equation in M_2:

$$f\left(\frac{2}{\gamma+1}\right)^{\frac{1}{\gamma-1}}\cdot\frac{1}{M_2}\left(1-\frac{\gamma-1}{\gamma+1}M_2^2\right)-\left(\frac{2}{\gamma+1}\right)^{\frac{1}{\gamma-1}}\cdot\frac{1}{M_1}\left(1-\frac{\gamma-1}{\gamma+1}M_1^2\right)=\gamma\left(\frac{2}{\gamma+1}\right)^{\frac{\gamma}{\gamma-1}}\cdot f(M_1-M_2)$$

This is simplified finally by some algebraic transformations to:

$$\frac{1}{M_2}+M_2 = \frac{1}{f}\frac{1}{M_1}+\left(\frac{2\gamma}{\gamma+1}-\frac{1}{f}\frac{\gamma-1}{\gamma+1}\right)M_1 \qquad (9)$$

or

$$M_2^2-\left[\frac{1}{f}\frac{1}{M_1}+\left(\frac{2\gamma}{\gamma+1}-\frac{1}{f}\frac{\gamma-1}{\gamma+1}\right)M_1\right]M_2+1=0 \qquad (9a)$$

The two solutions of this quadratic equation are designated by $M_{2\alpha}$ (+sign) and $M_{2\beta}$ (−sign)

$$M_{\substack{2\alpha\\2\beta}} = \frac{\left(\frac{2\gamma}{\gamma+1}-\frac{1}{f}\frac{\gamma-1}{\gamma+1}\right)M_1^2+\frac{1}{f}}{2M_1} \pm \sqrt{\left\{\frac{\left(\frac{2\gamma}{\gamma+1}-\frac{1}{f}\frac{\gamma-1}{\gamma+1}\right)M_1^2+\frac{1}{f}}{2M_1}\right\}^2-1} \qquad (10)$$

Hence, the final ~~states~~ velocities $M_{\substack{2\alpha\\2\beta}}$ can be calculated by (10), if the initial ~~state~~ velocity M_1 is given. It follows from (9a), that

$$M_{2\alpha}\cdot M_{2\beta} = 1 \qquad (11)$$

where $M_{2\alpha}>1$ and $M_{2\beta}<1$

Hence, it should be emphasized, that our problem has one supersonic solution $M_{2\alpha}$ and one subsonic solution $M_{2\beta}$. Their velocities are connected in the same way as the velocities before and behind the normal shock. It is demonstrated later (See Sec. 4, A2) that the

thermodynamic states (M_2 ; P_2) also of both solutions are interconnected by a normal shock.

It must be investigated carefully whether one or both solutions actually exist in accordance with the second law of thermodynamics by determination whether the entropy of the final state has not decreased compared with that of the initial state (See Sec. 4, C).

We determine now the second unknown of equation (6), the total pressure ratio K, which we designate from now on as K_D because it denotes the diffuser losses. According to the two solutions for M, we obtain two values of K_D

$$K_{D\alpha} = f\frac{\Theta(M_1;s_1)}{\Theta(M_{2\alpha};s_1)} \qquad \text{and} \qquad K_{D\beta} = f\frac{\Theta(M_1;s_1)}{\Theta(M_{2\beta};s_1)} \tag{12}$$

Now, the solution of the problem is completed. Equation (10) gives M_2, (12) gives K_D and (5a) with (5) determines P_2 and Θ_2

Thus, velocity, pressure, mass flow (and therefore density), and total pressure ratio of the final state are known. As the next step the diffuser efficiency will be calculated.

For this calculation we introduce by definition (See Sec. 1, C, 4) the diffuser efficiency as the total pressure ratio of the diffuser K_D compared with the total pressure ratio $K_{NS}(M_1)$ of a normal shock at the test section velocity M_1. As a result, it follows

$$\left.\begin{aligned} \eta_{D\alpha} &= \frac{K_{D\alpha}}{K_{NS}(M_1)} = f\,\frac{\Theta(M_1)}{\Theta(M_{2\alpha})\cdot K_{NS}(M_1)} \\ \eta_{D\beta} &= \frac{K_{D\beta}}{K_{NS}(M_1)} = f\,\frac{\Theta(M_1)}{\Theta(M_{2\beta})\cdot K_{NS}(M_1)} \end{aligned}\right\} \tag{13}$$

Equations (12) and (13) allow calculation of total pressure ratio and efficiency of the diffuser. For further discussion and numerical calculation of η_β, the introduction of a new function

$$\vartheta(M) = \frac{\Theta(M}{K_{NS}(M)} \tag{14}$$

defined in the supersonic range only is advantageous. It is the ratio of the narrowest downstream cross section, attainable after a normal shock at M has occurred, to the shock area. K_{NS} can be written as follows:

$$K_{NS}(M) = \left[M^{2\gamma}\,\frac{1-\frac{\gamma-1}{\gamma+1}M^2}{M^2-\frac{\gamma-1}{\gamma+1}} \right]^{\frac{1}{\gamma-1}}$$

With Θ according to (5), ϑ becomes

$$\vartheta(M) = \left(\frac{\gamma+1}{2}\right)^{\frac{1}{\gamma-1}} \cdot \frac{1}{M}\left(1-\frac{\gamma-1}{\gamma+1}\,\frac{1}{M^2}\right)^{\frac{1}{\gamma-1}} \qquad \text{valid for } 1 \le M \le M_{max} \tag{14a}$$

$$M_{max} = \sqrt{\frac{\gamma+1}{\gamma-1}}$$

Comparing both equations for Θ and ϑ , it is evident that the following condition is satisfied:

$$\left.\begin{aligned} \vartheta\left(\frac{1}{M_{SUBSONIC}}\right) &= \Theta\left(M_{SUBSONIC}\right) \\ \vartheta\left(M_{SUPERSONIC}\right) &= \Theta\left(\frac{1}{M_{SUPERSONIC}}\right) \end{aligned}\right\} \qquad (14b)$$

which can also be deduced from its physical significance. In addition to this behavior, ϑ has a non-vanishing limiting value, if the Mach number approaches infinity, which will be of importance for many future calculations.

$$\lim_{M \to M_{max}} \vartheta(M) = \left(\frac{\gamma-1}{\gamma+1}\right)^{\frac{1}{2}} \cdot \left(\frac{2\gamma}{\gamma+1}\right)^{\frac{1}{\gamma-1}} = 0.602645 \quad (\text{for } \gamma = 1.405) \qquad (14c)$$

The ϑ values decrease monotonically from 1 at Mach No. 1 to the limiting value (14c) at Mach No. infinity. The ϑ - function is represented in graphs 9, 10 or 11 by the curves for f = 1.

Comparing)11) and (14b) one obtains

$$\Theta(M_{2\beta}) = \vartheta(M_{2\alpha}) \text{ for } 1 \leq M_{2\alpha} \leq M_{max} \qquad (14d)$$

Equation (13) combined with (14) and (14d) results in:

$$\eta_{DB} = f \frac{\vartheta(M_1)}{\Theta(M_{2\beta})} \qquad (15a)$$

or

$$\eta_{DB} = f \frac{\vartheta(M_1)}{\vartheta(M_{2\alpha})} \qquad (15b)$$

Equation (15b) expresses the diffuser efficiency of the subsonic solution mathematically by the ϑ function at the supersonic velocity which physically does not exist (see later). However, this equation is very convenient for numerical calculations.

Section 4 - Discussion of the Solutions.

Survey

Complete numerical evaluation of the solution according to equations 10, 12, 5, 5a, 15a, 15b, 24, is represented in Fig. 2 to 8. They show final velocities $M_{2\alpha}$, $M_{2\beta}$ (Fig. 2), static pressure P_2 and total pressure ratio K_D (Fig. 3, 4), total pressure ratio K_D (Fig. 5), and diffuser efficiency η_D (Fig. 6, 7, 8) of the β-solution with initial velocity M_1 or initial Mach number Ma_1 and f as independent variables or parameters.

Fig. 2 represents the numerical evaluation of equations 10 and 12. It shows the final velocities $M_{2\alpha}$ and $M_{2\beta}$ as a function of initial velocity M_1 with parameter f. Also the total pressure ratio $K_{D\alpha}$, $K_{D\beta}$ is given as a function of M_1 and f. It is seen that for $f<1$ the velocities of the subsonic solution $M_{2\beta}<1$ are connected with the total pressure ratio $K_{D\beta}<1$ or even $\eta_{D\beta}<1$ (see also Fig. 5), while the velocities of the supersonic solution $M_{2\alpha}>1$ are connected with imaginary $K_{D\alpha}$ or with $K_{D\alpha}>1$. Because this latter means entropy decrease (equation 4b) of the final state, the supersonic (α) solution has no physical significance. However, before discussing this problem in detail (Part C), the following paragraphs (Parts A and B) deal first with the discussion from the mathematical point of view.

A. Velocity and Total Pressure Ratio of the α - and β -Solution.

1. Some Special Cases.

(a) In case of $f=1$, which is equivalent with free jet length zero, equation (9) is reduced to:

$$\frac{1}{M_2} + M_2 = \frac{1}{M_1} + M_1$$

For M_1 in the supersonic range, this gives:

$M_{2\alpha} = M_1$; $M_{2\beta} = \frac{1}{M_1}$ and according to (12) with (14b) and (14):

$$K_{D\alpha} = 1 \quad \text{and} \quad K_{D\beta} = \frac{\Theta(M_1)}{\Theta\left(\frac{1}{M_1}\right)} = \frac{\Theta(M_1)}{\vartheta_1(M_1)} = K_{NS}(M_1) \qquad (16a)$$

which means, we have either no change of state or a normal compression shock. For M_1 in the subsonic range, it results in:

$M_{2\alpha} = \frac{1}{M_1}$; $M_{2\beta} = M_1$ and correspondingly:

$$K_{D\alpha} = \frac{\Theta(M_1)}{\Theta\left(\frac{1}{M_1}\right)} = \frac{\vartheta\left(\frac{1}{M_1}\right)}{\Theta\left(\frac{1}{M_1}\right)} = \frac{1}{K_{NS}\left(\frac{1}{M_1}\right)} \quad \text{and } K_{D\beta} = 1 \qquad (16b)$$

This means we have either no change of state or a normal "rarefaction shock", (the opposite of a normal compression shock), which is connected with $K_{D\alpha} > 1$. In Fig. 2, the curves for f=1 form the exterior boundaries of a lower and upper realm, which contain the subsonic and supersonic solution.

(b) To study the case of f=0, which corresponds to a jet discharging in an infinitely large reservoir, we first multiply equation (9a) with f and then take f=0, which yields a linear equation

$$\left(\frac{1}{M_1} - \frac{\gamma-1}{\gamma+1} M_1\right) M_2 = 0$$

Assuming $M_1 < M_{max}$, the expression within parentheses does not vanish and we obtain

$$M_{2\beta} = 0 \qquad (17a)$$

while the supersonic solution evidently is indeterminate (see Fig. 2). $M_1 = M_{max}$ gives no determinate value for $M_{2\beta}$. For determining $K_{2\beta}$, equation (12) fails, but equation (6) gives

$$K_{D\beta} \cdot P(M_{2\beta}; s_1) - P(M_1; s_1) = 0$$

Because $P(M_{2\beta}; s_1) = 1$, it follows

$$K_{D\beta} = P(M_1; s_1) \quad \text{and} \quad \eta_{D\beta} = \frac{P(M_1; s_1)}{K_{NS}(M_1)} \qquad (17b)(17c)$$

Discharge of a free jet in an infinitely large reservoir gives the total pressure equal to the static pressure of the jet, a result well known for incompressible fluids.

(c) In case of $Ma_1 = \infty$, we have to assume f≠0 and insert in equ (10) $M_1 = M_{max} = \sqrt{\frac{\gamma+1}{\gamma-1}}$, which gives (see Fig 2)

$$M_{2\alpha} = \sqrt{\frac{\gamma+1}{\gamma-1}} = M_{max} \text{ and } M_{2\beta} = \sqrt{\frac{\gamma-1}{\gamma+1}} = \frac{1}{M_{max}} \qquad (18a)$$

The total pressure ratio is given by equ (12):

$$K_{D\beta} = 0 \qquad (18b),$$

while $K_{D\alpha}$ is indeterminate. The diffuser efficiency $\eta_{D\beta}$ is indeterminate by equ (13), but can be calculated from equ (15b), which gives the limit:

$$\eta_{D\beta} = f \frac{\mathfrak{N}(M_{max})}{\mathfrak{N}(M_{max})} \quad \text{or} \quad \lim_{Ma_1 \to \infty} \eta_{D\beta} = f \qquad (18c)$$

This result, as important as it is simple, shows the convenience of using our definition of the diffuser efficiency. The advantage in practical application for higher Mach numbers lies in the fact that $\eta_{D\beta}$ for Mach numbers above 3 and for f values > 0.6 used in conventional wind tunnel design, differs only 5% or less from its limiting value f (see Fig. 6). Evidently (see Fig. 8) equ (18c) is valid for f=0, too. Nevertheless,

the point $Ma_1 = \infty$, f=0 is singular, as seen in the discussion of $\frac{d\eta}{df}$ (see Section 4, C, 1, equ (32)).

2. Relation between the α and β -Solution.

We investigate now the relation between the α- and β -solution. Equ (11) indicates that their velocities are interconnected in the same way as the velocities before and behind a normal shock. Considering the total pressure ratios $K_{D\alpha}$ and $K_{D\beta}$ according to (12), and assuming $M_{2\alpha} \leq M_{max}$ and using (14d) and (14), we obtain:

$$\frac{K_{D\beta}}{K_{D\alpha}} = \frac{\Theta(M_{2\alpha})}{\Theta(M_{2\beta})} = \frac{\Theta(M_{2\alpha})}{\vartheta(M_{2\alpha})} = K_{NS}(M_{2\alpha})$$

$$K_{D\alpha} \cdot K_{NS}(M_{2\alpha}) = K_{D\beta} \quad \text{or} \quad p'_{o\alpha} \cdot K_{NS}(M_{2\alpha}) = p'_{o\beta} \qquad \text{(19a), (19b).}$$

The total pressures of the α and β -solution are connected by the total pressure relation of a normal shock occurring at the velocity $M_{2\alpha}$. Equ (11) with (19b) demonstrate that the state of the supersonic solution is connected with the state of the subsonic solution by a normal compression shock occurring at the velocity of the supersonic solution. It should be emphasized that this statement deals with the relation between two possible final states. The relation between the initial and either one of the final states is not that of a normal shock (except for f=1), as shown in the following paragraph.

3. Relation between the Initial and Final Velocity.

In order to give a simplified representation, we exclude from this paragraph the three special cases dealt with in paragraph 1, namely f=1, f=0, $Ma_1 = \infty$. Then we may prove the following two statements (a) and (b):

(a) If $1 < M_1 < M_{max}$ then

$$\frac{1}{M_{2\alpha}} = M_{2\beta} < \frac{1}{M_1} < 1 < M_1 < M_{2\alpha} = \frac{1}{M_{2\beta}} \qquad \text{(20a)}$$

In other words: If the velocity (1) of the free jet is supersonic, then the velocity after the transformation process of the supersonic solution (2α) is greater than that of the free jet, while the velocity of the subsonic solution (2β) is less than that after a normal compression shock in the jet.

Equ (9) can be written for the solution $M_{2\alpha}$ as follows:

$$\frac{1}{M_{2\alpha}} + M_{2\alpha} = \frac{1}{f}\frac{1}{M_1} + \left(\frac{2\gamma}{\gamma+1} - \frac{1}{f}\frac{\gamma-1}{\gamma+1}\right) M_1$$

The right side is larger than $\frac{1}{M_1} + M_1$, as can be seen by transforming into

$$\left(\frac{1}{f} - 1\right)\frac{1}{M_1} + \left(\frac{2\gamma}{\gamma+1} - \frac{1}{f}\frac{\gamma-1}{\gamma+1} - 1\right) M_1 > 0$$

or $\left(\frac{1}{f} - 1\right) > \left(\frac{1}{f} - 1\right)\frac{\gamma-1}{\gamma+1} M_1^2$, which is true for $M_1 < M_{max}$.

Hence $\frac{1}{M_{2\alpha}} + M_{2\alpha} > \frac{1}{M_1} + M_1$ and because $\frac{1}{M} + M$ is a monotonically increasing function for $M > 1$, it follows $M_{2\alpha} > M_1$, and according to (11), $M_{2\beta} < \frac{1}{M_1}$, where $\frac{1}{M_1}$ is the velocity after a normal shock occurring at M_1.

(b) If $0 < M_1 < 1$, then

$$\frac{1}{M_{2\alpha}} = M_{2\beta} < M_1 < 1 < \frac{1}{M_1} < M_{2\alpha} = \frac{1}{M_{2\beta}} \qquad (20b).$$

In other words: If the velocity (1) of the free jet is subsonic, then the velocity after the transformation process of the subsonic solution (2β) is smaller than that of the free jet, while the velocity of the supersonic solution (2α) is greater than that which would be obtained after a normal "rarefaction shock" in the jet had occurred. The first part of the proof for the solution $M_{2\beta}$ is the same as for $M_{2\alpha}$ above. Hence $\frac{1}{M_{2\beta}} + M_{2\beta} > \frac{1}{M_1} + M_1$, but because $\frac{1}{M} + M$ is a monotonically decreasing function for $M < 1$, it follows $M_{2\beta} < M_1$ and with (11): $M_{2\alpha} > \frac{1}{M_1}$. Here $\frac{1}{M_1}$ is the supersonic velocity, from which the velocity M_1 would be attained by a normal compression shock. In a mathematical not physical sense we can say also, $\frac{1}{M_1}$ is the velocity after a normal "rarefaction shock" at the velocity M_1 had occurred.

B. Changes of State in the Pressure-Velocity Diagram.

1. Representation of the β -Solution.

Fig. 3 is a dimensionless pressure-velocity diagram and gives a representation of the final state ($M_{2\beta}$, $P_{2\beta}$), which belongs to each initial state (M_1, P_1). Each initial state lies on the upper isentropic line s_1 corresponding to a total pressure ratio K=1. As known, the isentropic lines for higher entropy $s_2 > s_1$ are affine to the upper one by being multiplied with $K < 1$, according to equ (5a). We designate them by the K-value which is identical with the dimensionless static pressure P at zero velocity (M=0). Only the subsonic (β) solution with physical significance is represented here, while the supersonic α -solution without physical existence is omitted. The graph contains the results of numerical evaluations of $M_{2\beta}$, $K_{p\beta}$ and of $P_{2\beta}$ out of equations (10), (12), and (5a) with (5).

All of the final states of the β -solution lie in a region which is bounded as follows: By the P-axis at the left-hand side; by the initial isentropic line from M=0 to M=1 at the upper right; by the well-known "normal shock polar" from M=1 to M= $\frac{1}{M_{max}}$ at the lower right; by the M-axis from M= $\frac{1}{M_{max}}$ to M=0 at the bottom.

The final states (M_2, P_2) are formed by the intersection of two families of curves, denoted by the parameter f and the initial Mach number Ma. The family of the parameter f ranges from f=0.6 to 0.1. The curve for

f=1 is identical with the above mentioned upper right border (see equ (16b)) and lower right border of the region (see equ (16a)), while the curve for f=0 is identical with the left border (17a), excluding the origin (f=0, $Ma_1 = \infty$). All f-curves start at one single point (M=0, P=1) and terminate (for f≠0) in one single point ($M = \frac{1}{M_{max}}$, P=0) according to equ (18a), (18b). The family of "initial Mach numbers" ranges in this graph from 0.2 to 4.5, in order to obtain clearness in representation, while evaluations for initial Mach numbers up to 10 or infinity are to be found in several of the following graphs of η_D (see Fig. 6, 8) and other wind tunnel characteristics. The curves for "initial Mach numbers" start for $Ma_1 \leqslant 1$ at the upper isentropic line on their corresponding isentropic values (16b); for $Ma_1 \geqslant 1$ they start at the normal shock polar on their corresponding values of a normal shock (16a). The case when f approaches one, which means a vanishing ~~short~~ jet length, is therefore identical with no change of state for $Ma_1 \leqslant 1$ and with a normal shock for $Ma_1 > 1$. The Ma_1-curves terminate at the P-axis (equ (17a) in points with pressure equal to the initial static pressure, $P_2 = P_1$ (equ 17b).

2. Graphical Solution.

The pressure velocity diagram offers a possibility of graphical determination of the solution, which is a generalized version of the well-known method for a normal shock process. Due to the fact that $\left(-\frac{\partial p}{\partial w}\right)_{s=const.} = w\varrho$, the conservation of mass and momentum can be represented by simple graphical processes. The state after a normal shock can be found by constructing the tangent to the initial isentropic line at the point of initial supersonic velocity and determining the second point of contact of the same straight line to another isentropic line in the subsonic range.

In our diagram of dimensionless coordinates, the tangential relation can be obtained by equ (5):

$$\left(-\frac{\partial P}{\partial M}\right)_{S=const.} = \gamma\left(\frac{2}{\gamma+1}\right)^{\frac{\gamma}{\gamma-1}} \cdot \Theta \qquad (21)$$

Our equation system (3) with f=1 describes the above mentioned graphical solution for a normal shock. The final state lies on the normal shock polar with $K=K_{NS}(M_1)$.

In case of f≠1, the equations (3) state that the tangent to the isentropic line s_1 at the point of initial state (M_1, P_1) has to be rotated counterclockwise, until its slope is multiplied with $f < 1$, and then the point of contact of this rotated straight line to another isentropic line has to be constructed. This new point of contact is the final state (M_2, P_2). The designation of its isentropic line gives K_D. It can be seen from the graph that we find always a subsonic solution in the above described region of Fig 3 with $K_{D\beta} < 1$ or even $K_{D\beta} < K_{NS}(M_1)$.

Additionally, there are many (M_1, f) combinations where a second point of contact at the right-hand side of (M_1P_1) in the supersonic range can be found which lies on an isentropic above the initial isentropic line. This means $K_{p\alpha} > 1$. In many other (M_1, f) combinations, which give $M_{2\alpha} > M_{max}$ (see Fig 2), no graphical representation of the α -solution is possible, because the respective pressure is imaginary (non-existent gas).

3. Approximation for Incompressible Flow.

Figures 2, 5, 6, 7, 8 show that the β -solution is steady throughout when the initial jet velocity decreases from the supersonic range through the sonic speed down to subsonic velocities and finally approaches the incompressible region. It seems desirable to compare the evaluation of the general compressible equations in the incompressible region with more simple formulas which describe the incompressible transformation process of a free jet, known as "sudden widening of a pipe".

The incompressible formulas can be obtained as follows: The continuity and momentum equ (2) become for $\varrho_2 = \varrho_1 = \varrho$

$$\frac{p_2 - p_1}{w_1 - w_2} = f \cdot w_1 \cdot \varrho \quad ; \qquad \frac{w_2}{w_1} = f \qquad (22a)(22b)$$

Elimination of w_2 gives:

$$p_2 - p_1 = w_1^2 \varrho \cdot f \cdot (1-f)$$

Introducing the total pressure of the initial state

$$p_o = p_1 + \frac{\varrho w_1^2}{2}$$ results in

$$p_2 = p_o - \frac{\varrho w_1^2}{2}\left(1 - 2f(1-f)\right) \qquad (23)$$

This equation together with (22b) presents the solution (w_2, p_2), if w_1, f and p_o, ϱ are given. If we prefer dimensionless values, we obtain, by neglecting terms of second order, the approximate solution:

$$\frac{p_2}{p_o} = 1 - \frac{\gamma}{2} Ma_1^2 \left\{1 - 2f(1-f)\right\} \quad \text{and} \quad M_2 = \sqrt{\frac{\gamma+1}{2}} \cdot f \cdot Ma_1 \qquad (24)$$

Denoting the total pressure of the final state with $p_o' = p_2 + \frac{\varrho w_2^2}{2}$ and eliminating w_2 and p_2 by means of (22b) and (23), we obtain the difference in total pressures:

$$p_o - p_o' = \frac{\varrho \cdot w_1^2}{2}(1-f)^2 \qquad (25)$$

For the total pressure ratio we obtain the incompressible approximation

$$K_p = \frac{p_o'}{p_o} = 1 - (1-f)^2 \frac{\gamma}{2} Ma_1^2 \quad \text{or} \quad K_p = 1 - (1-f)^2 \frac{\gamma}{\gamma+1} M_1^2 \qquad (26)$$

Evaluation of (26) and comparison with the exact values of (12) give for $Ma_1 = 0.2$ differences in K_p between 3×10^{-5} at $f = 0.8$ and 5×10^{-4} at $f = 0$.

Fig. 4 gives the enlarged upper left-hand corner of the pressure velocity diagram, showing the exact calculated compressible values for $Ma_1 = 0.2$ and 0.4 (same as in Fig. 3), compared with values for $Ma_1 = 0.1$, 0.2, 0.3, and 0.4, obtained by the incompressible approximate formula (24) above. The comparison is an excellent check for the results of the general compressible equations.

C. Proof that the Diffuser Efficiency of the β -Solution is Smaller than one and that the α -Solution has no Physical Existence.

1. Establishing the Equations for $\frac{dK}{df}$ and $\frac{d\eta}{df}$.

As already explained in the survey of this Section 4, it can be seen by numerical evaluation represented in Figs. 2, 5, 6, 7, and 8 that, assuming $f < 1$, K_α is either larger than one or is imaginary, while always $K_\beta < 1$ or even $\eta_\beta < 1$. This means that the α -solution has no physical significance. However, the subsonic β -solution exists physically and shows that the actual diffuser losses are larger than those of a normal shock at test section velocity. It seems desirable to prove these important results directly from the equations in addition to the numerical evaluations given.

The proof will be made using the fundamental equations (3), by proving first that $\frac{dK_\alpha}{df} > 1$ and $\frac{d\eta_\beta}{df} < 1$. Because the pressure and mass flow functions (equ 5) are transcendental and the latter cannot be written explicitly in the velocity M, a proof with these special functions is very inconvenient. Instead of that, a more general proof will be given, using a generalized form of isentropic curves in a pressure (y) versus velocity (x) diagram.

In the following only positive values of x and y are considered. The equation $y = K \cdot F(x)$ shall represent the family of isentropic lines denoted by the total pressure ratio K, with $F(0) = 1$. $F(x)$ shall be a monotonically decreasing function with steady first and second derivatives. $F'(x) = 0$ is allowed for $x = 0$ only, while the second derivative shall not vanish at any point. Hence, $F(x)$ can be concave or convex, but any inflection point is excluded. (x_1, y_1) is an arbitrarily chosen fixed point, from which a tangent with the slope m is drawn to one isentropic line out of its family, where (x_T, y_T) is the point of contact. We define m as positive for clockwise rotation of the tangent around (x_1, y_1), so that $m \geq 0$ covers all possible cases. (x_1, y_1) does not necessarily lie on the initial isentropic with $K = 1$. This is an important fact for later application when the test chamber pressure is not equal to the Laval nozzle exit pressure. Then the following equations are valid:

$$\frac{y_T - y_1}{x_1 - x_T} = m \quad ; \quad y_T = K \cdot F(x_T) \quad ; \quad -m = K \cdot F'(x_T) \qquad (27a, b, c)$$

Equation (27a) corresponds to (3a), (27b) to (5a), and (27c) corresponds to (3b) with (5a). We consider (x_1, y_1) as fixed and m as independent variable, while (x_T, y_T) and K are dependent variables. If we denote for simplification that $\frac{-d\,F(x)}{dx} = g(x)$ and $\tilde{g}$ as the inverse function of g, (27c) becomes $g(x_T) = \frac{m}{K}$ or $x_T = \tilde{g}\left(\frac{m}{K}\right)$; and (27b) gives $y_T = K \cdot F\left[\tilde{g}\left(\frac{m}{K}\right)\right]$.

Elimination of x_T and y_T in (27a) by means of the last two equations yields

$$\Phi(K;m) \equiv K \cdot F\left[\tilde{g}\left(\frac{m}{K}\right)\right] - y_1 - m x_1 + m\tilde{g}\left(\frac{m}{K}\right) = 0$$

Dividing with K and introducing $\mu = \frac{m}{K}$ and K as new variables with

$$\frac{\partial \mu}{\partial m} = \frac{1}{K} \quad \text{and} \quad \frac{\partial \mu}{\partial K} = -\frac{m}{K^2}$$

gives $G(\mu,K) = F\left[\tilde{g}(\mu)\right] - \frac{y_1}{K} - \mu x_1 + \mu \cdot \tilde{g}(\mu) = 0$. Now we obtain the derivative

$$\frac{dK}{dm} = -\frac{\left(\frac{\partial G}{\partial m}\right)_K}{\left(\frac{\partial G}{\partial K}\right)_m} = -\frac{\frac{1}{K}\left(\frac{\partial G}{\partial \mu}\right)_K}{-\frac{m}{K^2}\left(\frac{\partial G}{\partial \mu}\right)_K + \left(\frac{\partial G}{\partial K}\right)_\mu}$$

In determining $\left(\frac{\partial G}{\partial \mu}\right)_K = \frac{\partial F}{\partial \tilde{g}} \cdot \frac{d\tilde{g}}{d\mu} - x_1 + \mu \frac{\partial \tilde{g}}{\partial \mu} + \tilde{g}$

we have to consider that $\frac{\partial F}{\partial \tilde{g}} = \frac{dF}{dx} = -g(x_T)$

and $\mu = g(x_T)$, and that $\frac{\partial \tilde{g}}{\partial \mu}$ remains finite under the aforementioned assumptions. Hence, it becomes $\left(\frac{\partial G}{\partial \mu}\right)_K = \tilde{g} - x_1$.

Finally we obtain

$$\frac{dm}{dK} = \frac{m}{K}\left\{1 + \frac{\frac{1}{m} y_1}{x_1 - \tilde{g}\left(\frac{m}{K}\right)}\right\} = \frac{m}{K}\left\{1 + \frac{y_1}{m(x_1 - x_T)}\right\} \qquad (28a)$$

or $$\frac{dK}{dm} = \frac{K}{m}\left\{1 - \frac{y_1}{y_T}\right\} \quad (\text{only for } m \neq 0) \qquad (28b).$$

These equations show two different cases, namely

(a) if $x_1 > x_T$ or, what is equivalent, $y_1 < y_T$, then $\frac{dK}{dm} > 0$ (29a)

(b) if $x_1 < x_T$ or, what is equivalent, $y_1 > y_T$, then $\frac{dK}{dm} < 0$ (29b)

If we now insert the physical quantities of our case and consider that m is proportional to f according to (3), we obtain for f≠0

$$\frac{dK_D}{df} = \frac{K_D}{f}\left\{1 - \frac{P_1}{P_2}\right\} \quad \text{and} \quad \frac{d\eta_D}{df} = \frac{\eta_D}{f}\left\{1 - \frac{P_1}{P_2}\right\} \qquad (30a)(30b)$$

or with the special value of m according to (3) in (28a):

$$\frac{df}{d\eta} = \frac{f}{\eta}\left\{1 + \frac{P_1}{f \cdot \Theta_1 \cdot \gamma\left(\frac{2}{\gamma+1}\right)^{\frac{\gamma}{\gamma-1}}(M_1 - M_2)}\right\} \qquad (31).$$

Determining the limit of (31) for f approaching zero, we have to exclude $Ma_1 = \infty$ and may then use (17a) for M_2 and (17c) for P_1, which results in:

(Note: $M_1 < M_{max}$!) $$\lim_{f \to 0} \frac{d\eta}{df} = \gamma\left(\frac{2}{\gamma+1}\right)^{\frac{\gamma}{\gamma-1}} M_1 \cdot \vartheta(M_1) \qquad (32)$$

Taking simultaneously the limits of f=0 and $Ma_1 = \infty$, the quantity of $\frac{d\eta}{df}$ is indeterminate. It might be mentioned that, violating the assumptions which had to be made, (18c) would give for f=0 the value 1, while (32) would give for $Ma_1 = \infty$ the value 1.08828 (for $\gamma = 1.405$). Nevertheless, this behavior is without practical significance, as Fig. 8 shows.

2. Discussion of the Equations.

Investigating the sign of $\frac{dK}{df}$ or $\frac{d\eta}{df}$ we have to differentiate between the following cases for the α- and for the β -solution (f≠0):

(a) If M_1 is in the supersonic or in the subsonic region, we have for $f < 1$ always $M_1 > M_{2\beta}$ according to (20a) and (20b), which results according to (29a) in $\frac{dK_{D\beta}}{df} > 0$ and $\frac{d\eta_{D\beta}}{df} > 0$. Hence, for increasing f, $K_{D\beta}$ and $\eta_{D\beta}$ must increase, too. Because for f=1 we have $\eta_{D\beta} = 1$, according to equ (16a), (16b), it follows

$$\text{for } f < 1 \text{ becomes } \eta_{D\beta} < 1. \qquad (33)$$

(b) If M_1 is in the supersonic range and $f < 1$, but large enough to give a real α- solution with $M_{2\alpha} < M_{max}$ (see Fig. 2), we have according to (20a), $M_1 < M_{2\alpha}$, which results according to (29b) in $\frac{dK_{D\alpha}}{df} < 0$. Hence, for increasing f from values $f < 1$ to f=1, $K_{D\alpha}$ must decrease until $K_{D\alpha} = 1$ is reached for f=1 (equ (16a)) and it follows

$$\text{for } f < 1 \text{ becomes } K_{D\alpha} > 1 \qquad (34a)$$

The case of $M_{2\alpha} > M_{max}$ involves imaginary pressures and is of no physical interest.

(c) If M_1 is in the subsonic range, we also need to consider only solutions with $M_{2\alpha} < M_{max}$. In this case, it becomes $M_1 < M_{2\alpha}$ for $f < 1$ (according to 20b)) and also for f=1 (according to 16b)), which results in $\frac{dK}{df} < 0$ (according to 29b). Hence, with f decreasing from f=1, it follows that

K_α increases from its value $\frac{1}{K_{NS}} > 1$ for f=1 (see 16b)), which means

for $f \leqslant 1$ becomes $K_{D\alpha} > 1$. (34b)

Evidently, in both cases (b) and (c), if M_1 is fixed, K_D increases monotonically with decreasing f until $K_{D\alpha} = \infty$ is reached (see Fig. 2). Decreasing f further gives $M_{2\alpha} > M_{max}$, which results in imaginary pressure and imaginary total pressure ratio.

(d) Of interest may be the special case of $Ma_1 = \infty$, which involves the limit $\frac{p_i}{\Theta_i} = 0$ (see equ (8)) and therefore transforms equ (31) for f+0 into $\frac{df}{d\eta} = \frac{f}{\eta}$. Integration with the arbitrary constant chosen so that $\eta_{D\beta} = 1$ for f=1, results in $\eta_{D\beta} = f$ in accordance to (18c).

Equations (33) and (34a), (34b) prove the statements made in the beginning of this Section 3 C.

Now, we can differentiate between the three regions of solutions in the M_2 vs. M_1 diagram (Fig. 2), excluding f=1.

(a) $0 \leqslant M_{2\beta} < 1$ are solutions with physical existence, because their change of state is connected with entropy increase, due to $K_{D\beta} < 1$ or even $\eta_{D\beta} < 1$.

(b) $1 < M_{2\alpha} \leqslant M_{max}$ are solutions without physical existence, because they belong to a change of state with $K_{D\alpha} > 1$, or entropy decrease, violating the second theorem of thermodynamics. The final state itself, however, belongs to a gas with physical existence.

(c) $M_{max} < M_{2\alpha}$ are solutions without physical existence, because the final state belongs to a non-existent gas with imaginary pressure.

Therefore, only the subsonic solution has physical existence. Or, in other words: If the initial velocity in the jet is either subsonic or supersonic, the final velocity in the diffuser after completion of the transformation process is subsonic in all cases.

This careful study concerning the physical existence was necessary because it cannot be stated in advance that the supersonic solution will have no physical existence. For instance, we will see in another report (Ref. 26) that in certain cases where the test chamber pressure is not equal to nozzle exit pressure, the supersonic solution exists physically in addition to the subsonic one.

3. Conclusions: The Physical Nature of the Diffuser Process.

Concerning the diffuser flow process the following conclusions can now be drawn. The final velocity after the transformation is smaller than that attained after a normal shock (equ 20a). Equ (33) states that

the diffuser losses are always larger than those of a normal shock at jet velocity. Hence, the diffuser process is not that of a normal shock at jet velocity. Neither does it correspond to that of a normal shock at a higher velocity, to which the jet velocity is accelerated by isentropic expansion from F_1 to a larger area. This was once assumed by H. Ramm (Ref. 2 and 3) for the purpose of discussing his experimental data on the pressure distribution along the diffuser and proved by him to be false. In the pressure velocity diagram (Fig. 3) the final states lie definitely on one side of and not on the normal shock polar (Sec. 4, B, 1).

Neither is the process an addition of losses in the jet or on its surface followed by a normal shock, as often presumed for explanation of the low diffuser efficiency. If the second process is a normal shock, the state upstream of it can be only the α - solution (see Sec. 4, A, 2), which has $K_\alpha > 1$, or total pressure increase. Hence, instead of jet processes with total pressure losses, such ones with total pressure gain (entropy decrease) should precede a normal shock, which leads to the final state calculated here. This same conclusion is valid also for the assumption of any combination of oblique shocks followed by a normal shock.

Neither is the process an addition of a normal shock at jet velocity, followed by a recapture and transformation process of a free jet with subsonic velocities. Such process would lead to higher total pressure ratios, because $K_D(\frac{1}{M_1}) = \eta_D(\frac{1}{M_1}) > \eta_D(M_1)$ and to smaller velocities and higher static pressures, as can be seen in Fig. 3.

It seems useless to search for explanations of this diffuser flow process after a jet expansion by means of a normal shock. The process here investigated is a more general process between the areas F_1 and $F_2 > F_1$, from which the normal shock is only a special case for F_2 approaching F_1. The special case never can explain the general case.

Section 5. Calculation of Other Wind Tunnel Characteristics.

A. Dimensions of the Diffuser Throat and Test Chamber Pressure Control.

The dimension of the second throat has been always an important feature in the design of supersonic wind tunnels. The result obtained above (Sec. 4, C, 2), that the velocity in the diffuser entrance section is subsonic after completion of the transformation process is very important to the following discussion. Assuming a certain restriction of area in the central part of the diffuser and a pressure maintained below a certain limit downstream of the diffuser by compressors or other means (as a vacuum tank), it follows that the diffuser acts as a conventional Laval nozzle with accelerated flow throughout. Therefore, the diffuser has subsonic velocity in its convergent part, sonic velocity in the minimum area and supersonic velocity in its divergent part. Because the minimum area of the diffuser F*' acts as a second throat following the first throat F* of the Laval nozzle, its size is determined by F* and the total pressure losses in between. The equations of continuity and energy give:

$$\frac{F^*}{F^{*)}} = \frac{\varrho^{*)}}{\varrho^*} = \frac{p^{*)}}{p^*} = \frac{p_o'}{p_o} = K_D \qquad (35)$$

The total pressure ratio involved here is K_D according to (12), because the flow in the convergent section of the diffuser downstream of the transformation zone is an accelerated subsonic flow which, as known, has practically no losses.

Using $\frac{F^*}{F_1} = \textcircled{M}_1$ (see (2b)) and η_D according to (13), we transform (35) into

$$\frac{F^{*)}}{F_1} = \frac{\vartheta}{\eta_D} \text{ for } Ma_1>1 \text{ and } \qquad \frac{F^{*)}}{F_1} = \frac{\textcircled{M}}{\eta_D} \text{ for } Ma_1<1 \qquad (36)$$

$\textcircled{M}$ or ϑ are functions of M_1 according to (5) or (14); η_D is a function of f and M_1 according to (13) or (15a), (15b). Sometimes it is convenient to use another ratio, deduced from (36):

$$\frac{F^{*)}}{F_2} = f\,\frac{\vartheta}{\eta_D} \text{ for } Ma_1>1 \quad \text{and} \quad \frac{F^{*)}}{F_2} = f\,\frac{\textcircled{M}}{\eta_D} \text{ for } Ma_1<1 \qquad (37)$$

Fig. 9 shows equ (36) as a function of f and nozzle Mach No. from 0 to 5, inclusive of the limit for Mach No. infinity. Fig. 10 shows equ (36) as a function of f and nozzle velocity in the reduced scale, to enable representation of small f. Fig. 11 shows equ (37) as a function of f and nozzle Mach No. from 0 to 5. The limit for Mach No. infinity is the same for all f-values and is equal to the limit of ϑ (equ (14c). The curves for f=1 in Fig. 9, 10, 11 represent the ϑ -function, due to η_D =1.

If the f-value and Mach No. in the test section are given, only one specific dimension of the second throat is determined by the equation (36) to which quantity the adjustable diffuser throat has to conform, in order to fulfill the fundamental assumption made in this analysis, namely: Equilibrium between the pressure of test chamber and Laval nozzle exit. Analysis in another report (Ref. 26) of the case $p_c \neq p_1$ shows that in a certain range $p_c < p_1$ results also in a subsonic solution but with K_D smaller than for pressure equilibrium, while $p_c > p_1$ results in K_D larger than for equilibrium. This fact causes, according to (35), an F*' larger and smaller, respectively, than that for pressure equilibrium. Or, expressed the other way: Varying the adjustable diffuser throat, changes the test chamber pressure. One specific dimension of the throat according to (36) gives chamber pressure equilibrium with the nozzle exit pressure, while an enlarged throat gives smaller chamber pressure, and a reduced throat gives higher chamber pressure than the nozzle exit pressure. It may be emphasized here that the control of the test chamber pressure by means of the adjustable diffuser as outlined above is an exact result of a one-dimensional calculation without consideration of friction. No assumption of pressure transfer upstream through subsonic boundary layers is necessary, as is sometimes done.

Evidently all conditions discussed above are independent of the downstream pressure as long as it is below a certain limit, so that sonic velocity in the minimum cross section with maximum mass flow per unit area is just maintained. Therefore, pressure equilibrium in the test chamber equivalent to a parallel jet, which is very important for actual wind tunnel testing, is independent of fluctuating intake pressure at the blowers for continuous operating tunnels. It is also independent of vacuum tank pressure increasing with time for intermittent suction type tunnels. To guarantee safe operation, actually an acceleration to a slightly supersonic flow is required at least for a short distance downstream of the second throat, with transition to final subsonic velocity by a normal compression shock at a low supersonic Mach No. with very little total pressure loss.

B. Volume Flow into Blowers.

The volume flow V_e per unit time into the blowers is an important characteristic in the power plant layout of supersonic wind tunnels. It can be calculated directly from the diffuser efficiency under the assumption that all additional losses occurring between second throat of the diffuser and the blower intake are negligible compared with the losses which have already occurred at the beginning of the diffuser. This is fairly valid for a reasonable subsonic diffuser and straight piping without corners or coolers for supersonic test section velocity, as measured in the Peenemuende wind tunnel (Ref. 3). Further, the intake velocity into the blowers is considered

to be so small that the static pressure and temperature can be replaced by their stagnation values p_e and T_e, with $\frac{p_e}{p_o} = K_D$.

In the following we make the special assumption that no intercooling shall be provided between test section and blowers. Hence the compressor inlet temperature is equal to the stagnation temperature of the air at the exit of the fixed diffuser and to that before entering the test section, or $T_e = T_o$. In case intercooling is provided, the formulas of paragraphs B, C, and D have to be changed accordingly.

The continuity of mass flow is expressed by

$$\varrho_e V_e = F^* \varrho^* a^*$$

which gives with

$$\frac{\varrho_e}{\varrho_o} = \frac{p_e}{p_o} = \eta_D \cdot K_{NS}$$

and with equation (14)

$$\left.\begin{aligned} \frac{V_e}{F_1} &= \frac{\varrho^*}{\varrho_o} \cdot a^* \frac{\vartheta}{\eta_D} \\ \text{or} \quad \frac{V_e}{F_1} &= \left(\frac{2}{\gamma+1}\right)^{\frac{\gamma+1}{2(\gamma-1)}} \frac{\vartheta}{\eta_D} \cdot a_o \end{aligned}\right\} \qquad (38a)$$

The velocity of sound a_o is taken at the stagnation temperature T_o. $\frac{\vartheta}{\eta_D}$ can be taken from Fig. 9 according to equ (36). The function ϑ in (38a) has to be replaced by Θ in case of subsonic velocities.

For numerical evaluation we choose $T_o = 293°$ K, and calculate a_o in (m/sec) by $a_o = 331.8\sqrt{\frac{T_o}{273}}$, which corresponds to V_e in (m^3/sec) and F_1 in (m^2). With $\gamma = 1.405$ the result is

$$\frac{V_e}{F_1}\left[\frac{m^3/sec}{m^2}\right] = 198.8 \cdot \frac{\vartheta}{\eta_D} \qquad (38b)$$

Figs. 12 and 13 are plots of (38b), as a function of Mach No. and with parameter f; Fig. 12 for Mach No. up to 5, Fig. 13 in a semi-logarithmic scale up to 8.5 with the limit for Mach No. infinity. For f-values of conventional wind tunnel design (f between 0.3 and 0.5), the V_e-curves above Ma=1 first show a slight increase with a maximum between Mach No. 1 and 2, whose location depends on the f-value, then a slight decrease and soon the curves approach the limit. The fact that V_e changes only slightly in the whole supersonic range is of great importance for engineering purposes in the layout of the blowers.

For instance, for f=0.64 we obtain the following $\frac{V_e}{F_1}$ -values:

at Ma=1: $\frac{V_e}{F_1} = 224 \frac{m^3/sec}{m^2}$; at Ma=1.1225: $\frac{V_e}{F_1} = 235 \frac{m^3/sec}{m^2}$ (maximum);

at Ma=∞: $\frac{V_e}{F_1} = 187 \frac{m^3/sec}{m^2}$

C. Energy Consumption of the Blowers

The energy consumption of the blowers can be calculated by the compression ratio of the blowers $\frac{P_o}{P_e} = \frac{1}{K_D}$, either for adiabatic or isothermic compression. As long as one blower unit may be with several internal stages, can be used (approximately up to Mach No. 2.5), the adiabatic compression is applicable. If for higher Mach numbers two or more blower units in series have to be applied, intercooling is necessary. Hereby the compression process approaches more nearly an isothermic compression as a greater number of external compressor stages are installed.

We start from the well-known equation of compression work per unit mass for a complete cycle, with the same assumptions as in Section B (compressor inlet temperature $T_e = T_o$)

$$W_{is} = R \cdot T_o \cdot \ln \frac{P_o}{P_e} \qquad \text{and} \quad W_{ad} = \frac{\gamma}{\gamma-1} R \cdot T_o \left[\left(\frac{P_o}{P_e} \right)^{\frac{\gamma-1}{\gamma}} - 1 \right]$$

We multiply by the factor of mass flow per unit time and unit nozzle exit area, $\frac{V_e \varrho_e}{F_1}$ and obtain the compression energy per unit nozzle exit area,

$$\frac{L_{is}}{F_1} = \left(\frac{2}{\gamma+1} \right)^{\frac{\gamma+1}{2(\gamma-1)}} \cdot a_o \cdot p_o \cdot \Theta \cdot \ln \frac{P_o}{P_e} \qquad (39a)$$

and L_{ad} correspondingly.

We choose the sound velocity a_o for the stagnation temperature $T_o = 293°K$ and the stagnation pressure $p_o = 1$ atm $= 10332 \frac{kg}{m^2}$ and we convert into international kilowatts by the relation 1 int KW = $102.00 \frac{m\,kg}{sec}$. We finally obtain the blower energy in int. KW per m^2, assuming 100% blower efficiency:

$$\frac{L_{is}}{F_1} \left[\frac{\text{int. KW}}{m^2} \right] = 20140 \, \Theta \cdot \ln \frac{1}{K_D} \quad \text{and} \quad \frac{L_{ad}}{F_1} = 20140 \frac{\gamma}{\gamma-1} \cdot \Theta \left[\left(\frac{1}{K_D} \right)^{\frac{\gamma-1}{\gamma}} - 1 \right] \qquad (39b)$$

Fig. 14 shows equ (39b) as a function of Mach number with f as the parameter. For incompressible flow (Mach number approaching zero), isothermic and adiabatic energy are identical. Fig. 15 shows the curves for f=0.64 in enlarged scale. For conventional wind tunnel design (f between 0.3 and 0.5) the energy curves have a peak between Mach No. 2 and 3. Fig. 14 shows also for the purpose of comparison the curve for the kinetic energy L_{Kin} in the test section for the same conditions. It might be noticed that for larger f at subsonic and small supersonic

Mach numbers L_{Kin} is larger than L_{is} or L_{ad}, but for higher supersonic Mach numbers the opposite is valid. The blower energy at no pressure recovery (f=0) is equal to the kinetic energy of the jet in the incompressible range only (see equ (42d)), while in the compressible range the blower energy is larger.

The kinetic energy L_{Kin} is calculated by $L_{kin} = \frac{1}{2} F^* \varrho^* a^* w^2$

which gives
$$\frac{L_{Kin}}{F_1} = \left(\frac{\gamma}{\gamma+1}\right)\left(\frac{2}{\gamma+1}\right)^{\frac{\gamma+1}{2(\gamma-1)}} \cdot a_o \cdot p_o \cdot \Theta \cdot M^2 \qquad (40a)$$

and with the same conditions for p_o, T_o as chosen above:
$$\frac{L_{kin}}{F_1}\left[\frac{int.KW}{m^2}\right] = \frac{\gamma}{\gamma+1} \cdot 20140 \cdot \Theta \cdot M^2 = 11770 \cdot \Theta \cdot M^2 \qquad (40b)$$

The last numerical factor is the kinetic energy for Mach No. 1. For $Ma = \sqrt{3}$ the maximum value $\frac{L_{kin}}{F_1} = 19520 \left[\frac{int.KW}{m^2}\right]$ is attained.

D. Energy Ratio

As explained before (Sec. 1, C, 3) the energy ratio depends on a specific but arbitrarily chosen compression and cooling process. We use the same assumptions regarding the cycle as outlined in Section 5, B. However, the values of these ratios are independent of the special choice of p_o, T_o. According to an isothermic or adiabatic compression process, we have to differentiate between the isothermic and adiabatic energy ratio. Considerable differences exist between those two terms in the higher supersonic range.

Dividing (40a) by (39a) we obtain the isothermic energy ratio
$$\zeta_{is} = \frac{L_{kin}}{L_{is}} = \frac{\gamma}{\gamma+1} \cdot \frac{M^2}{\ln \frac{1}{K_D}} \qquad (41a)$$

and the adiabatic energy ratio
$$\zeta_{ad} = \frac{L_{kin}}{L_{ad}} = \frac{\gamma-1}{\gamma+1} \cdot \frac{M^2}{\left[\left(\frac{1}{K_D}\right)^{\frac{\gamma-1}{\gamma}} - 1\right]} \qquad (41b)$$

Fig. 16 is a semi-logarithmic plot of equ (41a) and (41b) as a function of Mach number with parameter f up to Mach No. 10. There is no finite limit for Mach No. infinity. The energy ratio is infinite for f=1 in the whole subsonic range, because this corresponds to total pressure ratio 1 (equ (16b)) with no compression work needed. In the supersonic

range, however, f=1 represents the normal shock (equ (16a)) with finite losses and finite energy ratio. When f=0, which means no pressure recovery, we obtain $\zeta = 1$ for Mach number approaching zero, but $\zeta < 1$ at compressible flow. It can be seen that in the supersonic range the ζ -values decrease rapidly and finally all become less than one. For conventional wind tunnel design corresponding to f between 0.5 and 0.8, this happens between Mach number 3 and 5 for both the adiabatic and isothermic energy ratio.

It might be mentioned that Ackeret's definition of the energy efficiency of the diffuser (Sec. 1, C, 1) can be written as

$\eta_E = 1 - \frac{1}{\zeta_{ad}}$, hence becoming negative in a broad supersonic range where $\zeta_{ad} < 1$, even though pressure recovery is actually present $(f > 0)$. Therefore the value of this definition, given primarily for the compressible subsonic region, seems doubtful in the supersonic range.

In the subsonic range we must note that the transformation losses in the entrance of the diffuser, which are represented in Fig. 16, are becoming comparatively small and the losses in the subsonic diffuser itself and in the other parts of the circuit (corners, honeycomb) which are not included here, cannot be neglected as in the supersonic range. Therefore, experimental values of energy ratio, which include all such losses, must be considerably smaller than the calculated values in Fig. 16. The highest known energy ratio of an incompressible free jet wind tunnel is that of the California Institute of Technology in its former arrangement with a very short free jet length of $\frac{l}{H} = 0.8$. Clark Millikan (Ref. 12) reported an overall energy ratio of 3.6, referred to motor output, which will correspond to approximately $\zeta = 4.8$, referred to blower output. The calculated energy ratio based on the transformation losses of this short jet (f= approx. 0.80, Ma=0.23) is $\zeta = 24$, according to Fig. 16

In the case of incompressible flow, Ma→0, we have

$$L_{is} = L_{ad} = W(p_o - p_e) \qquad (42a)$$

and $L_{min} = \frac{1}{2} \rho_o W^3$ which gives (42b)

$$\zeta_{is} = \zeta_{ad} = \frac{\frac{1}{2} \rho_o W^2}{p_o - p_e} \qquad (42c)$$

Equation (42a) can be obtained also from (39b) as well as equation (42c) can be obtained from(41a) by a limiting process Ma → 0, considering that $\ln \frac{p_o}{p_e} \to \frac{p_o - p_e}{p_o}$. Using the difference in total pressures

expressed by f (equ (25)), the energy ratio (42c) for incompressible flow becomes finally

$$\zeta_{is} = \zeta_{ad} = \frac{1}{(1-f)^2} \qquad (42d)$$

Now, it will be analyzed how the needed blower energy depends upon the length of the free jet test section. For this purpose, Fig. 17 shows the reciprocal isothermic energy ratio $\frac{L_{is}}{L_{kin}}$ according to (41a) and (42d) as a function of the relative free jet length with the Mach No. as parameter varying between 0 and 10. In this graph, the parameter f used in all previous plots is eliminated and $\frac{l}{H}$ is substituted with the aid of equ (43), using for the expansion angle ε an experimental value of $\varepsilon = 0.061$ (see Sec. 6, A).

The subsonic curves start at zero energy for free jet length zero. For incompressible flow (Ma=0) the blower energy for small $\frac{l}{H}$ increases approximately parabolic, according to (42d) and (43). The supersonic curves start at a finite blower energy for free jet length zero to overcome the normal shock losses, and increase nearly linear with the jet length. Hence it follows that for subsonic and especially low speed wind tunnels, increasing the free jet length increases the required blower energy considerably. For supersonic velocities, however, and especially for high Mach numbers, increasing the free jet length increases the blower energy by only a relatively small amount. For instance, increasing the free jet length from 1 to 2 increases the blower energy at Ma=0 approximately 200%, at Ma=1 approximately 50%, at Ma=4.5 only 8%, and at Ma=10 only 3%. Reducing the length of free jet in order to keep the blower energy small is therefore important for subsonic wind tunnels only. In supersonic wind tunnels, especially for high Mach numbers, the length of the free jet need not be considered from the standpoint of saving power but can be chosen in favor of optimum testing conveniences.

Section 6. Discussion of Experimental Results

A. Experimental Values of Area Ratio f

As seen in the preceding sections, the area ratio f is the important parameter of all the theoretical calculations and discussions. Actually, it represents the boundaries of our one-dimensional problem, the nozzle exit and the diffuser intake cross section $\frac{A^{area}}{A^*}$. If f is given in a special case, the flow process through the diffuser and its efficiency can be calculated. Another problem is which f-value belongs to a certain relative length $\frac{l}{H}$ of the free jet. Or expressed more exactly: What diffuser intake area is necessary to produce a smooth recapture process of the jet of a given length at pressure equilibrium in the test chamber? The answer to this question shall be given in the present report purely experimentally and is represented in Fig. 18 as a plot of f vs $\frac{l}{H}$ from data used in different German free jet wind tunnels, which have been in successful operation and testing. In order to replace the relation between f and $\frac{l}{H}$ by one value, the expansion angle ε is introduced by the equation (see Fig. 1)

$$f = \frac{1}{(1 + 2\varepsilon\frac{l}{H})^2} \qquad (43)$$

This formula assumes similarity of the jet expansion in reference to the trailing edge of the Laval nozzle, as known by the two-dimensional analysis of the jet boundary by W. Tollmien (Ref. 8).

The following explanations are given for the data shown in Fig. 18. The Goettingen AVA supersonic free jet wind tunnel 11 cm x 13 cm was operated with model and bell mouth at an expansion angle $\varepsilon = 0.053$ by O. Walchner (Ref. 13). The Goettingen KWI supersonic wind tunnel 6 cm x 8 cm was equipped with recapturing knife edges. The test section was half closed - half open. Without model the expansion angle ε for the free jet boundaries was determined by K. Oswatitsch (Ref. 14) to $\varepsilon = 0.061$. For the purpose of comparison in Fig. 18 f is calculated with this ε-value from equation (43) for a completely free jet.

The Aachen AIA free jet supersonic wind tunnel 10 cm x 10 cm (Ref. 15) was operated by the author with model and bell mouth at an expansion angle of $\varepsilon = 0.061$. The Peenemuende, later Kochel, free jet supersonic wind tunnels I and II of 40 cm x 40 cm were designed by the author (Ref. 16) for long models with a free jet length of $l/H = 1.75$ and with a bell mouth of $\varepsilon = 0.071$. The Mach number range is 1 to 3.2 for the Goettingen and Aachen tunnels and up to 4.4 for the Peenemuende and Kochel tunnels. The fact that all data in Fig. 18 lies close together proves that ε is fairly independent of different variables such as bell mouth, knife edge, model, Reynolds number and Mach number. Even the experimental range of several low speed subsonic Goettingen tunnels with free jet with ε varying from 0.033 to 0.066 according to L. Prandtl (Ref. 17) is close to the supersonic data.

In addition to the test points, two curves are drawn in Fig. 18 according to equation (43) with the values of $\varepsilon = 0.061$ and $\varepsilon = 0.071$ which cover most of the supersonic data. A theoretical understanding of this experimental value of ε can be obtained with the aid of velocity distribution in the turbulent mixing zones. The curves can be used to determine f- values for free jet length l/H values other than those experimentally established. Because (43) is based on two dimensional flow, these curves in Fig. 18 will become gradually invalid for larger l/H values. They might be used up to approximately $l/H = 4$, according to the velocity distribution calculated by A. Keuthe (Ref. 9; its Fig. 9, 11). This also is approximately the region where the interior core of undisturbed velocity disappears according to experiments of P. Ruden (Ref. 18) and A. Kuethe (Ref. 9).

For conventional wind tunnel purpose a relative free jet length of 2 or 3 seems to be the upper limit. For the purpose of application of this theory to turbo-jet or ram-jet test stands, where sometimes longer jets are required, the curves might be extended with caution into the dotted regions. It shall be mentioned that the increase of ε from 0.061 in the Aachen design (1934) to 0.071 in the Peenemuende design (1937) was made by the author intentionally to overcome some difficulties in establishing pressure equilibrium at Mach number around 1.5 when large models were installed. In all other cases, the curve for $\varepsilon = 0.061$ can be used.

B. Pressure Distribution Measurements along the Diffuser

As explained before (Sec. 1, B) the present analysis was instigated by the results of the pressure distribution measurements along the diffuser of the Peenemuende wind tunnel by H. Ramm (Ref. 2) which now shall be compared with the theoretical results. The author himself designates in Part I these measurement results as "preliminary"; "the purpose of the investigation *** was chiefly the testing of small pressure gages;" "Since it was realized that measurement techniques were still far from perfect *** the results should be used only as a general survey."

Therefore, a quantitative agreement between theoretical and experimental results cannot be expected. However, quoting his major qualitative results will show an interesting and complete confirmation of our theoretical conclusions. We shall disregard all experimental results dealing with the so-called "throttling flap", and omit those concerning various test chamber pressures. In Ramm's recond report (Ref. 3), Sec. No. 4, Experimental Results, he says, "The figures (3, 4, 5 & 6) show the following characteristics valid for free jet wind tunnel: A pure subsonic flow in the diffuser never occurs at the test Mach numbers 1.22, 1.56, 1.86, and 2.50. Transition to a pure supersonic flow takes place only with a diffuser opening which is very large compared with the free jet cross section. In all other cases, the normal flow pattern shows a zone of losses in the first half of the "supersonic diffuser" characterized by a great pressure increase and a rapid change into a subsonic flow with an adjacent zone of increasing velocity. In the narrowest cross section of the diffuser, velocity of sound is attained the second time. Then a second expansion to supersonic velocity takes place."

The detailed discussion of his experimental results is condensed by Ramm in the following theorems:

"Theorem 1: In most cases the diffuser does not act as a device for pressure regain, but as a second Laval nozzle.

"Theorem 2: The ratio of the two narrowest cross sections of the diffuser and Laval nozzle determines the losses in the diffuser.

"Theorem 3: The transition from supersonic flow to subsonic flow in the "supersonic diffuser" does not occur by a simple normal compression shock.

"Theorem 5: In the supersonic diffuser, pressure losses take place which are greater than those of the normal shock wave at the Mach number of the nozzle. The losses in the adjacent subsonic diffuser are comparatively small."

Evidently, this summary of experimental results agrees very well with the important qualitative conclusions of the present theory.

Due to the restrictions concerning the accuracy of Ramm's tests a numerical comparison of the data in his Fig. 10 is not given in general. Only the diffuser efficiency calculated from the $p^{*)}$ values at pressure equilibrium and at Mach No. 1.22 and 1.56 are plotted in Fig. 20 (double circles); those at Mach No. 1.86 and 2.50 are omitted as much too low. The values of the diffuser efficiency calculated from the pressure ratio $\frac{p_e}{p_o}$ of the entire tunnel (see small table in his Fig. 10) show fair agreement with the more exact measurements at the same tunnel with mercury manometers (Fig. 20, Curve 7), but are omitted due to larger scattering. Values of F*' at pressure equilibrium from Fig. 10(Ref. 3) are not plotted in Fig. 19. They agree at Mach No. 1.22 with the other measurements at the same tunnel, but are between 7% and 15% larger at the other 3 Mach Nos.

C. Diffuser Throat Dimension Measurements

A comparison between measured and calculated diffuser throat dimensions (Fig. 19) gives a very reliable check of the theory, due to the following reasons:

1. The value of the diffuser throat depends inversely upon the value of the diffuser efficiency without any other experimental quantities involved. (Equ. 36).

2. The value of F*' according to (36) is connected with the sonic velocity in F*' and therefore is a direct consequence of the primary conclusion of the theory that subsonic velocities (β-solution) takes place in the beginning of the diffuser.

3. The value of F*' is independent of all losses which occur downstream, as in the divergent diffuser. However, those losses are included in η-values determined by the total pressure ratio of the entire tunnel. (See par. D, and Fig. 20).

4. The experimental determination of F*' is simple. It represents automatically an average across the area and does not involve complicated pressure measurements which are very sensitive to deviation of strictly one-dimensional flow.

5. The only disadvantage in using F*' is a possible falsification of its value by the boundary layer displacement thickness. Its value can be scarcely calculated because the initial thickness at the end of the transformation zone is unknown. Nevertheless, accelerated subsonic flow in the convergent part of the diffuser will keep it very thin as it is known from the converging part of the Laval nozzle.

Fig. 19 shows the theoretical curve of the diffuser throat for f = 0.64, according to Equ. (36), which is identical with the corresponding curve in Fig. 9. In addition, the experimental data of three different series are plotted from tests taken in the supersonic wind tunnels at Peenemuende and later at Kochel (Ref. 16). Test Section No. 1 and 2 had tunnels of the same size and the same diffuser area ratio f = 0.64 but belonged to different tunnels. The data not yet published are taken from test records and graphs in the hands of my former associate, H. U. Eckert, who carried out the last series in Feb. 1945. The subsonic values are taken from an average curve drawn through many test points. The subsonic Mach Nos. have been calculated from static pressure measurements in the axis of the nozzle by means of a long probe. The F*' values at Ma = 4.28 are those obtained after supersonic flow through the tunnel had been established. In order to start the tunnel approximately 10 - 20% larger F*' values were needed producing test chamber pressure smaller than the nozzle exit pressure. It might be mentioned that the second throat area is sensitive to inleakage. Sealing the tunnel was a difficult problem for Mach number 3 and higher. The test series above were carried out with glass windows. Other tests in February 1945 with the so-called steel windows, which had, as it was known, insufficient sealing, needed much higher F*' values (up to 50%) due to entrance of additional mass and increased transformation losses.

As a result, Fig. 19 represents an excellent quantitative confirmation of the theoretical calculations. The maximum deviations of the averaged test points from the theoretical curve are +4% and -7%.

D. Experimental Data of Total Pressure Ratio of the Entire Wind Tunnel.

There are test data available to the author concerning the total pressure ratio of several European supersonic wind tunnels. Assuming that the additional losses downstream of the diffuser throat are comparatively small as determined experimentally in the Peenemuende tunnel (see Sec. 6,B, Theorem 5), these data allow a third check of the theory, completely independent of those made in Par. B and C. of this section.

1. Peenemuende - later Kochel Wind Tunnel

The main proof in Fig. 20 is established by comparison of curve A with curve 7. Curve A represents the theoretical η_D - curve for f = 0.64 as shown before in Fig. 6. Curve 7 shows test data on the Peenemuende-Kochel free jet tunnel (Ref. 16) with 40 cm x 40 cm nozzle exit area and 50 cm x 50 cm diffuser intake area, corresponding to f = 0.64. The tests, not yet published, are carried out in tunnel No. 2 in Kochel by my former associate H.U. Eckert and recorded in Kochel Graph No. FL 666 from Mar 5, 1945. The following critical remarks should be made. Purpose of these tests was the furnishing of design data, and not checking of any theoretical calculations. The central arc shaped model support was installed. Due to the intermittent tunnel operation, the pressure readings (simple mercury manometers) for maximum efficiency were taken just before breakdown of the constant conditions in the test chamber, the time of which sometimes is not exactly defined. For Mach No. 4.3 the tunnel needed larger throat area for starting, producing pressure in the test chamber smaller than the nozzle exit pressure with higher losses. This throat area could be reduced during operation. It is uncertain if any final constant state could be reached during the short running time of about 16 seconds. The η_D - value plotted in curve 7 corresponds to this reduced area, while the η_D belonging to the first area would lie about 11% below. The η_D-values are sensitive to the exact test section Mach No. for which the K_{NS} is taken, therefore

average value in the tunnel axis over at least ± 20 cm was used for evaluation. Considering these remarks, the agreement between theory and experiment is good. The maximum deviation of the tests is about 8% below the calculated curve between Ma = 1 and 1.6. This can be explained by additional losses in the subsonic diffuser. The small positive deviation (2%) at Mach No. 4.3 is attributed to the aforementioned difficulties.

Fig. 21 and 22 give other comparisons between the same test results and the theory, using other variables and plotted up to Mach No. 10 in a semi-logarithmic scale. Fig. 21 shows the total pressure ratio, the test points taken for the entire tunnel $\frac{p_e}{p_o}$, while the curve is calculated from the diffuser theory $\frac{p_o'}{p_o}$. Fig. 22 is the reciprocal plot of Fig. 21, showing the compression ratio needed for the blowers if no additional losses occur. This representation is sometimes favored, for instance in the book by Liepmann & Puckett (Ref. 19) Fig. 5.16. The curve of this figure, going up to Mach No. 4.2 and designated "conservative values based on performance of several actual wind tunnels," is practically identical with the test values of the Kochel tunnel shown in Fig. 22. Fig. 21 and 22 show the great advantage for engineering purposes of having a diffuser theory extending up to high Mach number.

It might be mentioned that P. R. Owen (Ref. 20) in his careful and detailed summary on equipment and test results of the Kochel wind tunnel gives compression ratios $\frac{p_o}{p_e}$ in the range from Mach No. 0.4 to 4.38 (Part I, Table 8), which are too high throughout in the amount of 5 to 20%. Evidently he obtained misleading information.

It was the author's desire to prove the theoretical results in other free jet wind tunnel data than those from Peenemuende and Kochel but this is possible only with limitation. Data are available from the Goettingen AVA and the Aachen AIA free jet wind tunnel.

2. Goettingen AVA Wind Tunnel

The Goettingen AVA free jet intermittent type supersonic tunnel has a nozzle exit area 11 cm x 13 cm and a diffuser intake area of 13 cm x 15 cm; hence an area ratio of 0.73. Tests of total pressure ratio (see Fig. 20, Curve 2) were carried out by O. Walchner, but are reported by K. Oswatitch (Ref. 14).

The test results lie far below the theoretical curve for 0.73, which would lie somewhat above the curve A, if shown. However, the diffuser in this tunnel (Ref. 13) has a completely different shape from that generally used, and as assumed in this analysis (Fig. 1). It has only the convergent part of the conventional diffuser up to the minimum area and then expands abruptly to about twice that area. Thus, a kind of second free jet with sonic velocity emerges in a large pipe. Trying to calculate this process by a second application of the present formulas fails and does not explain the low diffuser efficiency. O. Walchner himself designates these data as "preliminary measurements in an incomplete war-time diffuser" (personal information to the author). The data themselves cannot be checked today. Dry air was used. K. Oswatitsch noticed this low pressure recovery also, but explained it as belonging to free jet wind tunnels in general, which obviously is an error.

3. Aachen AIA Wind Tunnel (10 cm x 10 cm)

The Aachen AIA free jet intermittent type supersonic tunnel has an exit area of 10 cm x 10 cm and a diffuser intake area of 11 cm x 13 cm, hence an area ratio of f = 0.70. Under the direction of C. Wieselsberger (Ref. 15) the author built and tested this tunnel from 1934 to 1937. Test records (from Nov. 29, 1936) concerning the total pressure ratio of the entire wind tunnel with model installed are in the possession of the author. The results, not yet published, are shown in Fig. 20 (Curve 6) and lie considerably below the theoretical curve for f = 0.70 (not shown). The difference can be explained by the fact that humid air was used. Hence, condensation shocks connected with total pressure loss and change in Mach number and velocity distribution will have occurred, all of which are functions of relative and absolute humidity, not yet quite known. The humidity conditions of these tests are likewise unknown. Recent evaluation of incomplete tests of that time by the author (Ref. 21) show that at so-called "medium humidity conditions" (approximately 40 to 50% relative humidity at Aachen) condensation shocks occurred with a total pressure ratio of approximately 0.90 at Ma = 1.42 and 0.80 at Ma = 2.28. The value of Ma = 3.15 could not be determined. Using these values for evaluation, the test data lie then in fair agreement and are only between 10% and 4% below the theoretical curve. However, this agreement cannot be considered as a reliable confirmation of the diffuser theory, due to the above mentioned uncertainties.

4. Aachen AIA Wind Tunnel (4 cm x 12 cm)

Investigations of the flow process and pressure measurements in the Laval nozzle of one smaller test section were performed by H. Eggink (Ref. 22) some years later. One part of his tests refers to a closed test section, another one to an "open jet arrangement." Whether this was a completely open jet or a "half open - half closed" test section could not be found out from his report. The author states (page 20 of the translation) that a "simple estimate of the pressure recovery for a free jet is not possible since the losses in the free jet are not yet understood." Nevertheless, he gives in his graphs 37, 38 a comparison of the pressure recovery in the closed and free jet test section. The term "pressure recovery" used in title, text, and figure captions referring to closed and free jet test section is misleading. It is not the total pressure ratio as commonly used but the ratio of two specific static pressures. These pressures have not been measured in or behind the diffuser but are calculated out of pressure measurements in the Laval nozzle with several doubtful assumptions for one specific diffuser expansion ratio behind the second throat. The report does not contain any measured static or total pressure in or behind the diffuser. Hence, Eggink's data of so-called "pressure recovery of the open jet" are not suitable to verify the present diffuser theory.

Further on, Eggink discusses the flow structure of the free jet arrangement at different diffuser openings and downstream pressures by means of Schlieren pictures in his figures 26, 27, and 28. It should be pointed out that the diffuser, which he commonly uses is extremely short and steep and quite different in shape from the slender diffuser type (Fig. 1) on which the present analytical treatment is based. The bell mouth of his diffuser acts at the same time as the steeply convergent part. Recapturing cross section F_2 and second throat area F^* are identical. No space for a transformation zone exists. The total length from diffuser intake lips to the second throat is 0.625 H only. Therefore, quantative agreement between his experimental results and the present theoretical calculations cannot be expected. But it is of interest that for a somewhat flatter diffuser intake at Ma = 1.3 and pressure equilibrium in the test chamber he observes (Fig. 26 g, h and 28 g, h) a strong pressure increase and transition from supersonic to subsonic speed in the beginning of the convergent diffuser part. This fact is in agreement with one of our main theoretical conclusions. Eggink interprets it falsely as a normal shock. At Ma = 2.0 no actual Schlieren pictures are given. Schematic sketches showing the steep diffuser intake and only the case of test chamber pressure smaller than the nozzle exit pressure give oblique shocks without transition to subsonic speeds.

Eggink himself notices (page 16) that the flatly converging diffuser (Fig. 26 g, h) has lower losses than the steeply converging diffuser. (Fig. 26 c, d). His proposal for improvement of pressure recovery for free jet (Pg. 21, Fig. 39) ends up with a very long and slender diffuser arrangement (distance from diffuser lip to second throat is approximately 5 H), which is similar to that of our Fig. 1. Nevertheless, our reasoning is quite different from his.

E. Supplement: Some Wind Tunnels with Closed Test Section

Although tunnels with closed test section are not considered in this paper, some brief remarks in connection with them are of interest for comparison. For this purpose Fig. 20 shows also the diffuser efficiency calculated from total pressure data of some supersonic wind tunnels with closed test sections.

The data of the Zuerich-ETH wind tunnel with continuous operation are given by J. Ackeret (Ref. 4, page 521) and involve the diffuser losses only without losses by corners, straightener or cooler (Curve No. 1). The test section area is 40 cm x 38 cm. The pressure distribution measurements range from Ma = 1.00 to Ma = 2.73 and have been extrapolated by Ackeret up to 3.00. The air was not dried but evidently the influence of humidity is low in his tests, probably due to reduced relative humidity by heating up the tunnel.

The data of the Goettingen KWI intermittent type wind tunnel are reported by K. Oswatitsch (Ref. 14) in a special study on pressure recovery in the diffuser. The tunnel dimensions are small, 6 cm x 8 cm. The tunnel was used with completely closed test section with either a short (31 cm) cylindrical diffuser (Curve 3) or a long (131 cm) cylindrical diffuser (curve 4) and sometimes with half-open - half-closed test section (curve 5). The air was not dried so that these results are somewhat affected by condensation as noted by Oswatitsch himself.

Because of many uncertainties test data of the Guidonia supersonic wind tunnel with closed test section (40 cm x 40 cm) and continuous operation are not included in Fig. 20. Gasperi himself (Ref. 23) notices that in the Laval nozzle ("Guidonia Nozzle No. 8"), designed for adiabatic expansion to Mach No. 2.14, large losses occur which lead to much smaller Mach numbers. His measurements of total pressure inside the flow, and static pressure at the tunnel side wall do not fulfill isentropic relation with the stagnation pressure in the stilling chamber. Furthermore, Gasperi interprets the pressure measured with the side orifices of the pitot tube as static pressure. The reliability of this interpretation seems doubtful. Calculations of Mach number using different combinations of these pressures from his Fig. 9 give 5 different values of Mach numbers ranging between 2.07 and 1.64. Gasperi gave the values 1.89 and 1.77 in the axis of the flow and 1.80 at the wall. Similar figures result by the evaluation of his Fig. 10. This fact indicates considerable losses most probably caused by condensation shocks of humid air, because for dry air the above mentioned isentropic relation between the pressures has been proved to be correct. Hence, proper evaluation of his diffuser pressure recovery values is impossible. It is unknown to the author if later measurements exist. In any case the value Ma = 2.00 given by Oswatitsch (Ref. 14) for the Mach No. of this nozzle is too high.

Not included either in Fig. 20 are results of pressure measurements by W. Kraus (Ref. 24) in the tunnel No. 5 of Peenemuende with 18 cm x 18 cm nozzle exit area and half-closed--half-open test section. In 1944 test chamber and diffuser were brought to the LFA at Braunschweig and connected with the compressor system of the supersonic tunnel there for continuous operation. Unfortunately, these tests were carried out with humid air because no air dryer in the

LFA installation was available, and thus all results are influenced considerably by condensation shocks. Efforts have been made by the author to evaluate these tests under consideration of condensation, but without success, since some data are missing required for this evaluation. The performance of these experiments was strongly affected by war time events.

Curve 8 represents the above (Sec. 1, C, 2) mentioned curve established by L. Crocco (Ref. 5, Fig. 1) and designated by him with "pressure recovery practically obtainable with steady compression." It is converted from Crocco's definition η_{cr} into the η_D- definition used in this paper by means of the corresponding formulas given before (Sec. 1, C, 2 and 4). He calls the curve a "mean experimental value" based on wind tunnel tests by Ackeret between Ma = 1 and 2.73 and by Castagna at Ma = 4.2 (one test point). The trend of Crocco's curve 8 seems to be fairly optimistic above Ma = 2.5 in comparison with the closed tunnel data of Zuerich ETH (Curve 1) and Goettingen KWI (Curves 3 and 4). Its fluctuations have no real meaning but are caused by inaccurate readings of the original curve.

F. Comparison Between Diffuser Efficiency of a Free Jet and a Closed Test Section Wind Tunnel. (Example)

Fig. 20 shows good agreement between the diffuser efficiency of the three closed test section tunnels. (Curves 1, 3, 4). They have somewhat higher diffuser efficiency (average of 8% between Mach No. 1 to 3) than the free jet (f = 0.64) tunnel (Curve 7). The efficiency value for the half-closed--half-open test section tunnel (Curve 5) lies somewhat below (average of 11%) that of the completely free jet tunnel. However, it would be incorrect to generalize these conclusions. For a correct comparison of different test section types one has to consider the same test section length. As shown in the present analysis in case of the free jet test section, the diffuser efficiency η_D depends greatly upon the area ratio f (Fig. 6, 7, 8) and therefore on the free jet test section length l/H, which requires this area ratio f (Fig. 18). The energy ratio decreases with increasing test section length (Fig. 17). In case of the closed test section, no such analysis is known up to now, but without doubt the diffuser efficiency will likewise decrease with increasing test section length.

For the purpose of comparison we take as an example the Zuerich and the Peenemuende-Kochel tunnel, both of practically the same size and operating at nearly the same Reynolds number and refer their efficiency values to the same test section length. We have to choose the test section length of l/H = 1.3 because this length was actually used in establishing the experimental data of the closed test section tunnel at Zuerich (H = 38 cm; Curve 1 in Fig. 20). The pressure recovery data of the free jet test section tunnel at Peenemuende-Kochel were measured with a test section length l/H = 1.75 and f = 0.64. In order to convert these experimental data to l/H = 1.3 we find first the corresponding area ratio f = 0.74 from Fig. 18 (for ε = 0.061). Then using the present analysis we find the theoretical η_D belonging to f = 0.74 from Fig. 8 as a function of Mach number. Finally we add or subtract the same percentage deviation from this theoretical η_D as found between the experimental and theoretical curve for f = 0.64 (difference between curve 7 and curve A in Fig. 20).

The result is given in the following table:

Comparison between diffuser efficiency of a free jet and a closed test section tunnel at the same test section length $l/H = 1.3$

Converted Experimental Data

Mach No.	η_D Free Jet conv. Kochel wind tunnel	η_D Closed test section Zuerich wind tunnel	$\frac{\eta_D \text{ Free Jet}}{\eta_D \text{ Closed Test Section}}$
1.0	0.859	0.827	1.039
1.2	0.810	0.810	1.000
1.5	0.779	0.789	0.987
2.0	0.768	0.795	0.966
2.5	0.763	0.777	0.982
3.0	0.758	0.763	0.993
		Average	0.995

Remark: The third decimal has limited physical meaning.

It is seen that the difference in diffuser efficiency between both test section types at this specific length is very small, maximum ± 4% at different Mach numbers and within 0.5% as average in the given supersonic Mach number range from 1 to 3. Evidently the superiority in efficiency of the closed test section, as it is known from the subsonic range (e.g. see Ref. 12) is vanishing in the supersonic range, according to this example. Between Mach No. 1 and 2 there might be still a slight difference. At about Mach No. 3 both tunnel types have practically equal diffuser efficiency.

It might be emphasized that even though the decelerating process in the diffuser behind the closed test section will be quite different from that behind the free jet, the diffuser efficiencies of both test section types are nearly equal in the supersonic range and at the test section length under consideration. A statement for Mach Nos. above 3 or for other test section length can be made only after a similar theoretical analysis is known for the closed test section diffuser as it is given here for the free jet test section diffuser or after more extended experimental data are established.

NOMENCLATURE

a = Velocity of sound

c_p = Specific heat at constant pressure

f = Ratio of nozzle exit cross section area to diffuser intake area

F = Cross section area (if with subscript)

$F(x)$ = Generalized isentropic line

$g(x)$ = Negative first derivative of $F(x)$

$\tilde{g}$ = Inverse function of g

G = Function symbol

H = Height of nozzle exit cross section

K = Total pressure ratio

l = Length of free jet

L = Energy

m = Slope of isentropic line

$M = \frac{w}{a^*}$ = Dimensionless velocity

$Ma = \frac{w}{a}$ = Mach Number

P = Pressure

P_o' = Total pressure after losses

$\mathfrak{P} = \frac{P}{P_o}$ = Dimensionless pressure

R = Gas constant

s = Entropy

T = Absolute temperature

V = Volume flow

W = Compression work per unit mass

w = Velocity

x = Velocity-variable for generalized isentropic lines

y = Pressure-variable for generalized isentropic lines

$(x_i; y_i)$ = Arbitrarily chosen fixed point

$(x_T; y_T)$ = Point of contact

γ = Ratio of specific heats; $\gamma = 1.405$ for numerical calculations of air

ε = Half of expansion angle from nozzle exit to diffuser intake (see Fig. 1)

ζ = Energy ratio

η = Efficiency factor

$\vartheta = \frac{\Theta}{K_{NS}}$ (See equation (14))

Θ = Dimensionless mass flow

$\mu = \frac{m}{K}$

ϱ = Density

Φ = Function symbol

SUBSCRIPTS

ad = Adiabatic process

B = Blower

C = Test chamber

Cr = Abbreviation for Crocco

D = Diffuser

E = Energy

e = Exit of diffuser; intake of blower

i = Inlet of diffuser

is = Isothermic process

kin = Kinetic

max = Maximum

NS = Normal shock

P = Pressure

α = Supersonic solution

β = Subsonic solution

1 = Nozzle exit

2 = Diffuser intake if area; properties of state after transformation process

0 = Stagnation

* = First throat

* = Second throat

BIBLIOGRAPHY

1. Busemann, A. Profilmessungen bei Geschwindigkeiten nahe der Schallgeschwindigkeit. Jahrbuch der Wissenschaftlichen Gesellschaft fuer Luftfahrt (WGL), pp 95-99. 1928
See also:

Busemann, A. and Walcher, O. Profileigenschaften bei Ueberschallgeschwindigkeit. Forschung, Vol. 4, p. 87. 1933

2. Ramm, H. Measurements of the Pressure Distribution in the entire Wind Tunnel, and especially in the Diffuser by means of small Pressure Gages. (English translation of WVA-Kochel Report No. 66/205 Sept 1945). No. F-TR-2137-ND GS-AAF-Wright Field No. 20, May 1947.

3. Ramm, H. Phenomena in Supersonic Diffusers, No. F-TR-2175ND GS-AAF-Wright Field No. 43. Nov 1947.

4. Ackeret, J. Windkanaele fuer hohe Geschwindigkeiten. Convegno di Scienze, Fisiche, Mathematiche e Naturali. 30 Sept - 6 Oct 1935. Roma. pp 487-537. Especially page 496 and following.

5. Crocco, L. Gallerie aerodinamice per alte velocita. Convegno di Scienze, Fisiche, Mathematiche e Naturali. 30 Sept - 6 Oct 1935. Roma. pp 542-557. Especially p545, Fig. 1.

6. Busemann, A. Gasdynamik. Handbuch der Experimentalphysik, Vol. 4, Part 1. Leipzig, 1930.

7. Tollmien, W. Stationaere ebene und rotationssymmetrische Ueberschallstroemungen. Chapter 5, No. 7. Peenemuende Archiv No. 44/5, p 16. 1941.

8. Tollmien, W. Berechnung turbulenter Ausbreitungsvorgaenge. ZAMM Vol 6, pp 468 to 478. 1926.

9. Kuethe, A. Investigations of the Turbulent Mixing Regions Formed by Jets. Journal of Applied Mechanics, Vol. 2, pp 87-95. 1935.

10. Liepmann, H. W. and Laufer, J. Investigations of Free Turbulent Mixing. NACA TN No. 1257, 1947.

11. Karman, Th. von The Fundamentals of the Statistical Theory of Turbulence. Journal of Aeronautical Sciences, Vol. 4, pp 131-138, 1937.

12. Millikan, C. B. Wind Tunnel at California Institute of Technology. Society of Automotive Engineers Journal, Vol. 25, pp 520-524. 1929

13. Walchner, O. Personal information to the author. No description of the tunnel available.

14. Oswatitsch, K. Untersuchungen ueber den Diffuserwirkungsgrad und ueber die Erzielung einwandfreier Parallelstrahlen bei Ueberschallwindkanaelen, HAP-Archiv No. 201/179. 1942.

15. Wieselsberger, C. Die Ueberschallanlage des Aerodynamischen Institutes der Technischen Hochschule Aachen. Luftwissen, Vol. 4, No. 10, p 301. 1937.

16. Hermann, R. The Supersonic Wind Tunnel of the Heereswaffenamt and its Application in External Ballistics. 1940. In: The Story of Peenemuende. pp 692-749, 1945. Translation of: HAP or Kochel Archiv 66/0.

17. Prandtl, L. Herstellung einwandfreier Windkanaele. Par. 3, p 73. Handbuch der Experimentalphysik, Vol. 4, Part 2, Leipzig 1930.

18. Ruden, P. Turbulente Ausbreitungs Vorgaenge im Freistrahl. Naturwissenschaften, Vol. 21, pp 375-378. 1933.

19. Liepmann, H. W. and Puckett, A. E. Introduction to Aerodynamics of a Compressible Fluid. John Wiley & Sons, New York, 1947.

20. Owen, P. R. Note on the Apparatus and Work of the WVA Supersonic Institute at Kochel, S. Germany. Parts I - VI. Royal Aircraft Establishment, Farnborough, Hants. Technical Note AERO 1711 et als. 1945 and 1946.

21. Hermann, R. Der Kondensationstoss in Ueberschall-Windkanaldueesen. Luftfahrt-Forschung, Vol. 19, pp 201-209, 1942. Especially Sec. 4, par 3.

22. Eggink, H. Stroemungsaufbau und Druckrueckgewinnung in Ueberschall-kanaelen. Forschungsbericht No. 1756, ZWB 1943. English translation by the University of Michigan: Flow Structure and Pressure Recovery in Supersonic Tunnels. ATI 3570. CGD 808.

23. Gasperi, M. Strumenti è metodi per le ricerche alla galleria del vento ultrasonora. Vortraege der Hauptversammlung 1937 der Lilienthal-Gesellschaft fuer Luftfahrtforschung, pp 187-213. With German translation in the same book: Geraete und Verfahren fuer Untersuchungen im Ueberschallwindkanal.

24. Kraus, W. Bericht ueber die bei der Verlagerung der Gruppe Thermodynamik nach Braunschweig durchgefuehrten Messungen. Kochel Archiv No. 66/169. 1945.

25. Hermann, R. Theoretical Calculation of the Diffuser Efficiency of Supersonic Wind Tunnels with Free Jet Test Section. Heat Transfer and Fluid Mechanics Institute, Berkeley, California, 1949. Volume of preprints published by: The American Society of Mechanical Engineers, May 1949, New York 18, New York.

26. Hermann, R. Diffuser Efficiency of Free Jet Supersonic Wind Tunnels at Variable Test Chamber Pressure. Not yet published.

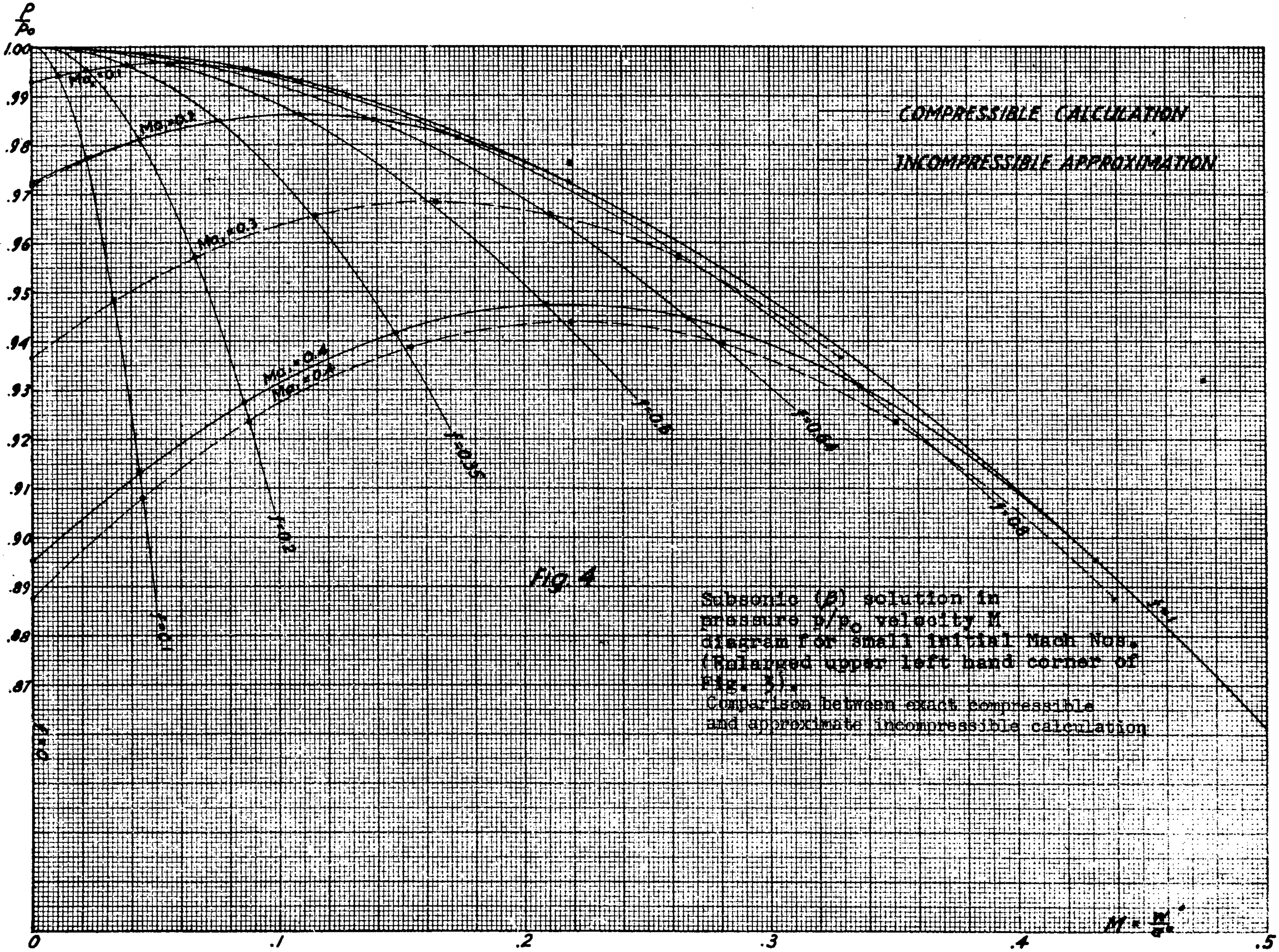

Fig. 4

Subsonic (β) solution in pressure p/p_0 velocity M diagram for small initial Mach Nos. (Enlarged upper left hand corner of Fig. 3).
Comparison between exact compressible and approximate incompressible calculation

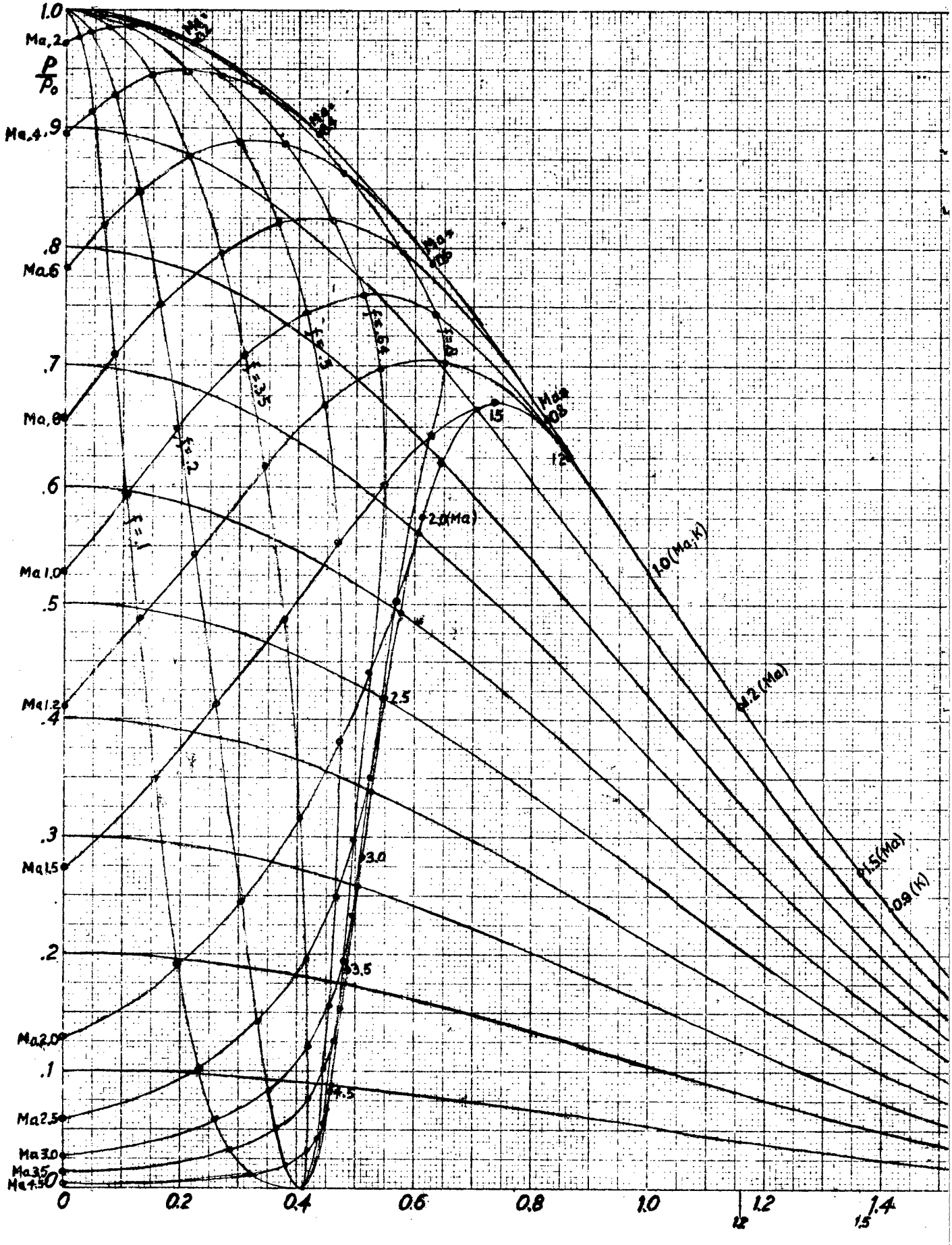
1.0
Ma.2
P/P₀
Ma.4
.9
.8
Ma.6
.7
Ma.8
.6
Ma1.0
.5
Ma1.2
.4
.3
Ma1.5
.2
Ma2.0
.1
Ma2.5
Ma3.0
Ma3.5
Ma4.0
0
0.2
0.4
0.6
0.8
1.0
1.2
1.4
1.5
1.2
Ma=1.0
Ma=1.05
Ma=1.08
Ma=1.15
Ma=1.2
Ma=1.4
Ma=1.5
Ma=1.8
Ma=2.0
Ma=2.5
Ma=3.0
Ma=3.5
Ma=4.0
1.5
2.0
2.5
3.0
3.5
4.0
1.0(Ma;K)
1.2(Ma)
1.5(Ma)
1.0(K)

AFTR -6334

Fig. 3

FLOW PROCESS IN DIFFUSER OF FREEJETS AT SUPERSONIC OR SUBSONIC VELOCITIES AT DIFFERENT EXPANSION RATIOS f

Subsonic (β) solution in pressure p/p_o vs. velocity M diagram with curves for constant area ratio f as parameter and curves for constant initial Mach number. Isentropics are curves with constant diffuser total pressure ratio K_D. Limiting curve is normal shock polar.

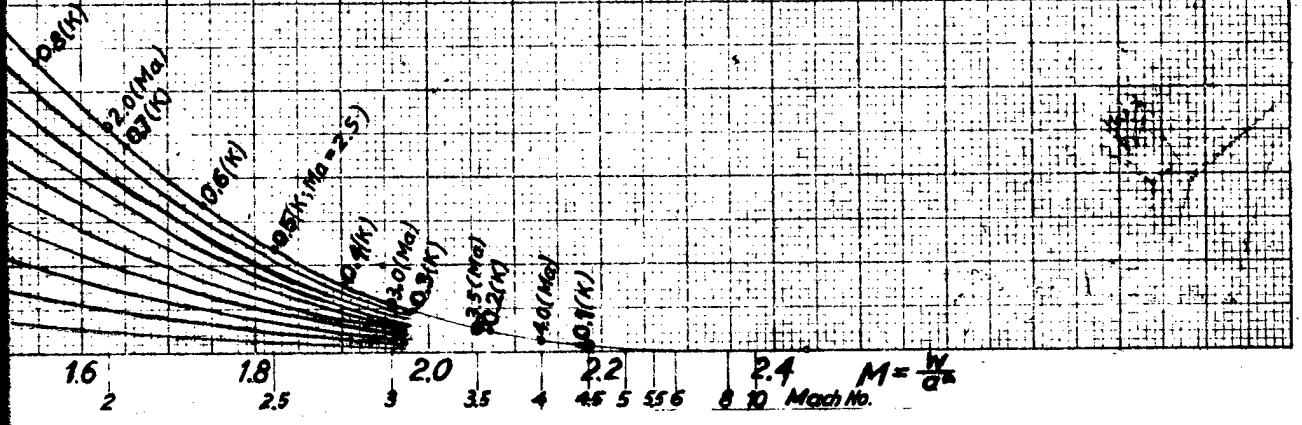

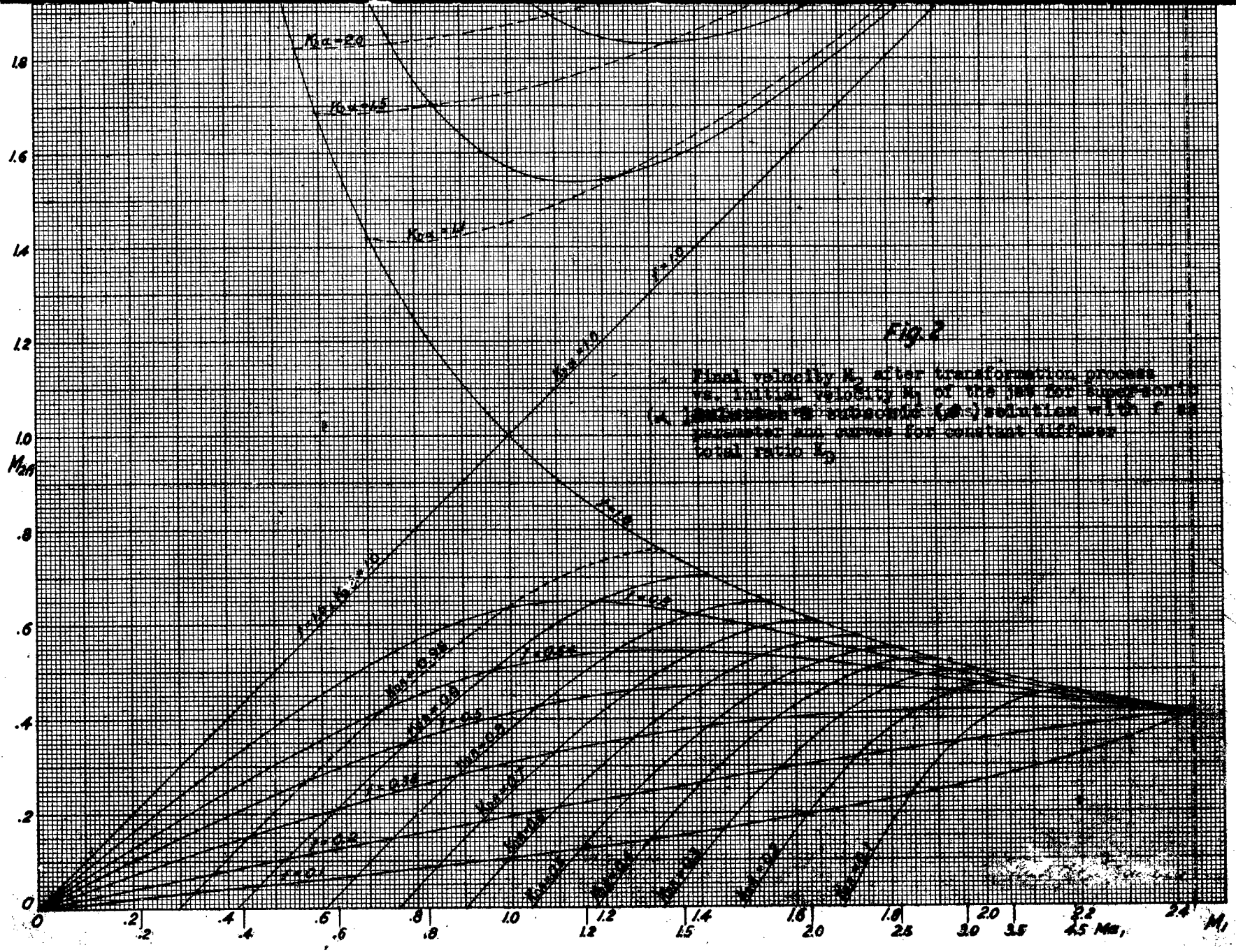

Fig. 2

Final velocity K_2 after transformation process vs. initial velocity K_1 of the jet for isentropic (= reversible) adiabatic ($\Delta s = 0$) reaction with ε as parameter and curves for constant diffuser total ratio κ_D

SCHEME OF SUPER SONIC WIND TUNNEL WITH FREE JET TESTSECTION

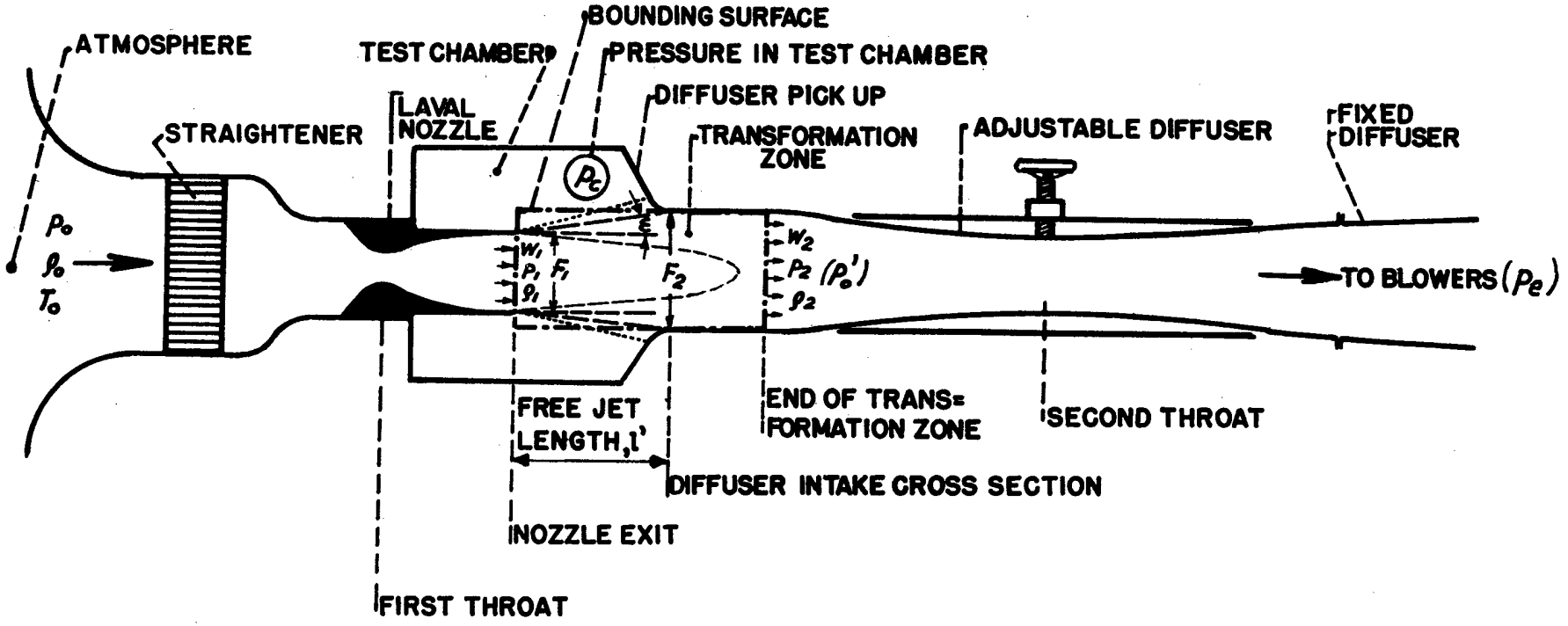

Fig. 1

Scheme of supersonic wind tunnel with free jet test section

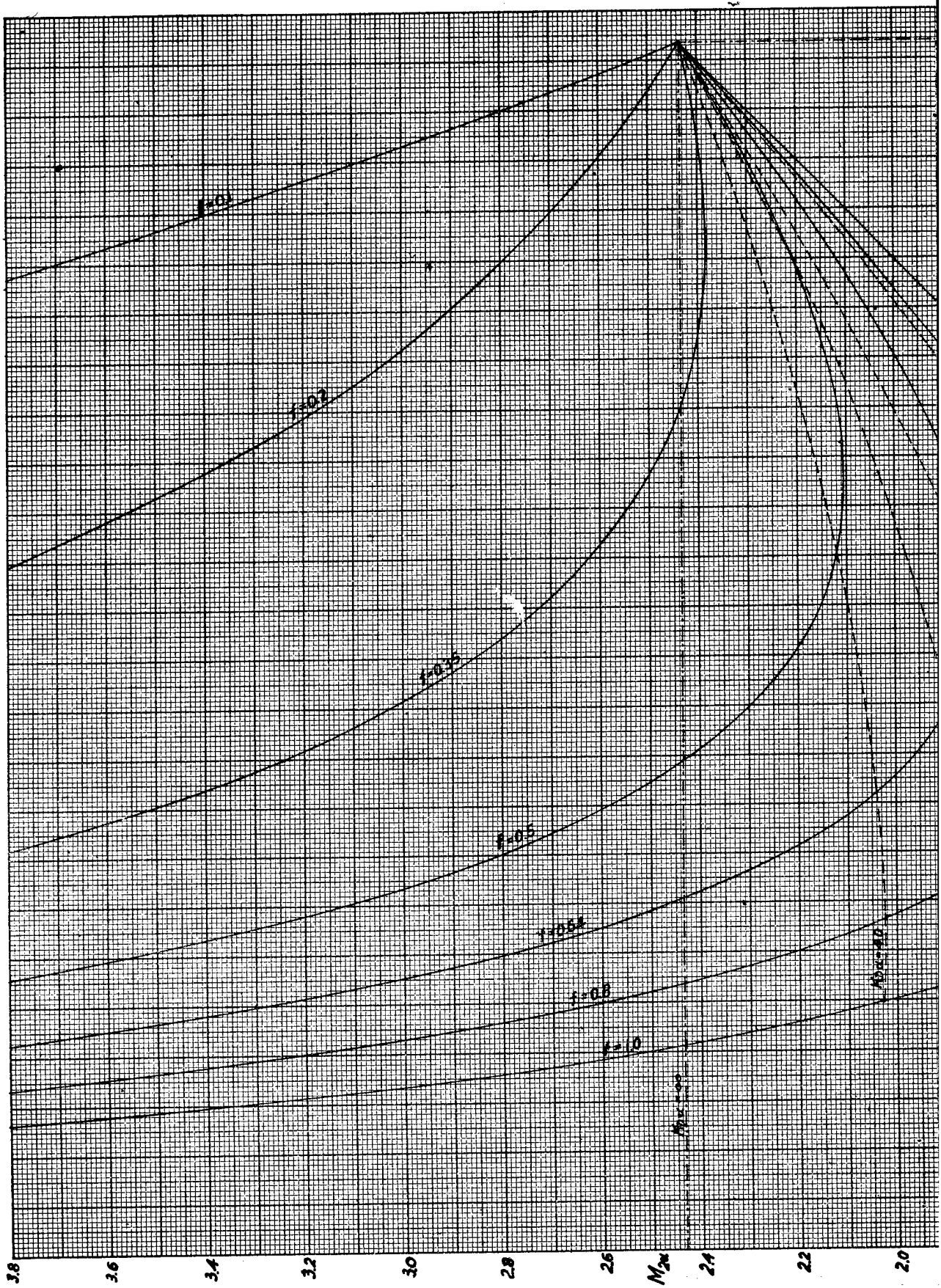
ε=0
ε=0.2
ε=0.35
ε=0.5
ε=0.65
ε=0.8
ε=1.0
Mcr=1.0
Abc=90°
3.8
3.6
3.4
3.2
3.0
2.8
2.6
M∞
2.4
2.2
2.0

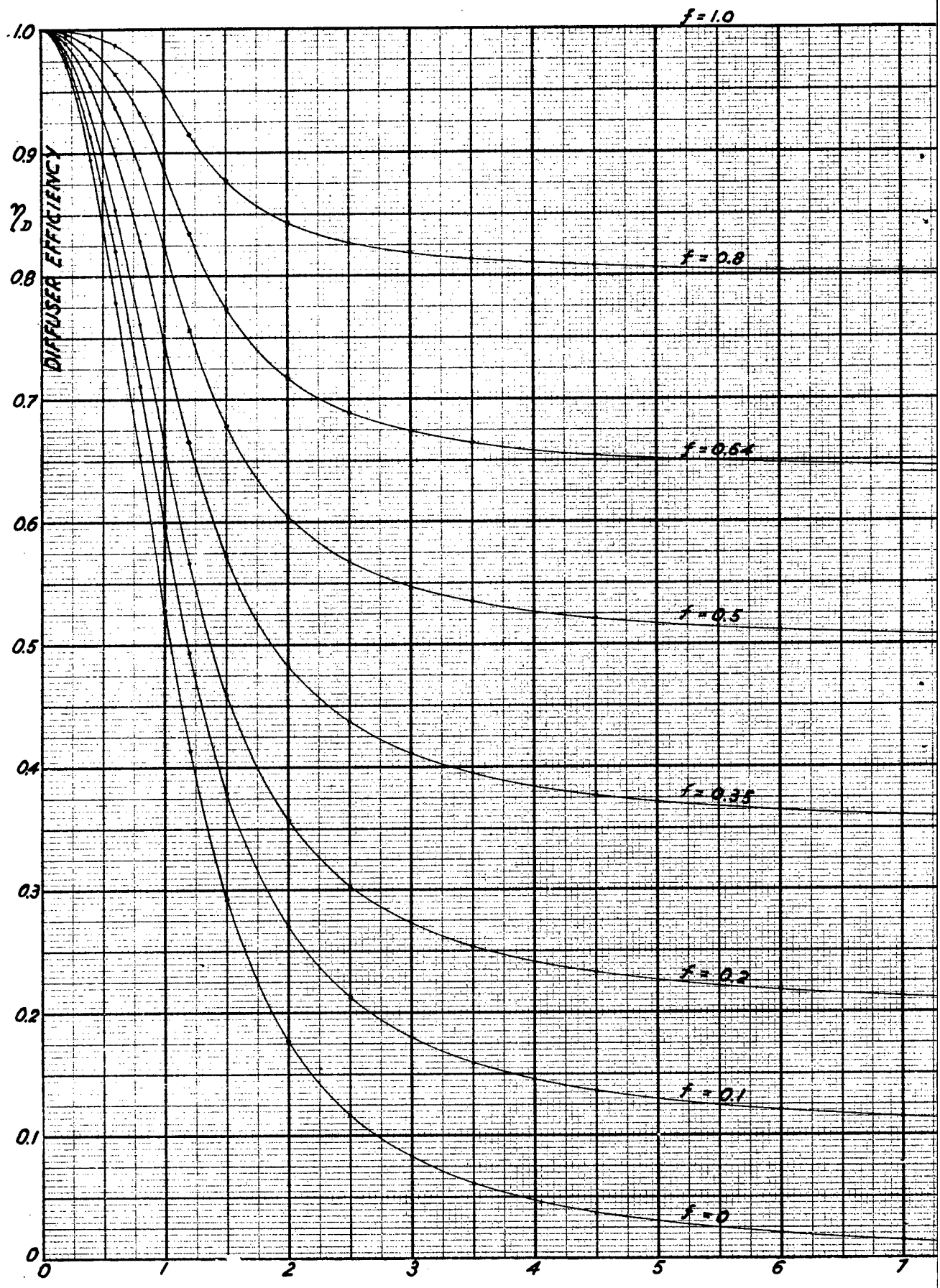
f = 1.0
f = 0.8
f = 0.64
f = 0.5
f = 0.35
f = 0.2
f = 0.1
f = 0
DIFFUSER EFFICIENCY
η_D
1.0
0.9
0.8
0.7
0.6
0.5
0.4
0.3
0.2
0.1
0
0
1
2
3
4
5
6
7

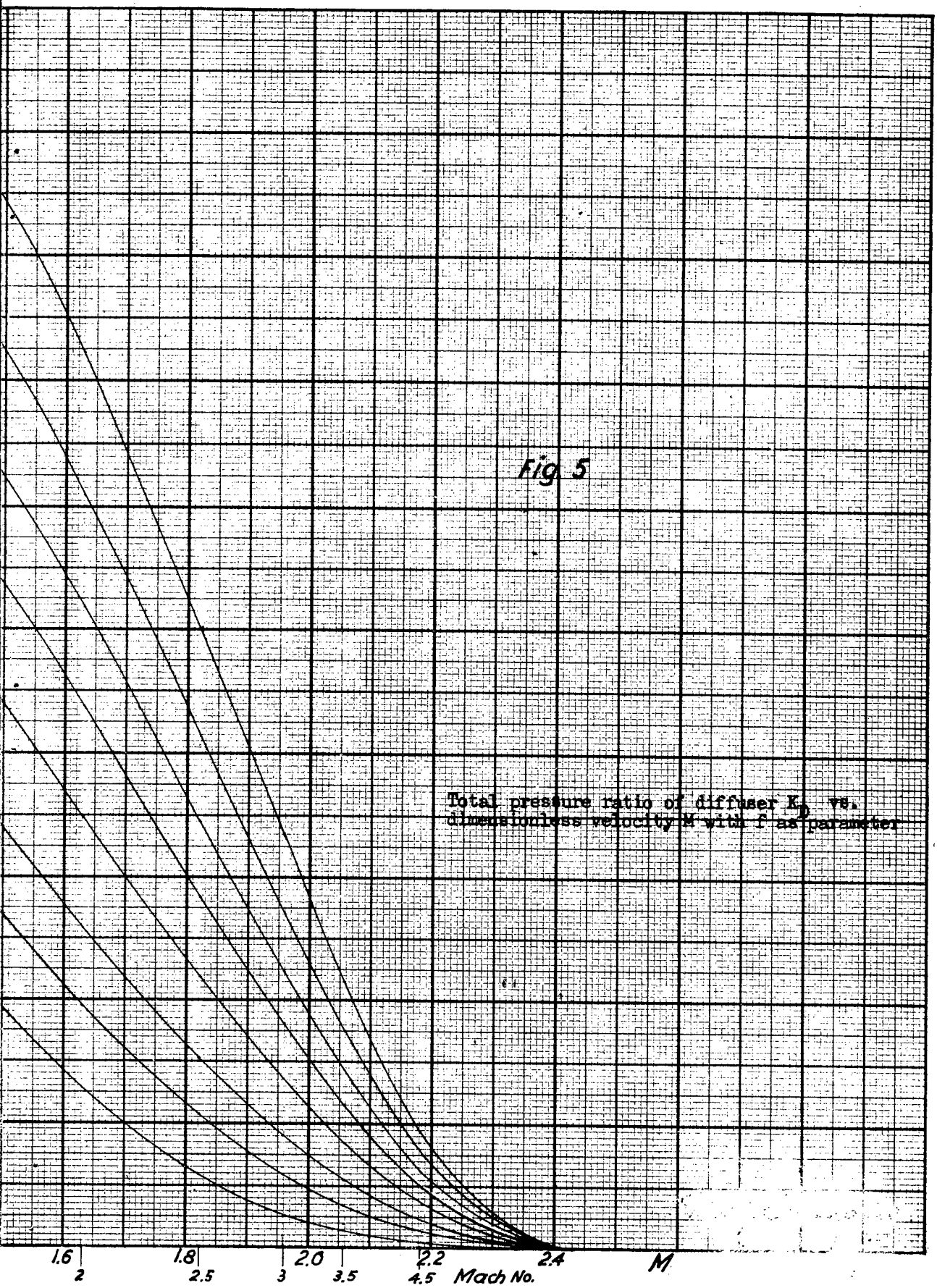

Fig. 5

Total pressure ratio of diffuser K_D vs. dimensionless velocity M with f as parameter

Fig. 6

Diffuser efficiency η_e vs. Mach number of the jet with area ratio $\bar{f}$ as parameter. Asymptotes for Mach number infinity

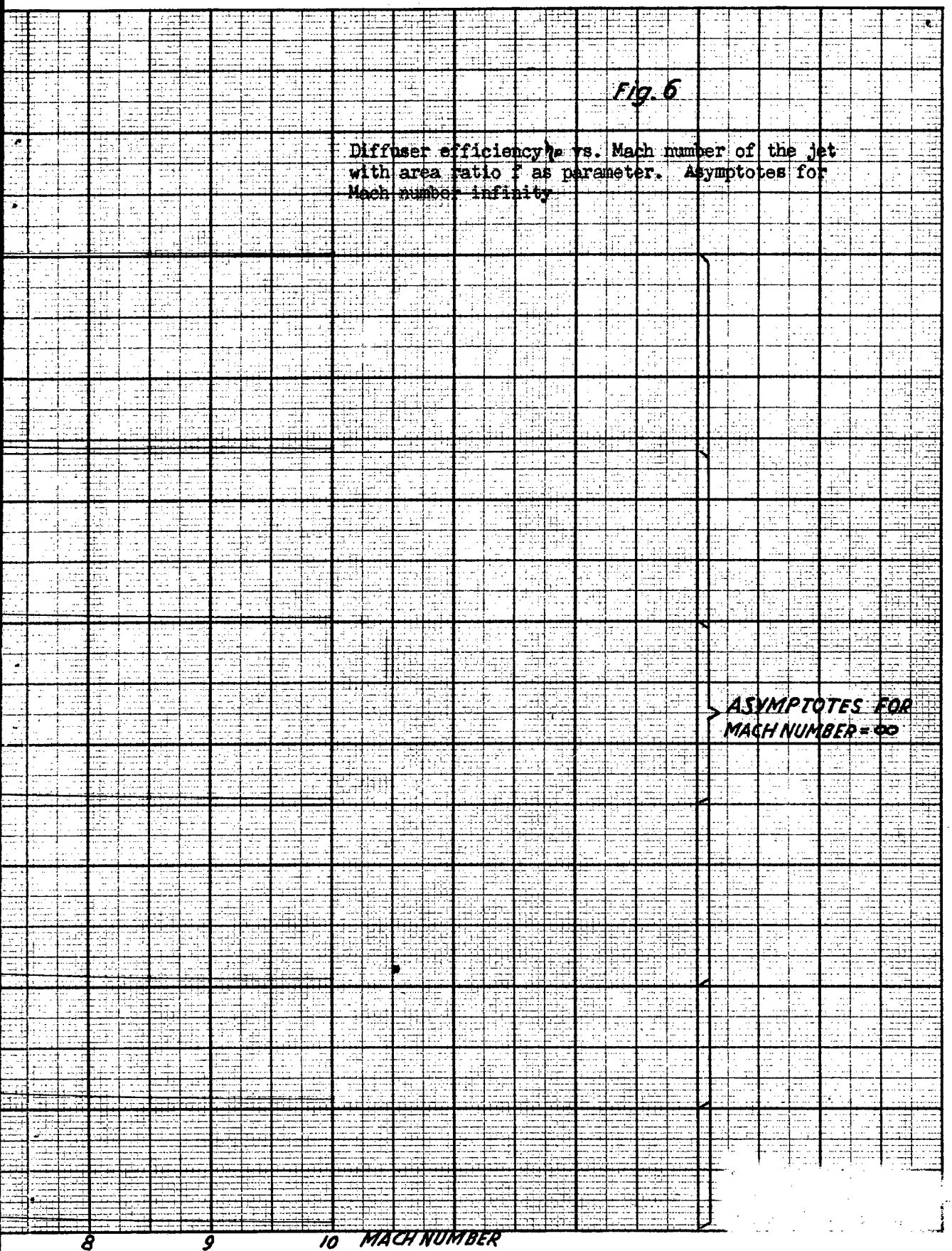

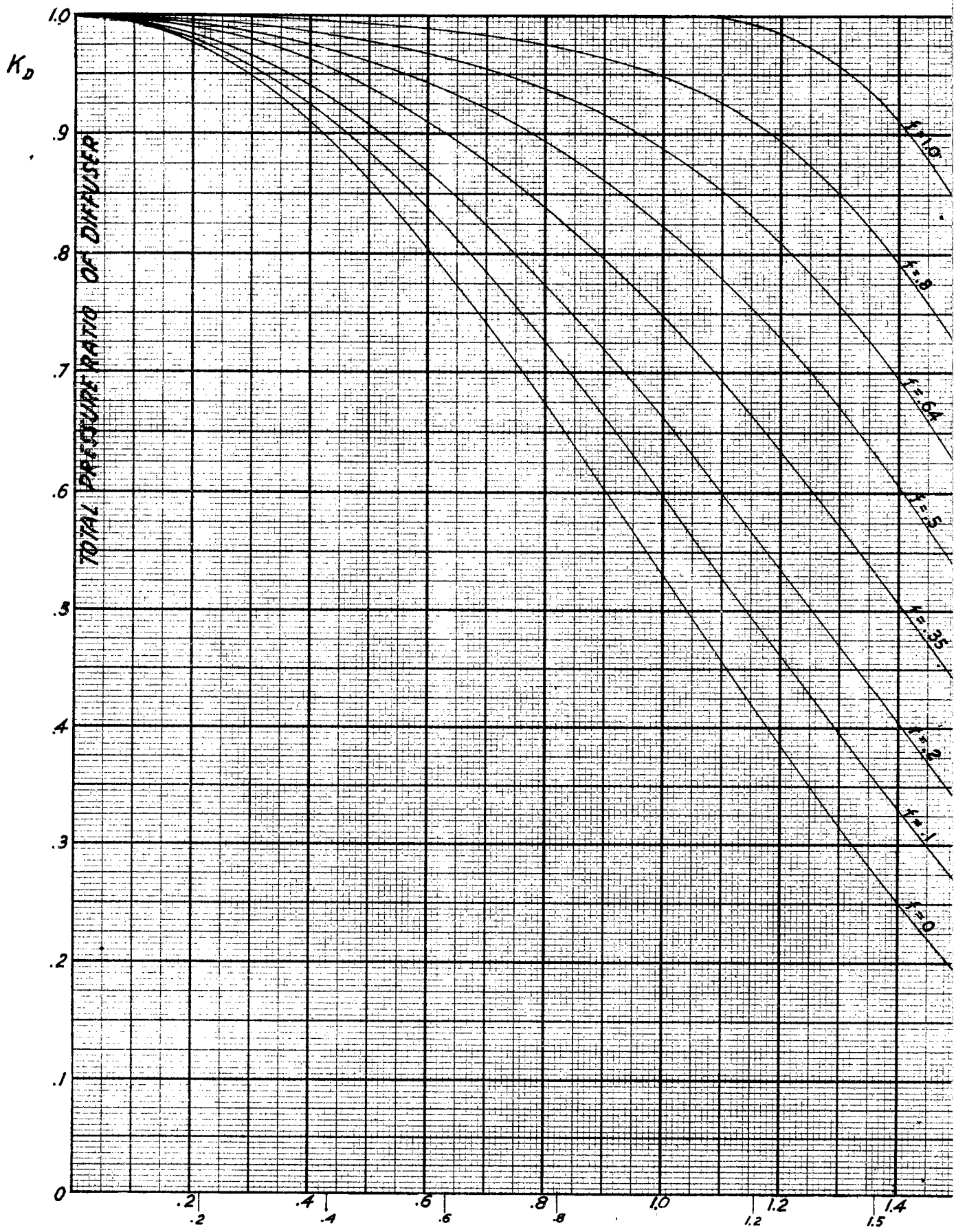
K_D
TOTAL PRESSURE RATIO OF DIFFUSER
1.0
.9
.8
.7
.6
.5
.4
.3
.2
.1
0
.2
.4
.6
.8
1.0
1.2
1.4
1.5
k=1.0
k=.9
k=.64
k=.5
k=.35
k=.2
k=.1
k=0

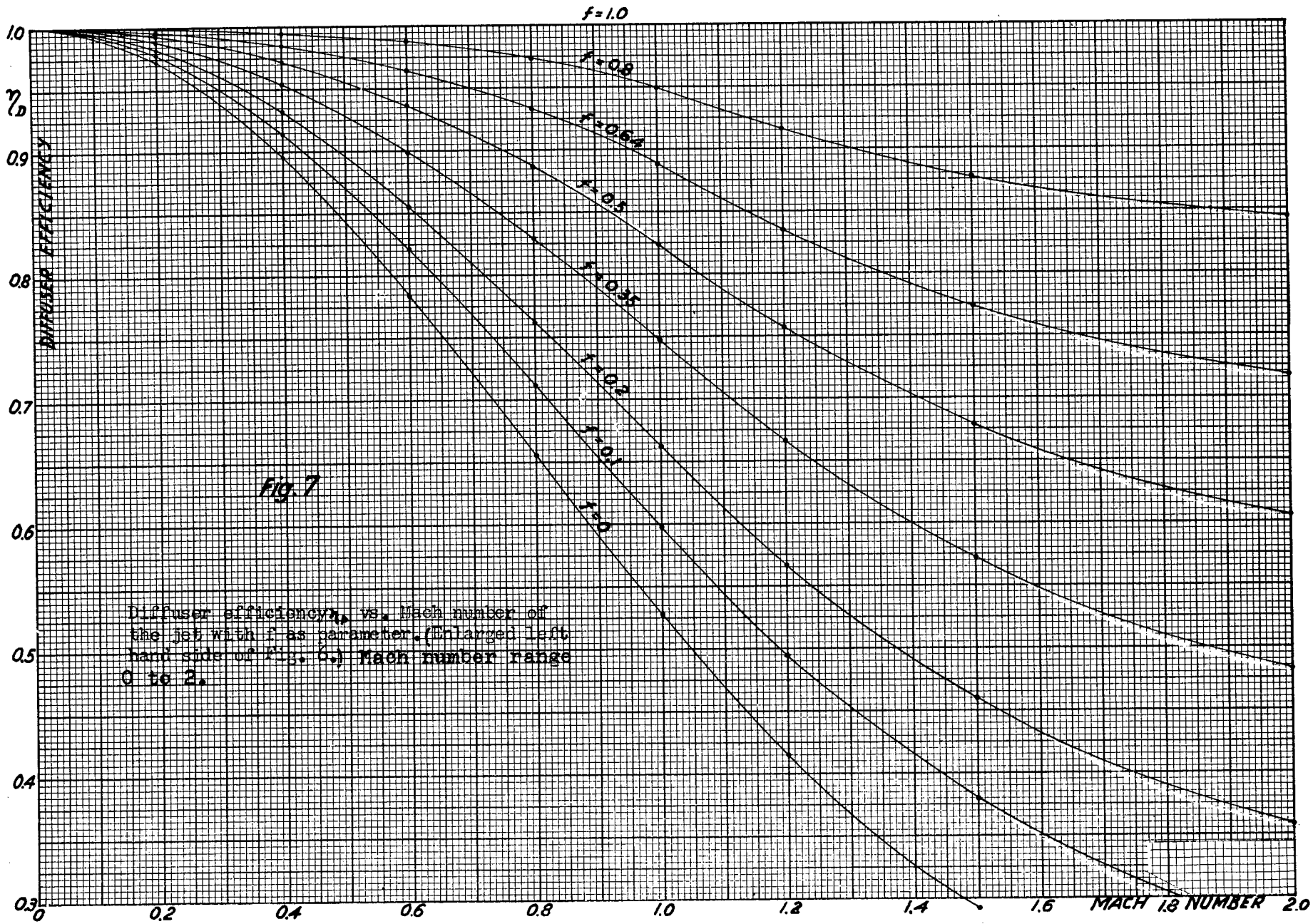

Fig. 7

Diffuser efficiency η_D vs. Mach number of the jet with f as parameter. (Enlarged left hand side of Fig. 6.) Mach number range 0 to 2.

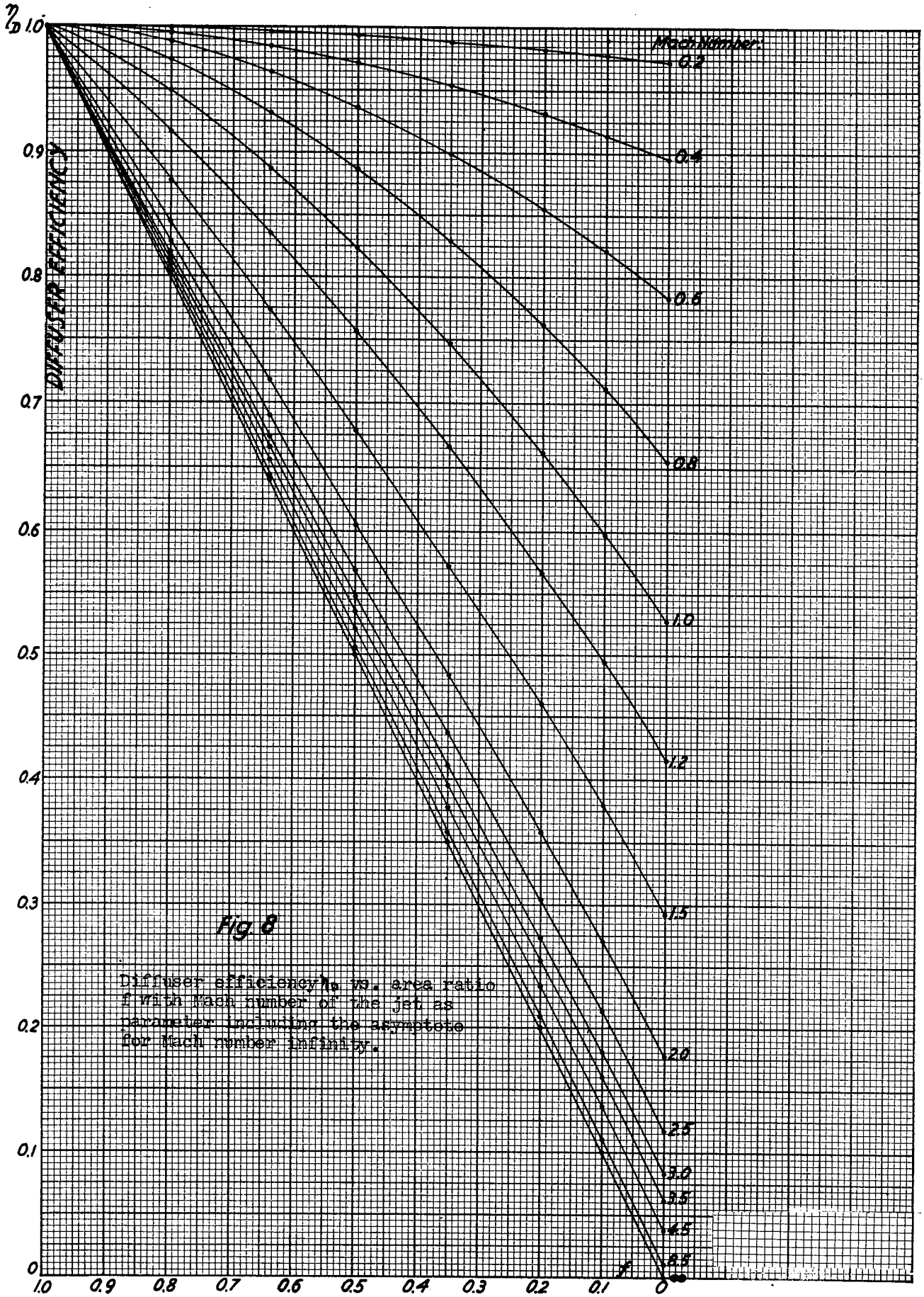

Fig 8

Diffuser efficiency η_D vs. area ratio with Mach number of the jet as parameter including the asymptote for Mach number infinity.

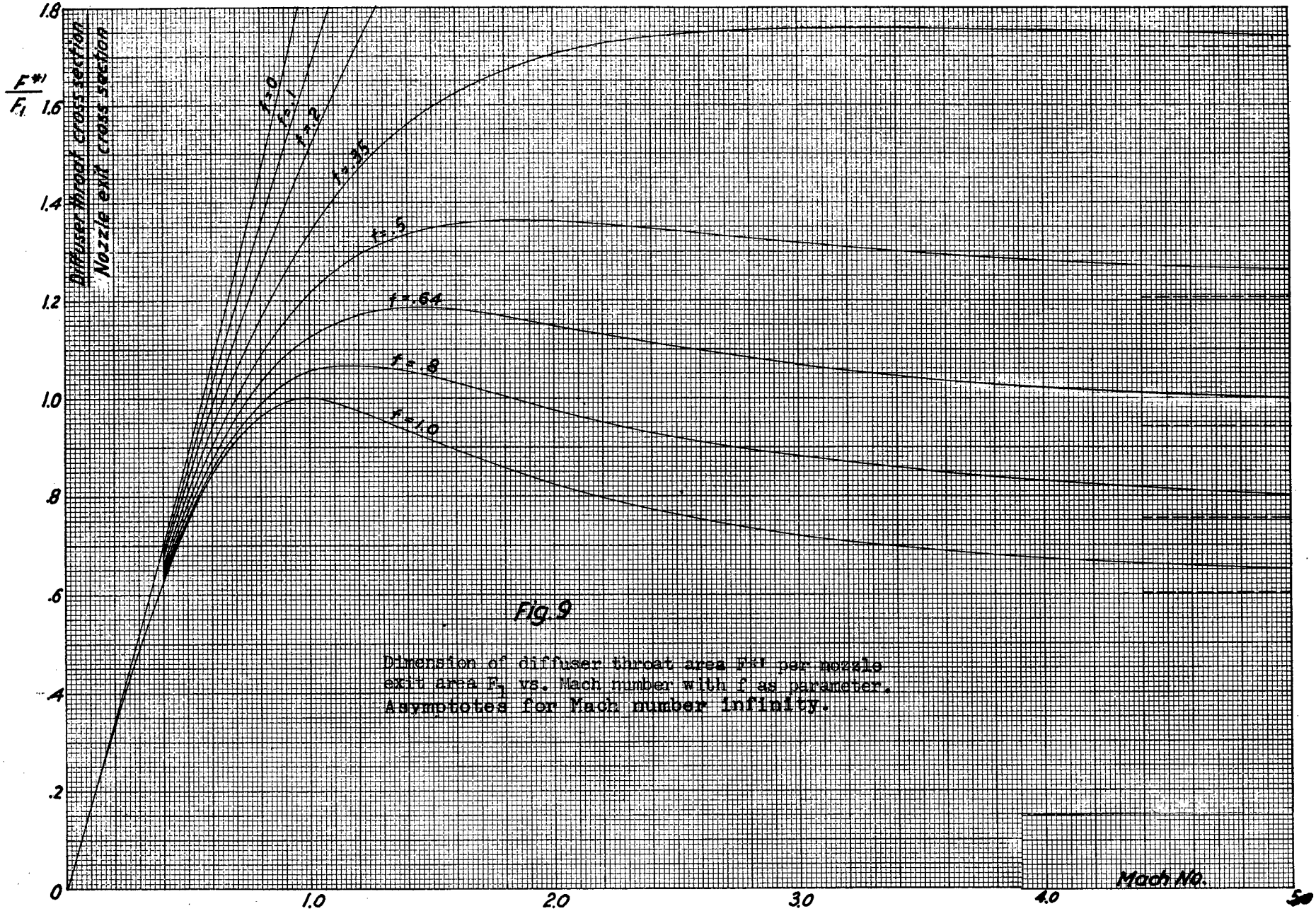

Fig. 9

Dimension of diffuser throat area F*1 per nozzle exit area F_1 vs. Mach number with f as parameter. Asymptotes for Mach number Infinity.

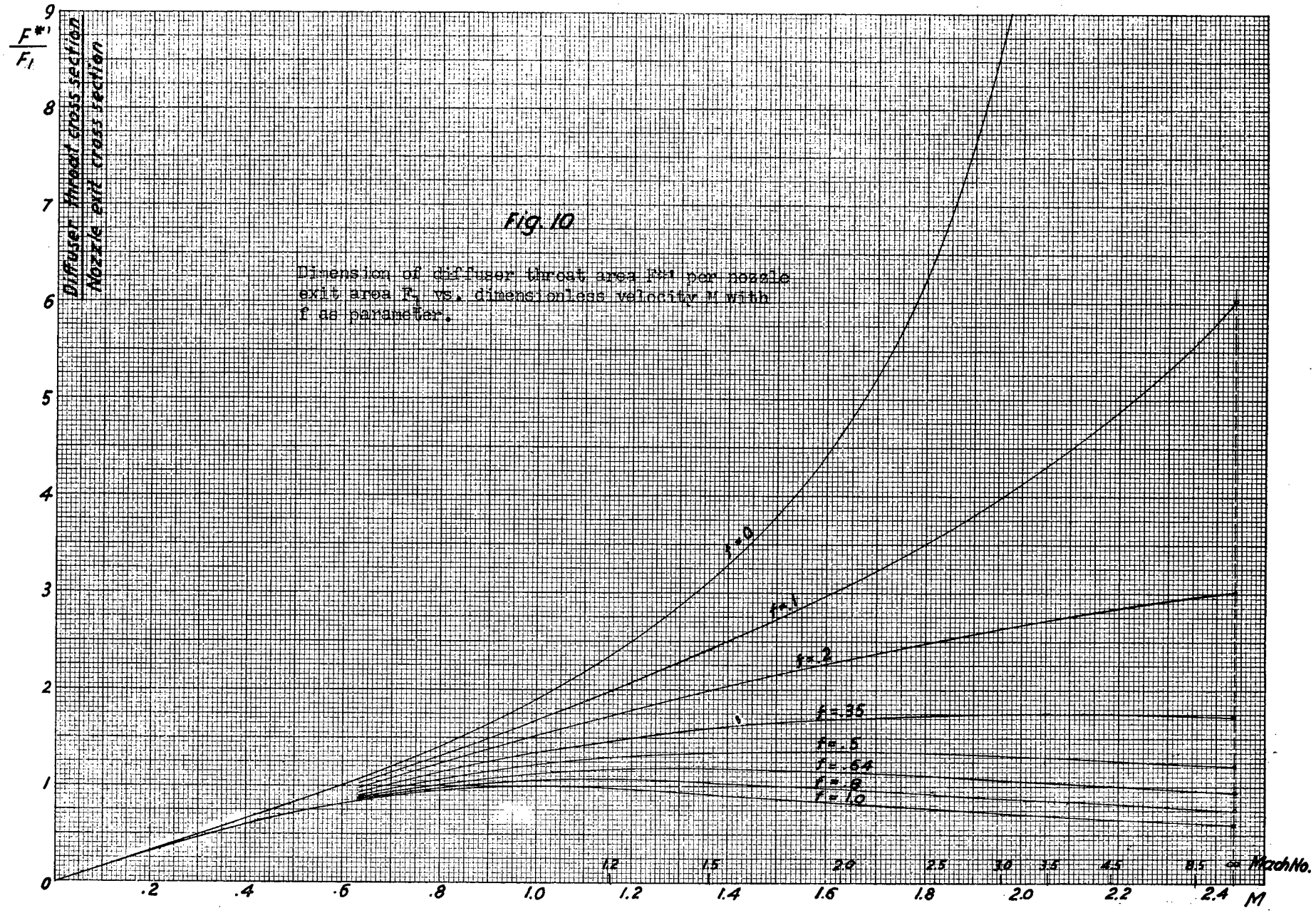

Fig. 10

Dimension of diffuser throat area F*1 per nozzle exit area F1 vs. dimensionless velocity M with f as parameter.

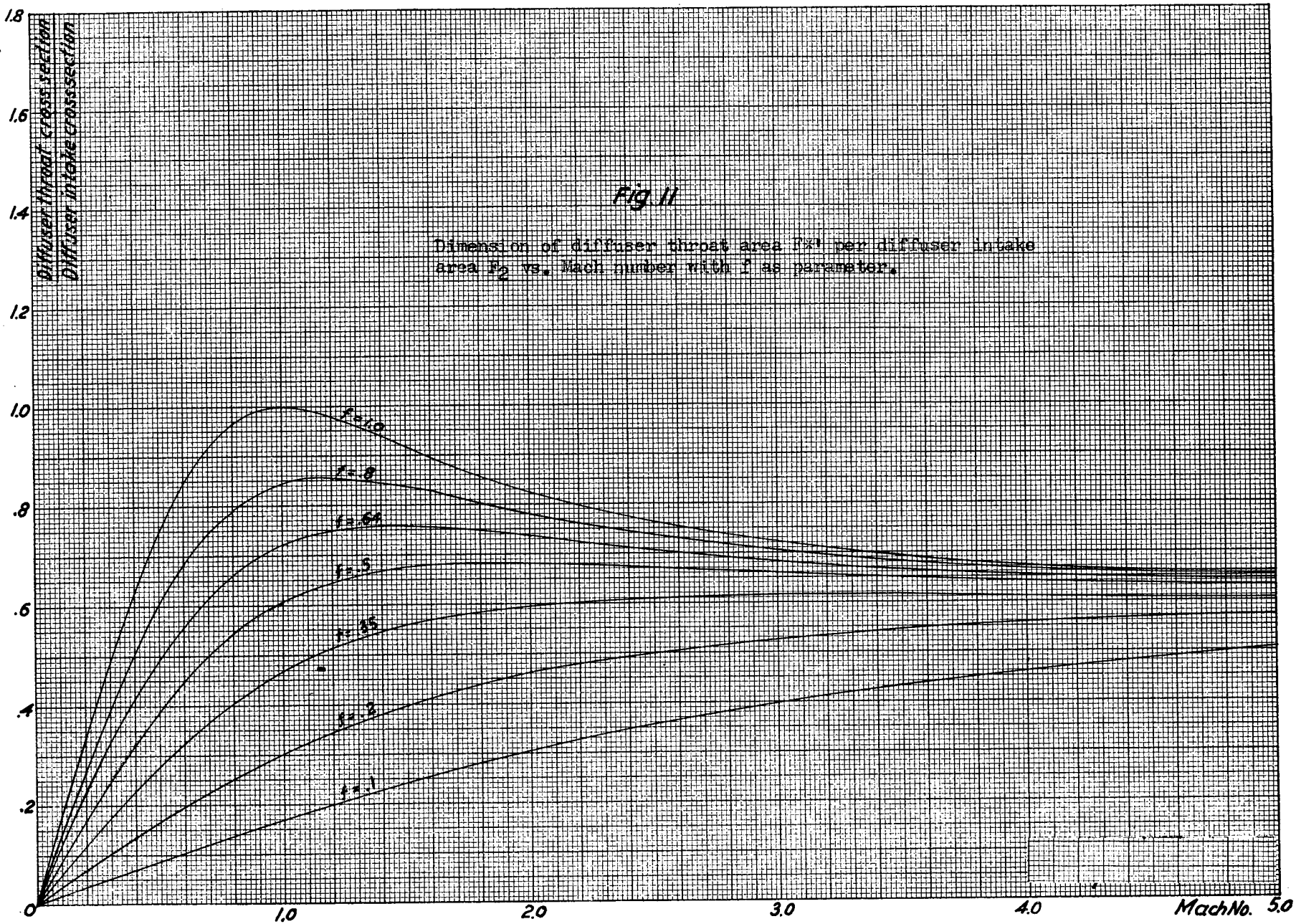

Fig. 11

Dimension of diffuser throat area F^{*1} per diffuser intake area F_2 vs. Mach number with f as parameter.

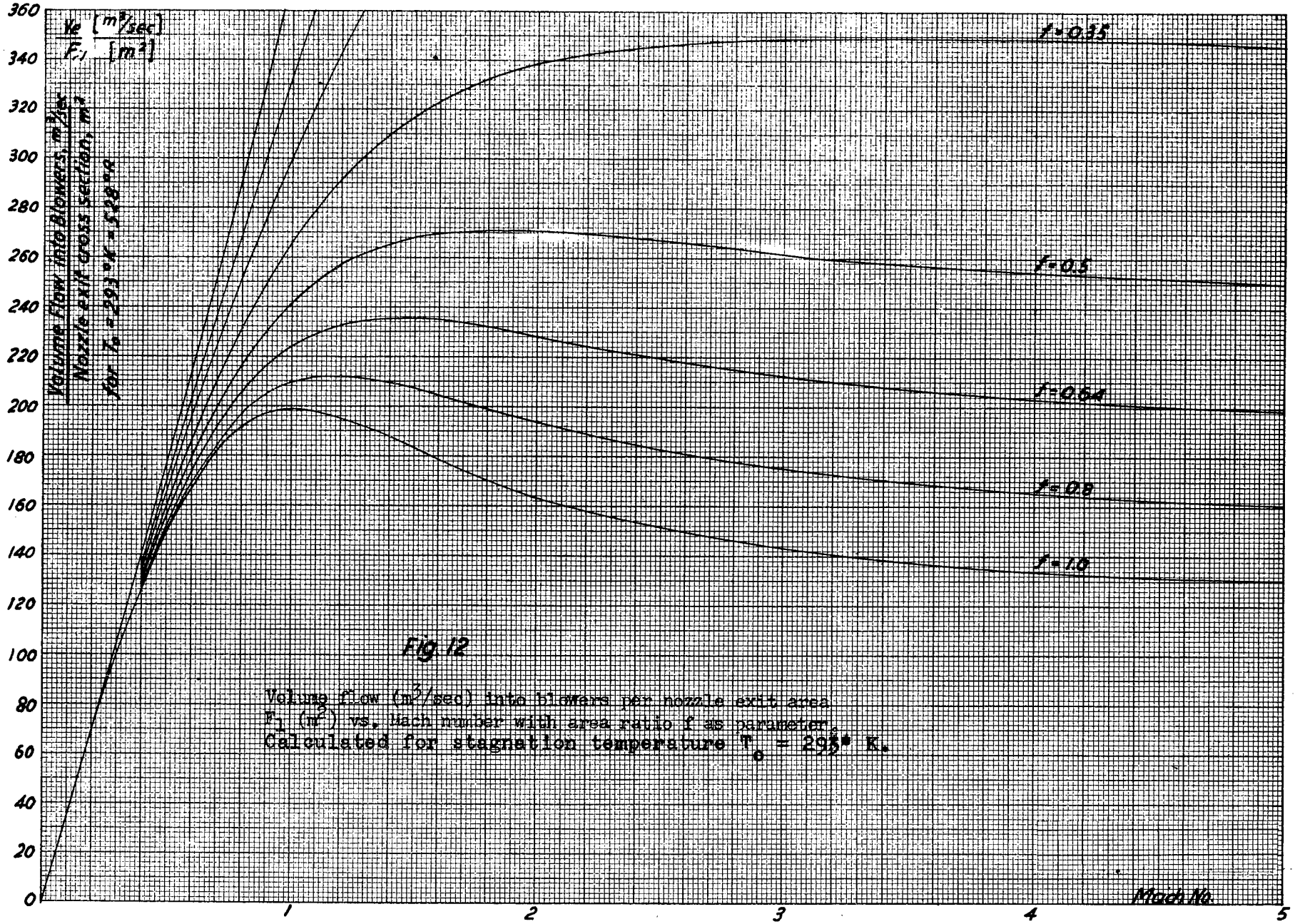

Fig 12

Volume flow (m^3/sec) into blowers per nozzle exit area F_1 (m^2) vs. Mach number with area ratio f as parameter. Calculated for stagnation temperature T_o = 293° K.

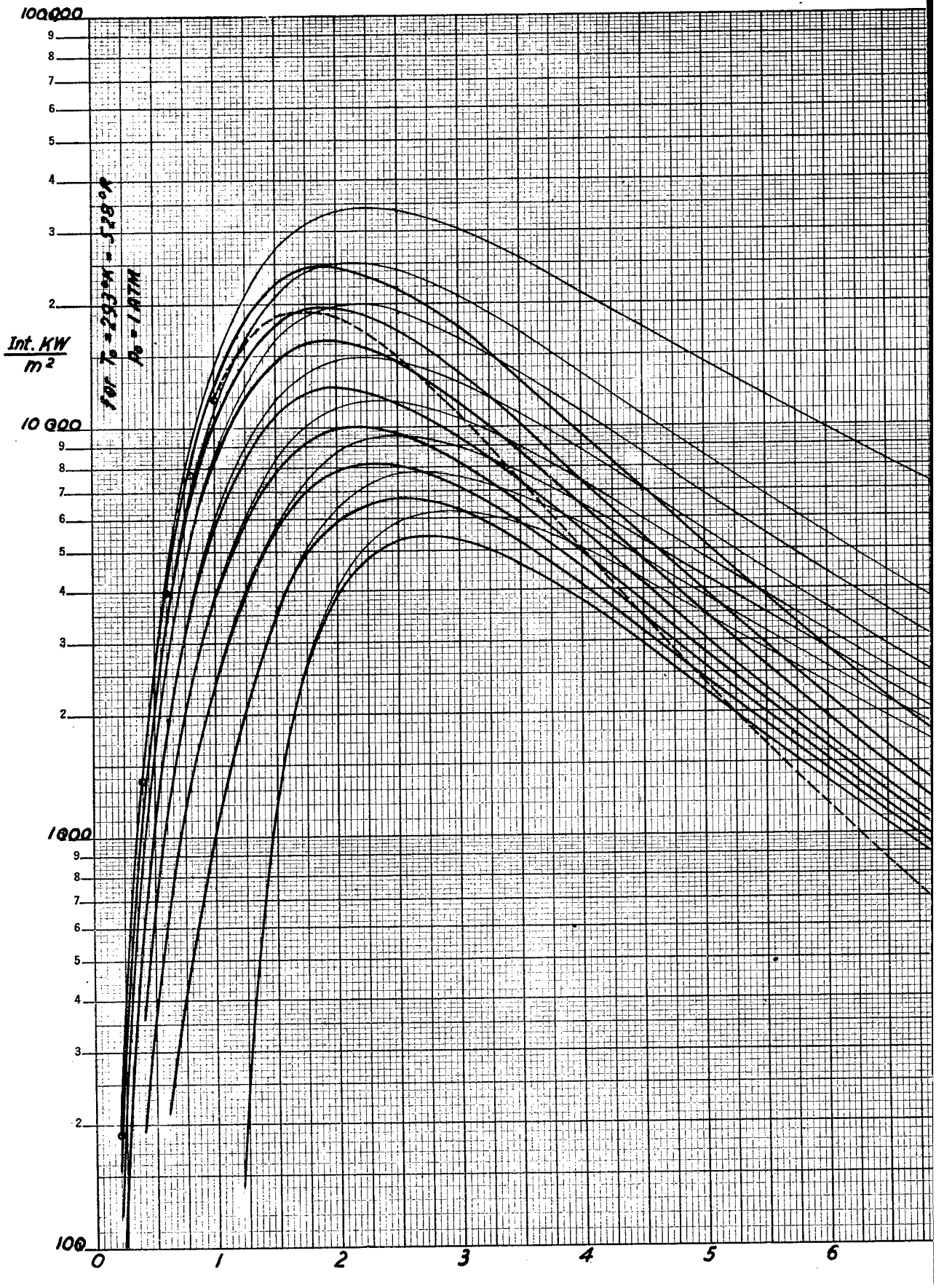
100000
9
8
7
6
5
4
3
2
Int. KW / m²
for T₀ = 293°K = 528°R
P₀ = 1 ATM
10 000
9
8
7
6
5
4
3
2
1000
9
8
7
6
5
4
3
2
100
0
1
2
3
4
5
6

AFTR-6334

Fig. 14

Adiabatic and isothermic blower energy and kinetic energy in test section per nozzle exit area vs. Mach number with f as parameter. Calculated for stagnation temperature T_o = 293°K and stagnation pressure p_o = 1 atm. abs. Ordinate in International Kilowatts per square meter.

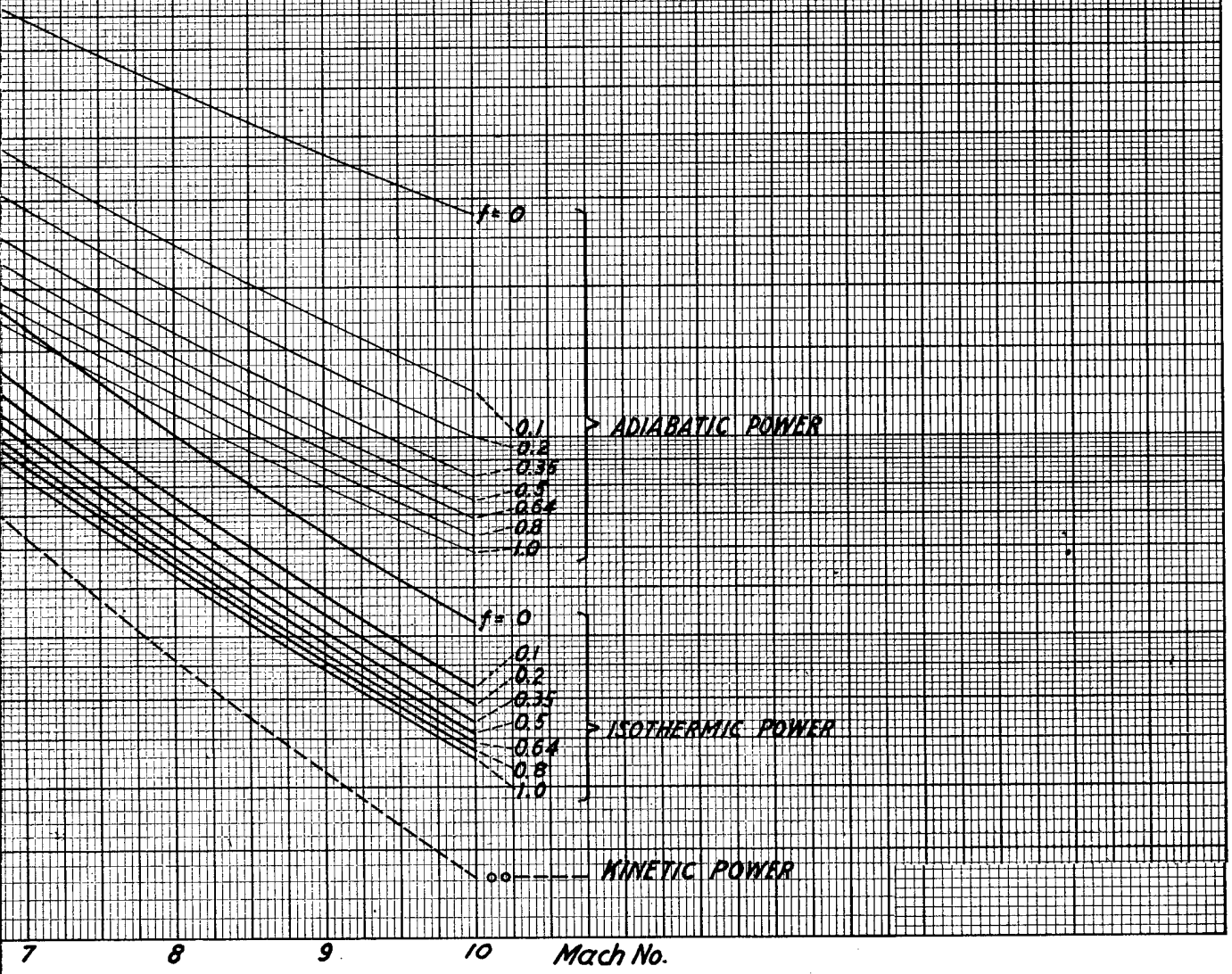

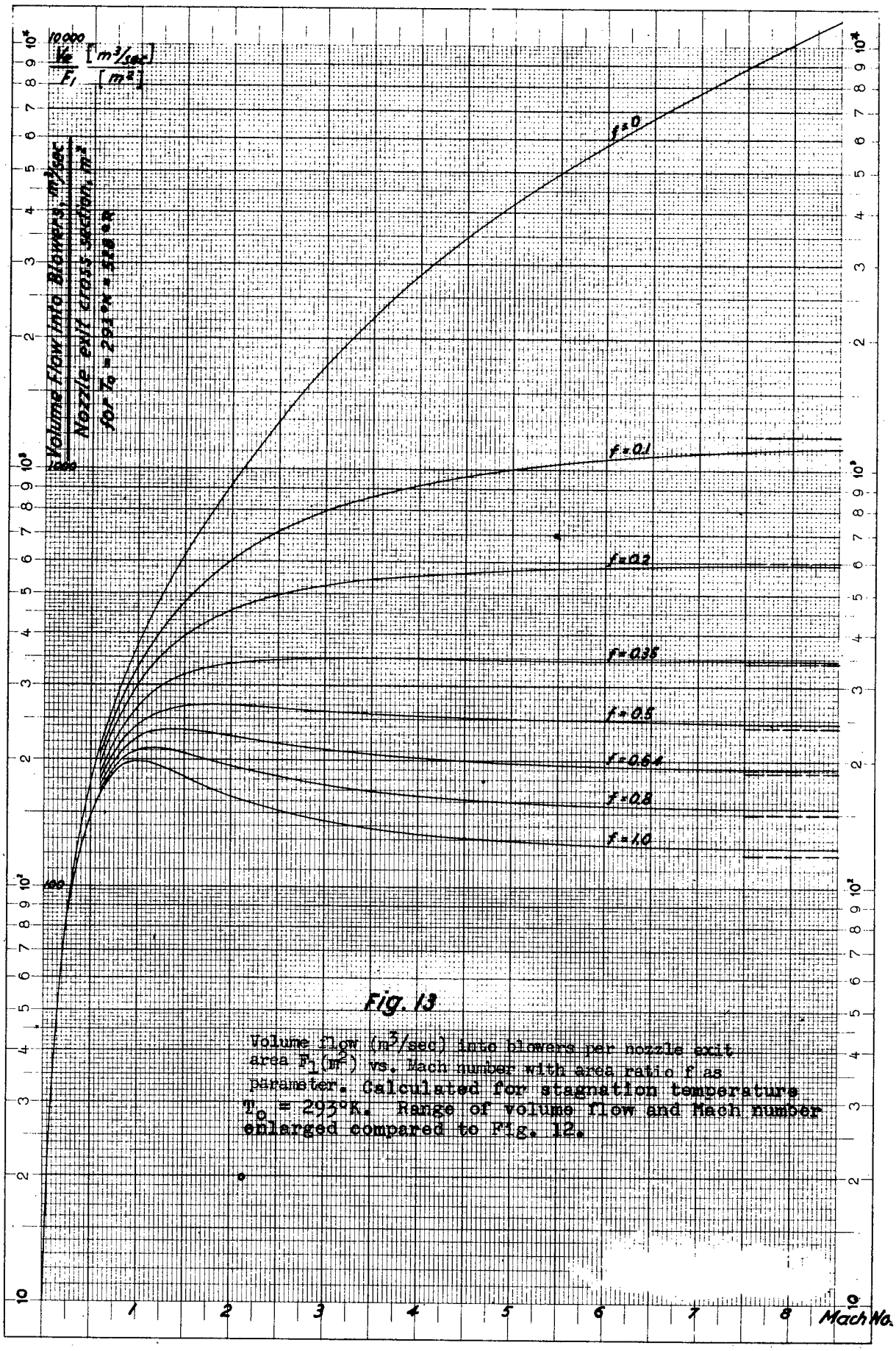

Fig. 13

Volume flow (m^3/sec) into blowers per nozzle exit area F_1 (m^2) vs. Mach number with area ratio f as parameter. Calculated for stagnation temperature T_o = 293°K. Range of volume flow and Mach number enlarged compared to Fig. 12.

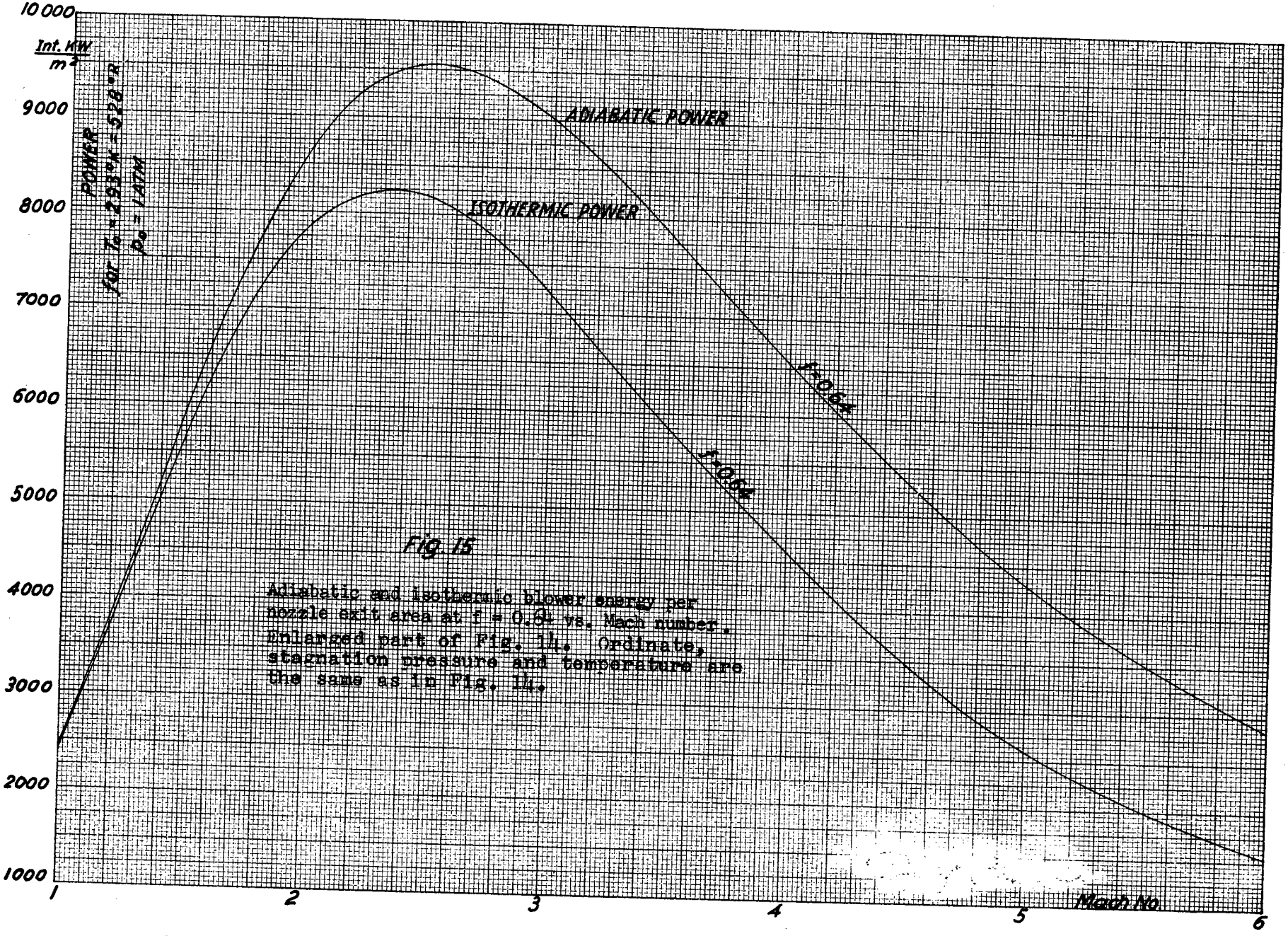

Fig. 15

Adiabatic and isothermic blower energy per nozzle exit area at f = 0.6% vs. Mach number. Enlarged part of Fig. 14. Ordinate, stagnation pressure and temperature are the same as in Fig. 14.

Fig. 16

Adiabatic and isothermic energy ratio ζ vs. Mach number with f as parameter

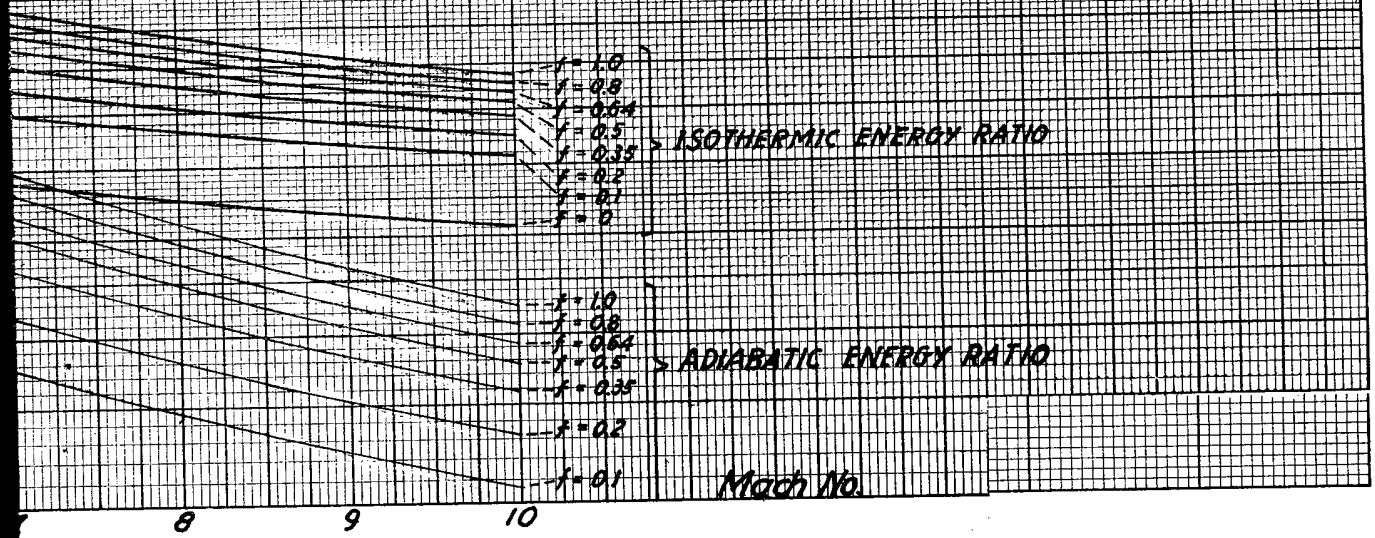

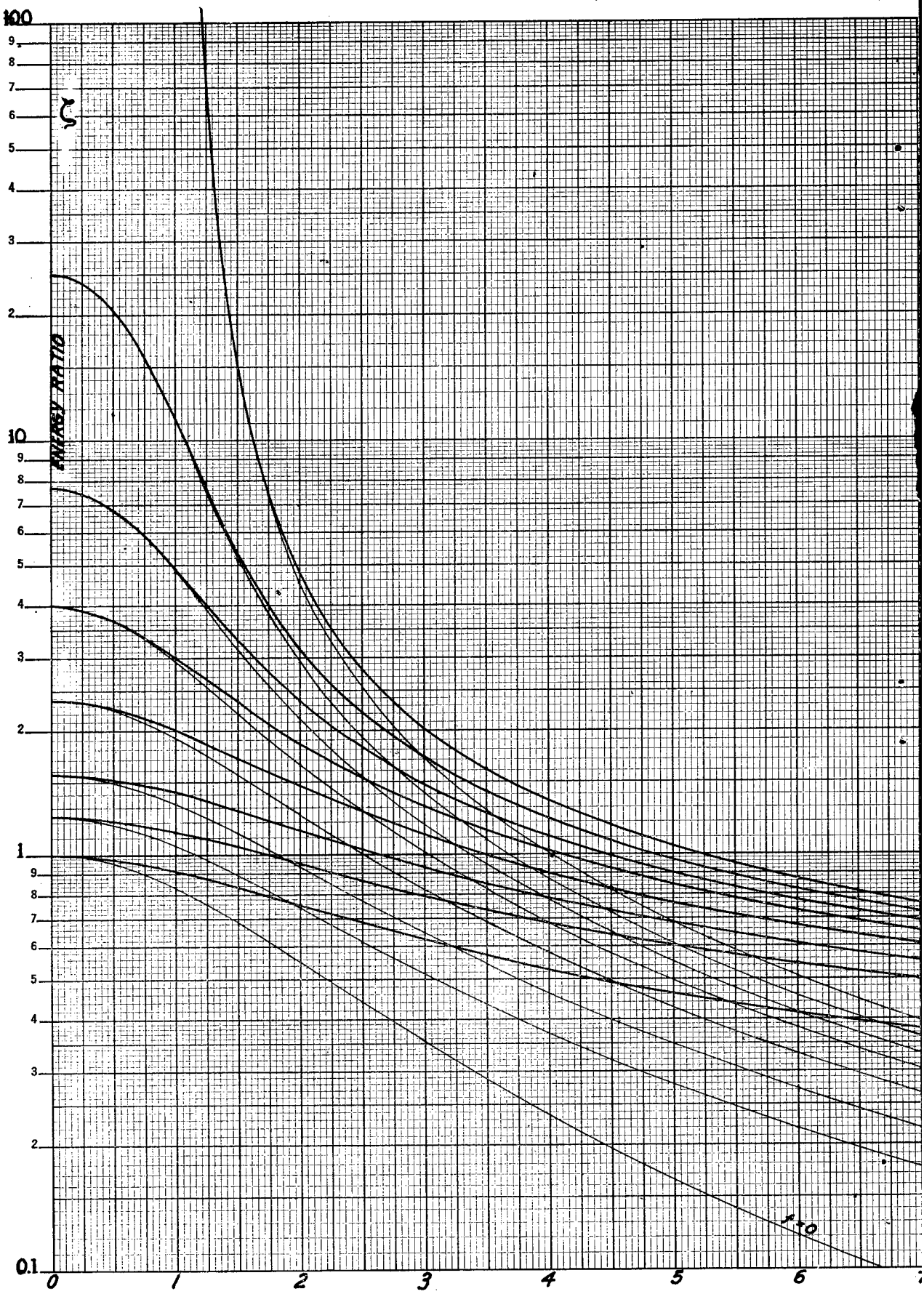
100
9
8
7
ζ
6
5
4
3
2
ENERGY RATIO
10
9
8
7
6
5
4
3
2
1
9
8
7
6
5
4
3
2
0.1
0
1
2
3
4
5
6
f=0

Fig. 17

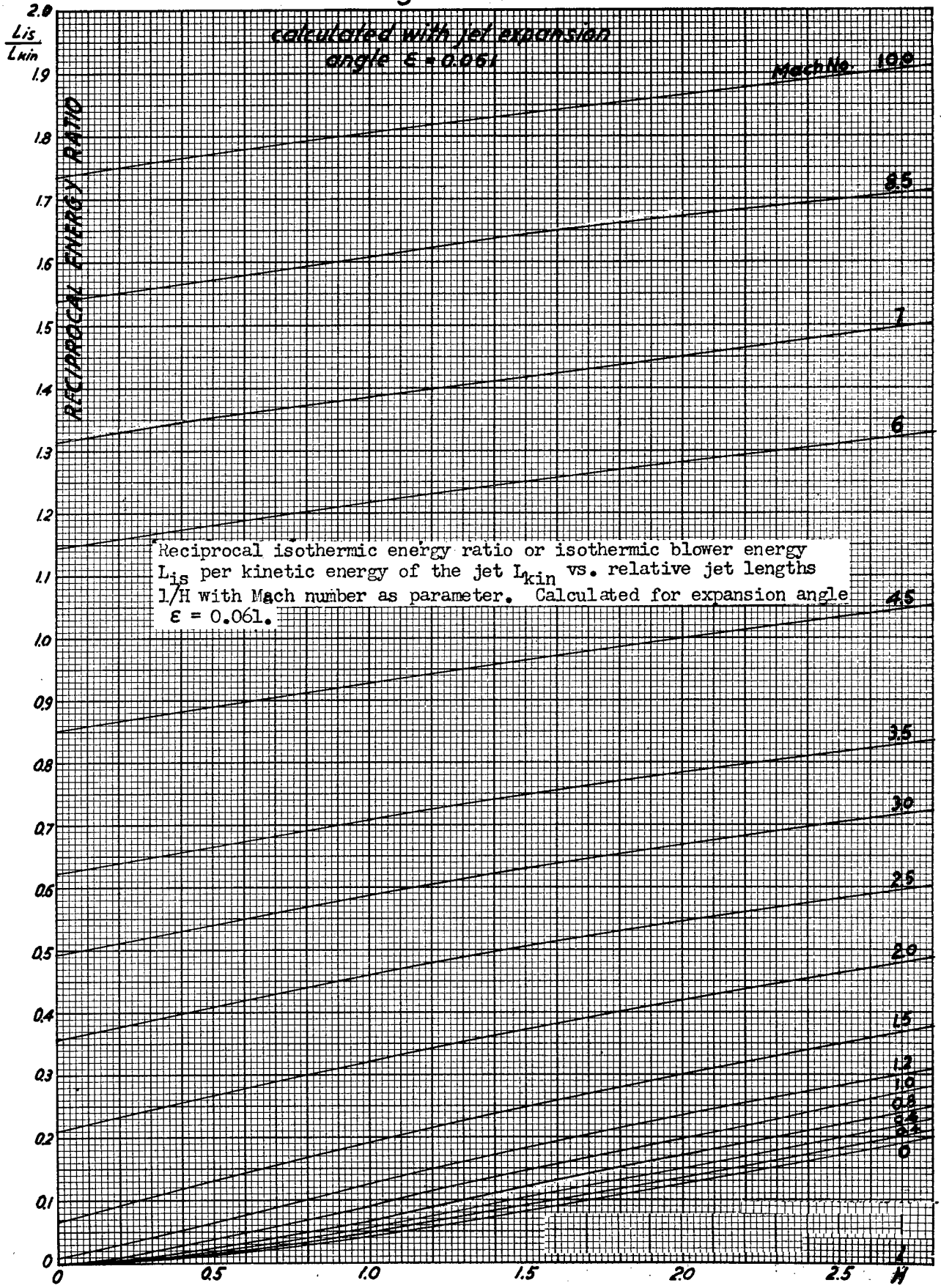

Reciprocal isothermic energy ratio or isothermic blower energy L_{is} per kinetic energy of the jet L_{kin} vs. relative jet lengths l/H with Mach number as parameter. Calculated for expansion angle $\varepsilon = 0.061$.

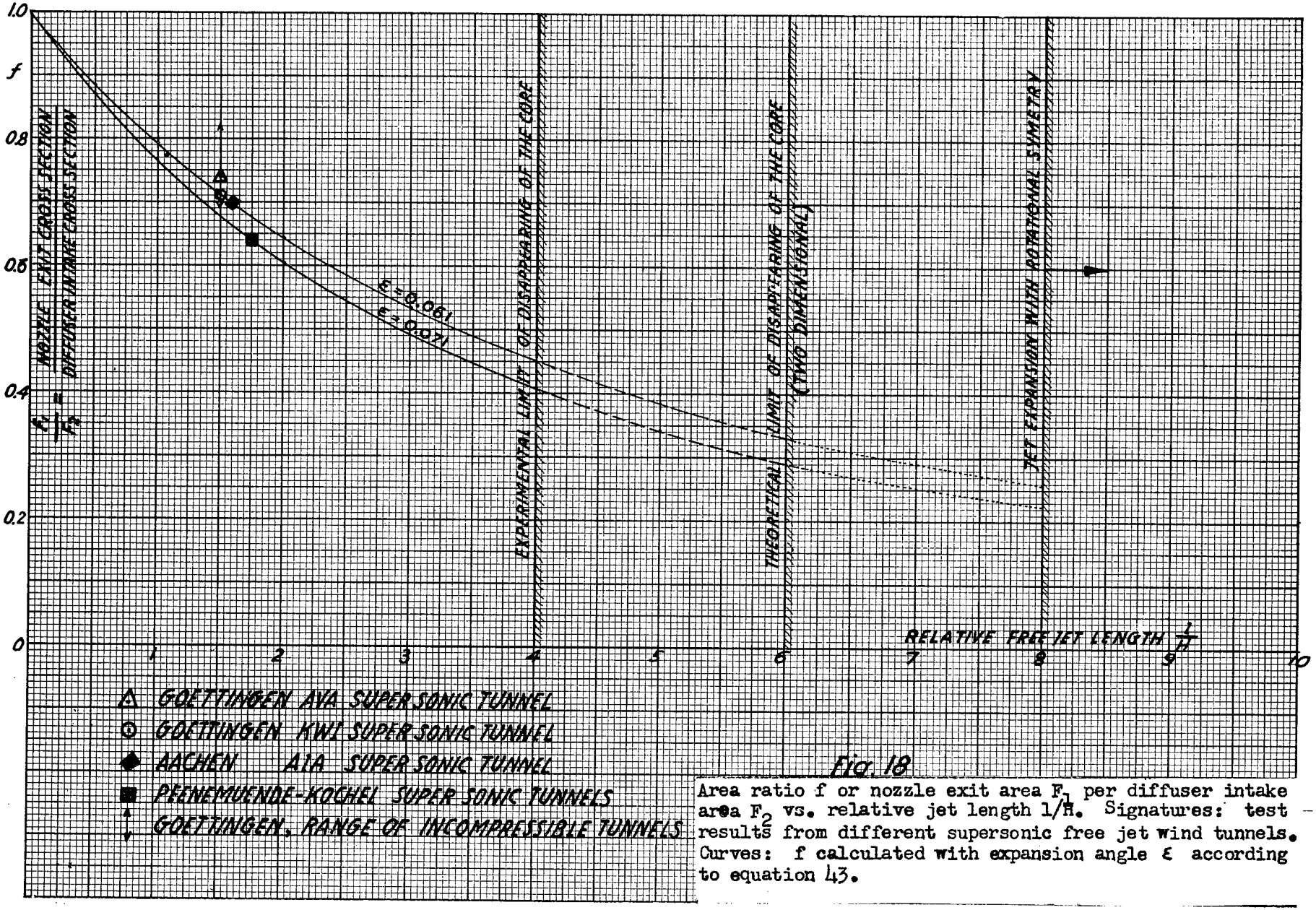

Fig. 18

Area ratio f or nozzle exit area F_1 per diffuser intake area F_2 vs. relative jet length l/H. Signatures: test results from different supersonic free jet wind tunnels. Curves: f calculated with expansion angle ε according to equation 43.

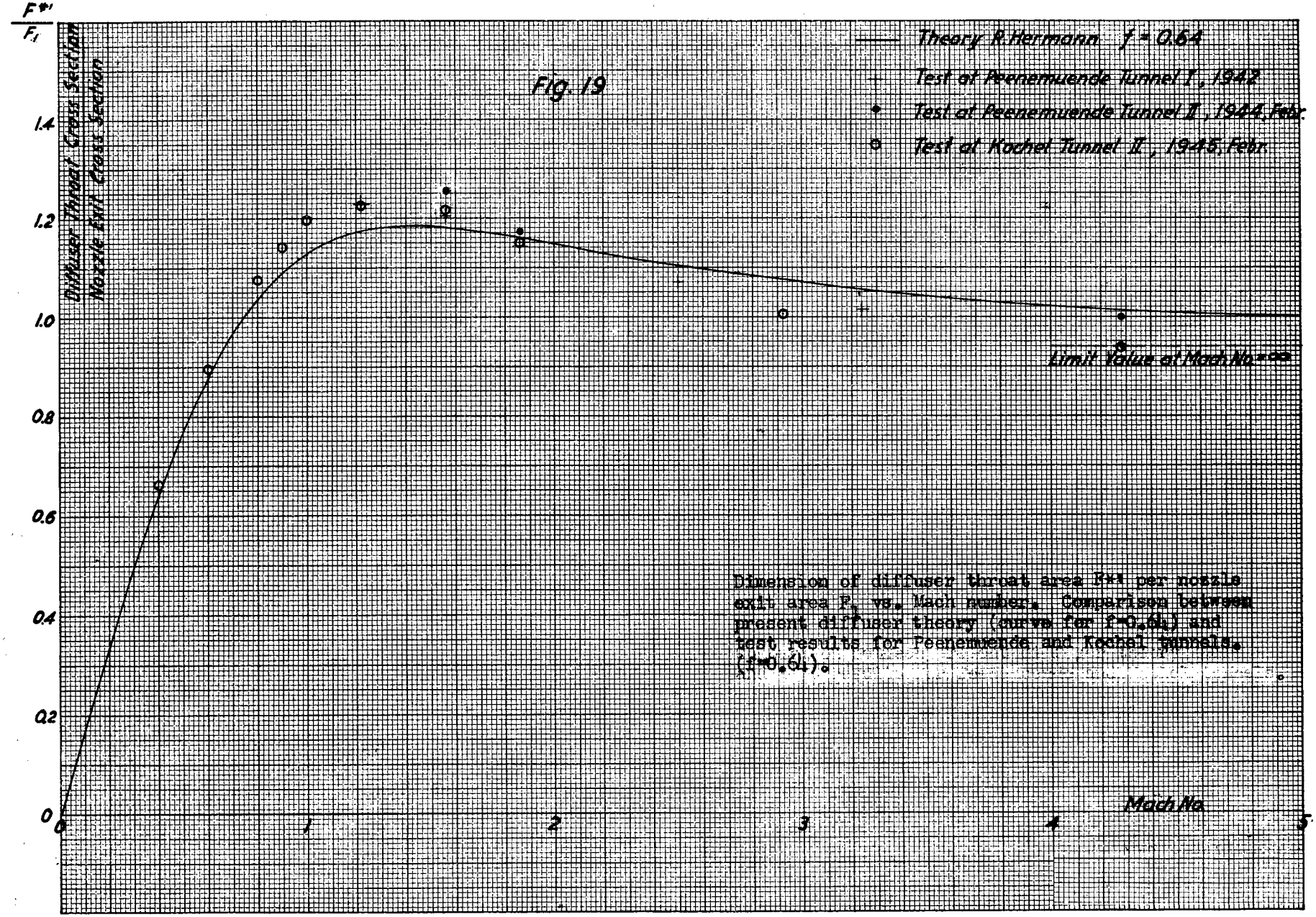

FIG. 19

Dimension of diffuser throat area F*1 per nozzle exit area F1 vs. Mach number. Comparison between present diffuser theory (curve for f=0.64) and test results for Peenemuende and Kochel tunnels. (f=0.64).

Fig 20

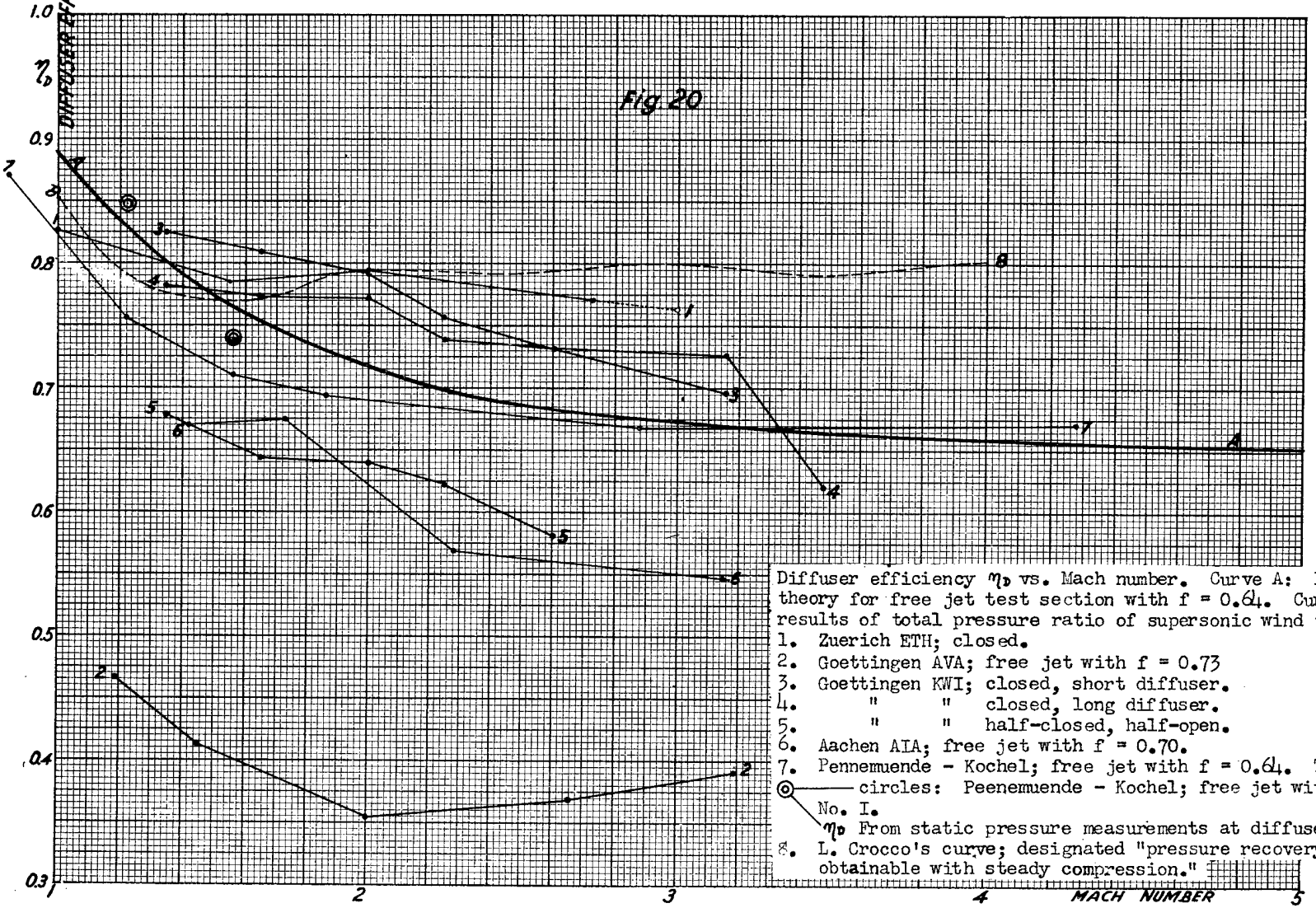

Diffuser efficiency η_D vs. Mach number. Curve A: Present diffuser theory for free jet test section with f = 0.64. Curves 1 - 7: Test results of total pressure ratio of supersonic wind tunnels.

1. Zuerich ETH; closed.
2. Goettingen AVA; free jet with f = 0.73
3. Goettingen KWI; closed, short diffuser.
4. " " closed, long diffuser.
5. " " half-closed, half-open.
6. Aachen AIA; free jet with f = 0.70.
7. Pennemuende - Kochel; free jet with f = 0.64. Tunnel No. II.
   ◎ circles: Peenemuende - Kochel; free jet with f = 0.64. Tunnel No. I.
   η_D From static pressure measurements at diffuser throat.
8. L. Crocco's curve; designated "pressure recovery practically obtainable with steady compression."

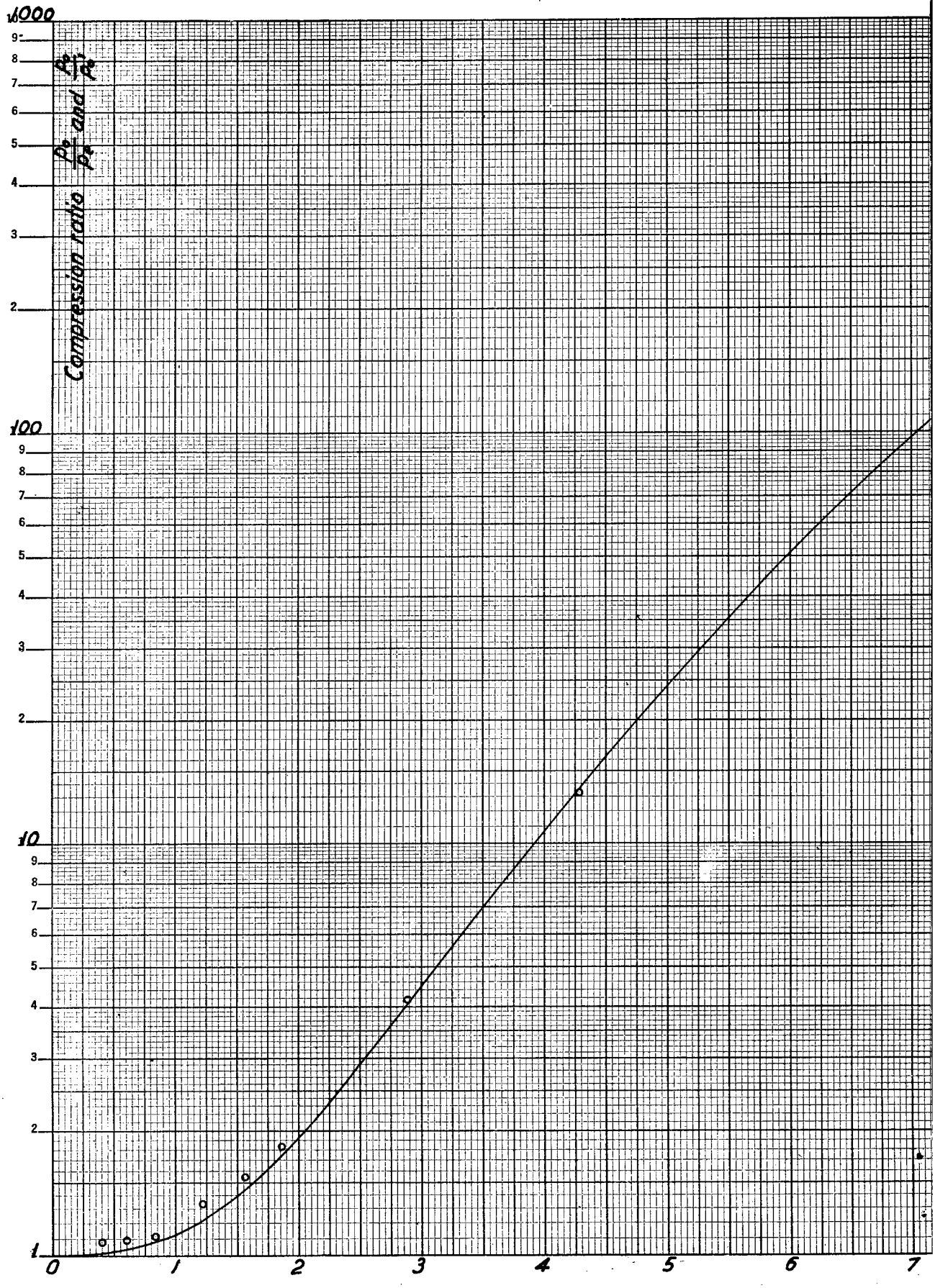
Compression ratio $\frac{p_0}{p_s}$ and $\frac{p_0}{p_s}$
1000
100
10
1
0
1
2
3
4
5
6
7

Fig. 21

—— Diffuser Theory for free jet testsection (f=0.64) by R. Hermann $\frac{p_e'}{p_0}$

• Test values of Peenemuende-Kochel Windtunnel (16"x16") $\frac{p_e}{p_0}$

Total pressure ratio vs. Mach number. Circles: Test results p_e/p_0 for entire Peenemuende - Kochel wind tunnel f = 0.64. Curve: Present diffuser theory p_e'/p_0 for free jet test section with f = 0.64.

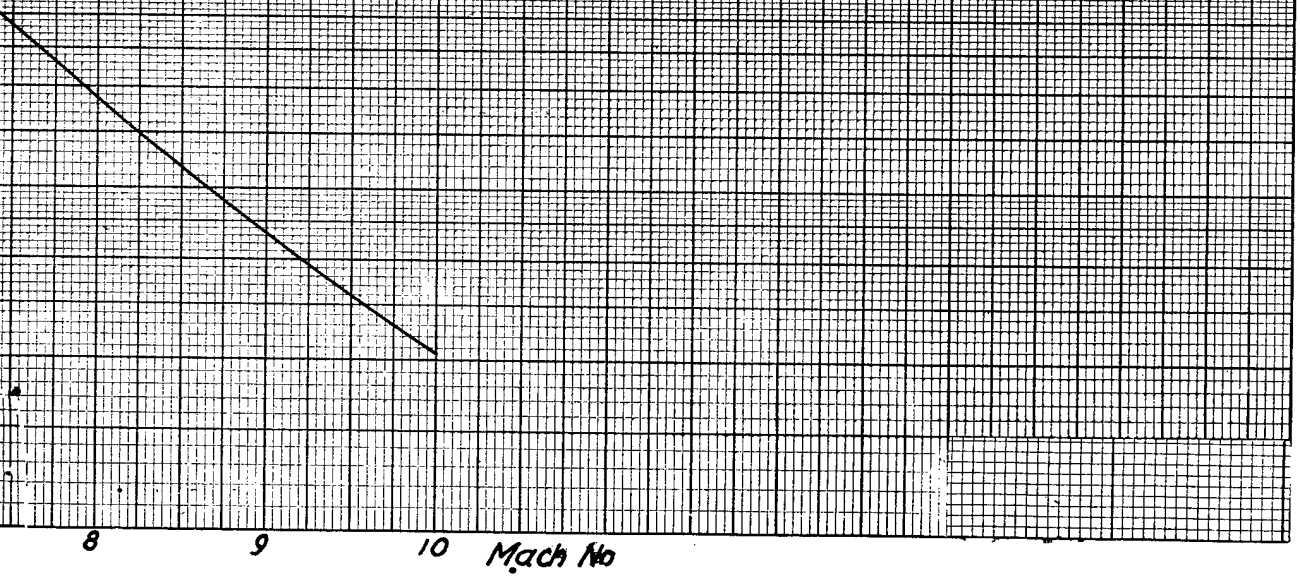

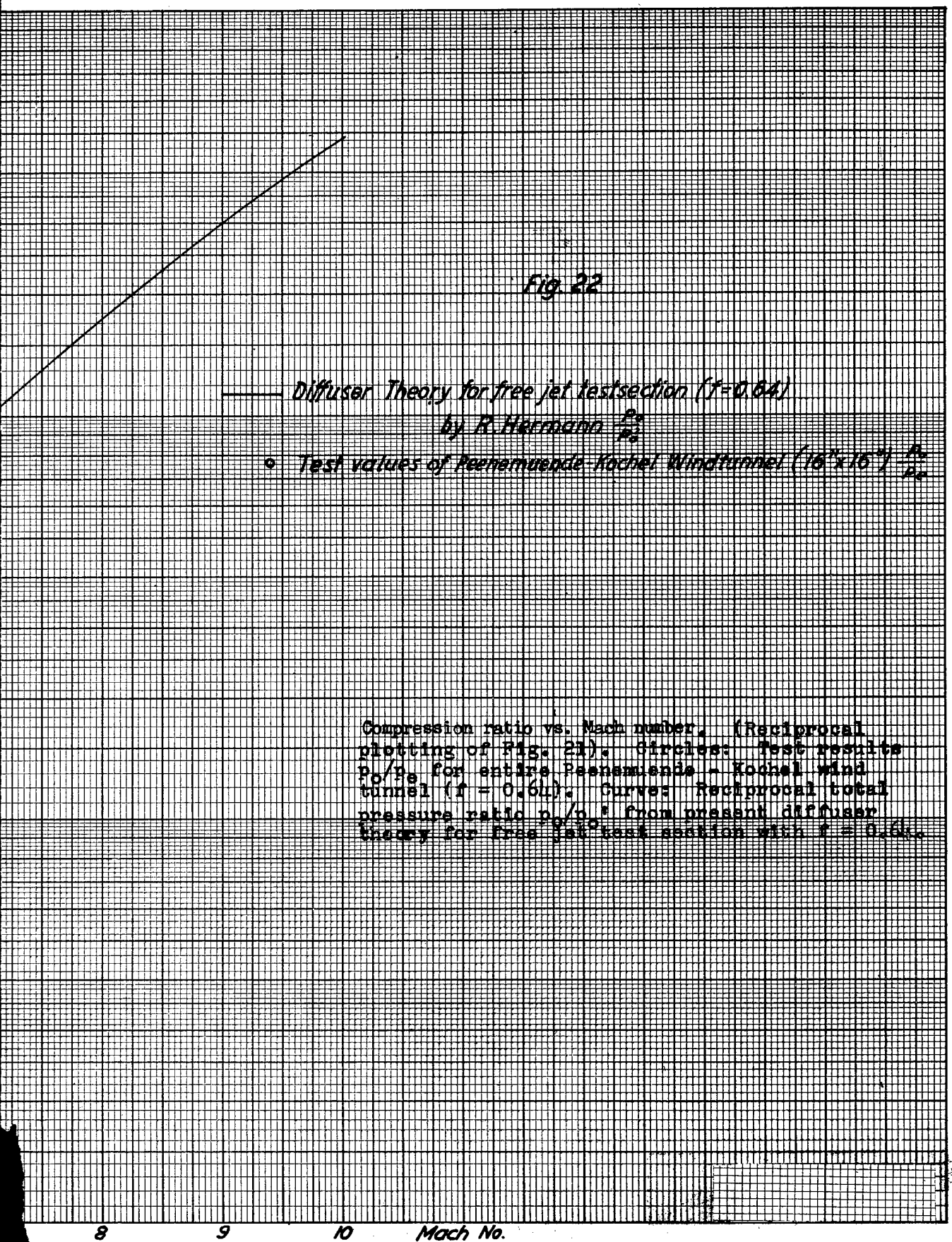

Compression ratio vs. Mach number. (Reciprocal plotting of Fig. 21). Circles: Test results p_o/p_e for entire Peenemuende - Kochel wind tunnel (f = 0.64). Curves: Reciprocal total pressure ratio p_e/p_o' from present diffuser theory for free jet test section with f = 0.64.

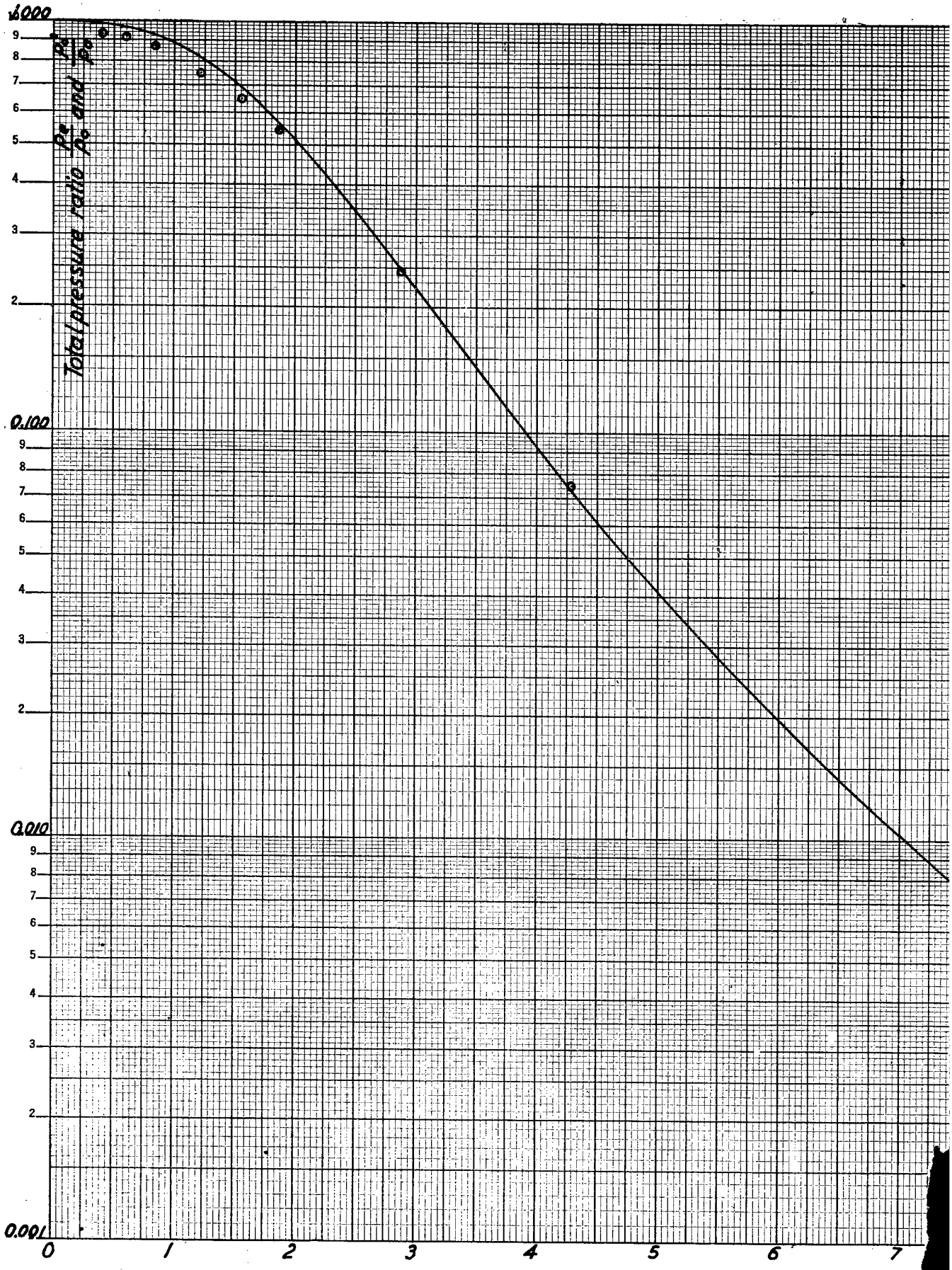

AFTR-6334